

ABSTRACT

Title of Document: EARLY AGE STRENGTH PREDICTION FOR
HIGH VOLUME FLY ASH CONCRETE
USING MATURITY MODELING

Sushant Upadhyaya, Ph.D Civil Engineering,
and 2008

Directed By: Associate Professor, Dr Dimitrios Goulias,
Department of Civil and Environmental
Engineering

The use of fly ash in concrete has received significant attention over recent years due to environmental concerns regarding its disposal and on the other hand its potential use as a cementitious material, with its ability to provide significant benefits to concrete. While a fly ash content less than 25% of total cementitious content is routinely used in concrete, high-volume fly ash (HVFA) contents are not common used due to perceived lower early-age strengths. The objective of this research was to demonstrate that the beneficial effects of high in-place hydration might be able to compensate the slower rate strength gain of HVFA concrete that is typically observed when tested in standard laboratory conditions, in this effort, the maturity-based technique was used. In addition, different

methods (match-cured cylinders and pullout testing) were used to estimate the early-age in-place strength of HVFA concrete to confirm the maturity predicted strengths. The results have shown that the standard and field-cured cylinder strengths underestimate the in-place concrete strength. Higher in-place temperatures due to the mass characteristics of structural elements resulted in increased early age in-place strengths, adequate for construction scheduling, as measured by match-cured cylinders, pullout testing, and the maturity approach.

Furthermore, an extensive investigation on the use of the traditional and alternative maturity principles was examined in order to first identify its applicability to these types of mixtures and, then identify potential adjustments to the maturity modeling as applicable to HVFA concrete mixtures. Two primary directions were followed, the constant and variable ultimate strength (S_u) for multiple curing temperatures.

Another objective of the study was to examine alternative methods of predicting activation energies (AE) for these cementitious systems, as compared to the traditional method identified by the maturity process. Among them, the setting time approach of mortar was considered. Finally, a maturity-based approach was developed for estimating in-place strength of HVFA mixtures to assist the construction industry in implementing the results of this study.

Keywords: Concrete, Fly Ash, Supplementary Cementitious Materials, Maturity, Pullout Test.

EARLY AGE STRENGTH PREDICTION FOR HIGH VOLUME FLY ASH
CONCRETE USING MATURITY MODELING.

By

Sushant Upadhyaya.

Dissertation submitted to the Faculty of the Graduate School of the
University of Maryland, College Park, in partial fulfillment
of the requirements for the degree of
Doctor of Philosophy
2008

Advisory Committee:
Dr Dimitrios Goulias, Chair
Dr. M. Sherrif Aggour
Dr. Amde M. Amde
Dr. Chung C. Fu
Dr. Sung lee, Dean's Representative

© Copyright by
Sushant Upadhyaya
2008

Preface

A major obstacle that limits the widespread use of High-Volume Fly Ash (HVFA) concrete is its lower early-age strength as documented in research studies conducted in the laboratory with standard-cured strength specimens. The objective of this research was to demonstrate that using a maturity-based technique that the actual in-place strength of HVFA concrete in a structure is higher than that indicated by strength measured on field-cured cylinders due to the higher in-place temperature resulting from the slower dissipation of heat of hydration due to the greater mass of structural members. The in-place strength of concrete in the structure can be determined by monitoring its temperature history over time, calculating the maturity, and by estimating the in-place strength from the pre-calibrated strength-maturity relationship. Maturity concepts are well established for Portland cement concrete but they are not so established for HVFA concrete mixtures containing chemical admixtures. The Arrhenius and Nurse-Saul maturity functions are usually used to establish the maturity index. The Arrhenius maturity function is considered more accurate and was used in this research. The Arrhenius maturity function requires the use of mixture-specific activation energy to improve predictions of strength. The activation energy quantifies the temperature sensitivity of the concrete mixture.

An initial task was to determine the activation energy of each of the concrete mixtures using the procedure outlined in ASTM C1074. Various fly ashes (Class C and Class F fly ash meeting the standard ASTM C618) with multiple dosages (20% to 50% by mass of

cementitious materials) were used in this research. Activation energies of these mixtures were determined. Some unexpected trends of strength were observed for these fly ash mixtures. The fly ash mixtures cured at elevated temperatures demonstrated higher long-term strengths than anticipated in comparison to the strength of specimens cured at lower temperatures.

The next step was to develop strength-maturity relationships in the laboratory for four of the concrete mixtures. Additionally, pullout forces versus compressive strength correlations were developed. To validate the strength predictions based on maturity, four concrete blocks and two slabs were prepared in the field during the period of October to December, when the ambient temperature ranged from 15.5°C (60°F) to 7.5°C (45°F).

The in-place compressive strength of the concrete blocks and slabs were predicted based on the following approaches:

1. Match-cured cylinder method;
 2. Pullout testing method by using the pullout versus compressive strength relationships;
 3. Maturity method based on the activation energy and strength-maturity relationships;
- and,
4. Field-cured cylinder approach

The compressive strengths of the concrete mixtures using the standard-cured cylinders were tested at several ages, as well.

Based on this research the following primary conclusions were reached:

1. Match-cured compressive strength data have clearly demonstrated that HVFA concretes in actual structural members achieve much higher early-age strengths than the strength indicated by testing field-cured cylinders. This observation will allow for further mixture optimization and possibly increased content of fly ash without negative impact on construction operations.
2. A maturity-based approach has been developed to estimate in-place strength in the actual structure from temperature measurement with time. This is based on the variable S_u approach even though the crossover effect of the hydration temperature vs. strength gain for the mixtures did not follow the trend that is typically observed for the conventional concrete.

Dedication

*To my late grandfather **Dr. Gaya Prasad Upadhyaya***

Acknowledgement

I would like to express my gratitude to all those people who helped me directly or indirectly in completion of this dissertation. I am deeply indebted to my advisor Dr. Dimitrios Goulias under whose guidance and encouragement, I chose this topic and enjoyed working on my dissertation. His stimulating suggestions, invaluable time and experience in the field helped me in overcoming the problems I faced, and putting up my best.

I would also like to thank the members of the committee, professor M. Sherif Aggour, professor Amde M. Amde, research professor Chung C. Fu, and professor Sung Lee, Dean's representative for agreeing to serve on my committee and for sparing their invaluable time reviewing the manuscript and providing comments for the dissertation.

I would like to extend my appreciation to Dr. Nicholas J. Carino (retired NIST investigator), and Dr. Anton K. Schindler (Auburn University), for guiding me throughout the research, and providing valuable suggestions. Members of the National Ready Mixed Concrete Association (NRMCA), Dr. Karthikeyan H. Obla who has given me advice, suggestions, and instruction in regards to my research and future professional plans. Dr. Colin Lobo for providing comments for the dissertation. Haejin Kim (manager of the NRMCA research lab) for supporting and giving valuable remarks throughout the

research. Soliman Ben-Barka and Stuart Sherman for assisting me during the experimental phase of this research.

I thank my parents and other family members because of whom I am here today. Their faith and inspiration is the only reason I have survived. No words can express my gratitude, but it is the least I can do.

Finally, I would like to thank my loving wife, for her continued support.

I also acknowledge Maryland Department of Natural Resources (MDNR), the Department of Energy (DOE) and its CBRC program officers, and the National Ready Mixed Concrete Association (NRMCA) for financially supporting my dissertation and its implementation.

Table of Contents

Preface.....	ii
Dedication.....	v
Acknowledgement.....	vi
Table of Contents.....	viii
List of Figures.....	xi
List of Tables.....	xv
Chapter 1 Introduction.....	1
1.1 Research Objectives.....	3
1.1.1 Maturity Modeling.....	4
1.1.2 Setting Time of Mortar Mixes.....	4
1.1.3 Pullout Load vs. Strength Modeling.....	4
1.1.4 Evaluate Proposed Strength vs. Age Models from Field and Lab Data.....	5
1.1.5 Effects of Different Lab and Field Monitoring Methods on Strength Measurements and Predictions.....	5
1.2 Description of Contents.....	8
Chapter 2 Background.....	10
2.1 Strength-age Model.....	10
2.2 Maturity Concept.....	12
2.3 Pullout Test.....	15
2.4 Match Curing.....	16
2.5 Pushout Cylinders.....	17
2.6 Literature Review of HVFAC.....	18
Chapter 3 Experimental Work – Mortar.....	22
3.1 Materials.....	22
3.2 Mixing Mortar.....	25
3.3 Mortar Testing.....	26
3.3.1 Fresh Mortar Tests.....	26
3.3.2 Hardened Mortar Tests.....	26
3.4 Mixture Proportions.....	28
3.5 Discussion of Test Results.....	30
3.5.1 Fresh Mortar Properties.....	30
3.5.2. Compressive Strength.....	36
3.5.3.1 Setting time method.....	48

3.5.3.2 Constant S_{uc} approach.....	50
Chapter 4 Experimental Work – Concrete.....	55
4.1 Materials	55
4.2 Mixing Concrete	55
4.3 Concrete Testing.....	55
4.3.1 Fresh Concrete Tests.....	56
4.3.2 Hardened Concrete Tests	56
4.4 Mixture Proportions.....	66
4.5 Discussion of Test Results	67
4.5.1 Fresh Concrete Properties	67
4.5.2 Standard Cured Strength Results and Strength-Maturity Relationship	67
4.5.3 Pullout force test results and pullout force versus strength correlation.....	71
4.5.4 In-Place Strength Estimates Based on Field-Cured and Match-Cured Cylinder Strengths	76
4.5.5 In-Place Strength Estimates Based on Pullout and Maturity	80
Chapter 5 Semi-Adiabatic Calorimetry Testing	92
5.1 Quantifying the Total Heat of Hydration of the Cementitious Materials	93
5.2 Quantifying the Degree of Hydration Development.....	94
5.3 Temperature Sensitivity of Cementitious Materials	96
5.4 Modeling the Heat Generation and Temperature Associated with Hydration.....	97
5.5 Experimental Work.....	98
5.6 Test Data and Discussion of Results.....	100
Chapter 6 Step by Step Procedure for Optimizing the Design of HVFA Mixtures.....	105
6.1 Step-by-Step Approach.....	105
6.1.1 Strength Requirement for Structural Application.....	106
6.1.2 Mix Design of HVFA Concrete.....	106
6.1.3 Selection of an Activation Energy	110
6.1.4 Develop Strength Maturity Relationship	112
6.1.5 Hydration Parameters for HVFA Concrete.....	113
6.1.6 Thermal Analysis using ConcreteWorks Thermal Modeling Software.....	113
6.1.7 In-Place Strength Predictions.....	114
Chapter 7 Conclusions	116
Appendix A.....	119
Appendix B.....	132
Appendix C.....	143

Appendix D.....	145
Appendix E.....	150
Appendix F.....	159
Appendix G.....	166
References.....	172

List of Figures

Figure 2.1 Pullout setup (Carino 2004).....	16
Figure 3.1 Temperature sensor (iButton®).....	28
Figure 3.2 Setting times of mortar mixtures	32
Figure 3.3 Compressive strength vs. actual age (35% FA-A mixture).....	37
Figure 3.4 Compressive strength vs. actual age (35% FA-C mixture).....	38
Figure 3.5 Rate constant vs. temperature-control mixture (AE-41400l J/mol)	41
Figure 3.6 Rate constant vs. temperature-20% FA-A (AE-48100 J/mol).....	42
Figure 3.7 Rate constant vs. temperature-35% FA-A (AE-15600 J/mol)	42
Figure 3.8 Rate constant vs. temperature-50% FA-A (AE-33400 J/mol).....	43
Figure 3.9 Rate constant vs. temperature-35% FA-B (AE-33000 J/mol).....	43
Figure 3.10 Rate constant vs. temperature-35% FA-C (AE-28300l J/mol).....	44
Figure 3.11 Arrhenius plot (Control mixture).....	44
Figure 3.12 Arrhenius plot (20% FA-A).....	45
Figure 3.13 Arrhenius plot (35% FA-A).....	45
Figure 3.14 Arrhenius plot (50% FA-A).....	46
Figure 3.15 Arrhenius plot (35% FA-B).....	46
Figure 3.16 Arrhenius plot (35% FA-C).....	47
Figure 4.1 Match cure system showing 8 match-cured cylinder molds connected to a micro-controller computer	58
Figure 4.2 Custom 20.32 cm (8 in.) cube mold	59
Figure 4.3 Cube molds with pullout inserts at the centers of the 4 side faces	59
Figure 4.4 Pullout Equipment.....	60
Figure 4.5: Field block with pullout inserts and temperature sensors	61
Figure 4.6 Concrete block curing in field.	63
Figure 4.7 Concrete slab with cast-in-place cylinders and temperature sensors	65
Figure 4.8 Slabs with cast-in-place cylinders, floating inserts and field cure cylinders...	65
Figure 4.9 Maturity model- control mixture	69

Figure 4.10 Maturity model- 35% FA-A mixture.....	70
Figure 4.11 Maturity model- 50% FA-A mixture.....	70
Figure 4.12 Maturity model- 35% FA-C mixture.....	71
Figure 4.13 Compressive strength vs. pullout force relationship-Control mixture	74
Figure 4.14 Compressive strength vs. pullout force relationship-35% FA-A mixture.....	75
Figure 4.15 Compressive strength vs. pullout force relationship-50% FA-A mixture.....	75
Figure 4.16 Compressive strength vs. pullout force relationship-35% FA-C mixture	76
Figure 4.17 Compressive Strength vs. age for different curing conditions (control mixture-block).....	77
Figure 4.18 Compressive Strength vs. age for different curing conditions (control mixture-slab)	78
Figure 4.19 Compressive Strength vs. age for different curing conditions (35% FA-A mixture-block).....	78
Figure 4.20 Compressive Strength vs. age for different curing conditions (35% FA-C mixture-block).....	79
Figure 4.21 Compressive Strength vs. age for different curing conditions (50% FA-A mixture-slab and block)	79
Figure 4.22 Comparison of strength obtained from various methods vs. equivalent age (control-mixture block).....	86
Figure 4.23 Comparison of strength obtained from various methods vs. equivalent age (50% FA-A block)	86
Figure 4.24 Comparison of strength obtained from various methods vs. equivalent age (35% FA-A block)	87
Figure 4.25 Comparison of strength obtained from various methods vs. equivalent age (35% FA-C block).....	87
Figure 4.26 Comparison of strength obtained from various methods vs. equivalent age (control mixture-slab).....	88
Figure 4.27 Comparison of strength obtained from various methods vs. equivalent age (50% FA-A-slab).....	88

Figure 5.1 Effect of change in fly ash proportions and w/cm on cumulative heat of hydration development.....	102
Figure 5.2 Effect of change in fly ash proportions and w/cm on rate of hydration	103
Figure 5.3 Effect of change in fly ash type and w/cm on cumulative heat of hydration development.....	104
Figure 5.4 Effect of change in fly ash type and w/cm on rate of hydration.....	104
Figure A.1 Specimens for task 3.....	126
Figure A.2 Schematic of field testing.....	127
Figure A.3 Concrete block and temperature sensor locations	129
Figure A.4 Concrete slab and temperature sensor locations.....	131
Figure D.1 Strength vs. pullout force (control mix)	146
Figure D.2 Strength vs. pullout force (35% FA-A)	147
Figure D.3 Strength vs. pullout Force (50% FA-A)	147
Figure D.4 Strength vs. pullout Force (35% FA-C).....	148
Figure E.1 Arrhenius Plot for setting time vs. temperature	150
Figure E.2 Maturity model-setting time approach (Control mix).....	151
Figure E.3 Comparison of strength obtained from various methods vs. equivalent age setting time (Control mixture-block)	151
Figure E.4 Maturity model-setting time approach (35% FA-A).....	153
Figure E.5 Comparison of strength obtained from various methods vs. equivalent age setting time (35%FA-A mixture-block).....	153
Figure E.6 Maturity model-setting time approach (50% FA-A).....	154
Figure E.7 Comparison of strength obtained from various methods vs. equivalent age setting time (50%FA-A mixture-block).....	154
Figure E.8 Maturity model-setting time approach (35% FA-C).....	155
Figure E.9 Comparison of strength obtained from various methods vs. equivalent age setting time (35%FA-C mixture-block).....	156
Figure E.10 Comparison of strength obtained from various methods vs. equivalent age setting time (control mixture-slab).....	157

Figure E.11 Comparison of strength obtained from various methods vs. equivalent age setting time (50% FA-A-slab).....	157
Figure F.1 Arrhenius plots (Constant S_{uc} approach).....	160
Figure F.2 Comparison of Arrhenius plot (Variable S_u and Constant S_{uc}) for combined data set.....	161
Figure F.3 Comparison of strength obtained from various methods versus equivalent age (control mixture-block).....	162
Figure F.4 Comparison of strength obtained from various methods versus equivalent age (35% FA-A-block).....	162
Figure F.5 Comparison of strength obtained from various methods versus equivalent age (50% FA-A-block).....	163
Figure F.6 Comparison of strength obtained from various methods versus equivalent age (35% FA-C-block).....	163
Figure F.7 Comparison of strength obtained from various methods versus equivalent age (control mixture-slab).....	164
Figure F.8 Comparison of strength obtained from various methods versus equivalent age (50% FA-A -slab).....	164
Figure G.1 Ambient temperature profile during field testing from October to November	166
Figure G.2 Temperature Profile of block (Control mixture).....	167
Figure G.3 Temperature Profile Control mixture.....	167
Figure G.4 Temperature Profile of Slab (Control Mixture).....	168
Figure G.5 Temperature Profile of block (50% FA-A).....	168
Figure G.6 Temperature Profile 50% FA-A.....	169
Figure G.7 Temperature Profile of Slab (50% FA-A).....	169
Figure G.8 Temperature Profile of block (35% FA-A).....	170
Figure G.9 Temperature Profile 35% FA-A.....	170
Figure G.10 Temperature Profile of block (35% FA-C).....	171
Figure G.11 Temperature Profile 35% FA-C.....	171

List of Tables

Table 3.1 Chemical and physical properties of cement and fly ash (ASTM C 150, ASTM C618).....	24
Table 3.2 Gradation and properties of aggregates (ASTM C 136).....	25
Table 3.3 Mortar mixture proportions (5.08 cm (2-inch) cubes –ASTM C1074)	29
Table 3.4Curing temperatures used for multiple trials	30
Table 3.5 Average curing temperature for mortar cubes	31
Table 3.6 Setting times for mortar mixtures (ASTM C403).....	31
Table 3.7 Flow results for mortar mixtures-trial I (ASTM C1437).....	33
Table 3.8 Flow results for mortar mixtures-trial II (ASTM C1437).....	33
Table 3.9 Flow results for mortar mixtures-trial II (ASTM C1437).....	34
Table 3.10 Flow results for mortar mixtures-trial IV (ASTM C1437).....	34
Table 3.11 Air content and density for mortar mixtures-trial II (ASTM C185).....	35
Table 3.12 Air content and density for mortar mixtures-trial III (ASTM C185)	35
Table 3.13 Air content and density for mortar mixtures-trial IV (ASTM C185)	35
Table 3.14 Best fit regression constants	41
Table 3.15 Calculated activation energies (ASTM C1074).....	47
Table 3.16 Activation energy using setting time approach.....	50
Table 3.17 Best fit regression constants-Constant S_{uc}	52
Table 3.18 Activation Energy computed based on constant S_u approach.....	52
Table 3.19 R square values for best fit linear fit.....	53
Table 3.20 Percent difference between predicted strength and maturity method.....	54
Table 4.1 Placement of concrete for blocks and slabs- over the first 96 hours	66
Table 4.2 Yield adjusted concrete mixture proportions.....	67
Table 4.3 Fresh concrete properties	67
Table 4.4 Control mixture.....	68
Table 4.5 35% FA-A mixture	68
Table 4.6 50% FA-A mixture	69
Table 4.7 35% FA-C mixture.....	69

Table 4.8 Regression constants for strength relationship	73
Table 4.9 Strength prediction using maturity and pullout correlation	89
Table 4.10 Strength comparison between various curing condition and predicted strength	90
Table 4.11 Average percent differences between match cured and various other in-place strength prediction techniques	91
Table 5.1: Mixture proportions used for semi-adiabatic testing	98
Table 5.2: Quality control data collected for batches produced for semi-adiabatic testing	100
Table 5.3: Best-fit hydration parameters obtained from semi-adiabatic testing ($T_r =$ 22.8°C)	101
Table 6.1 Activation energies for mixtures	111
Table A.1 Mixture Proportions	119
Table A.2 Initial Activation Energy	121
Table B.1 Compressive strength -trial 1 (control mixture)	132
Table B.2 Compressive strength -trial 2 (control mixture)	133
Table B.3 Compressive strength -trial 1 (20% FA-A)	134
Table B.4 Compressive strength -trial 1 (35% FA-A)	135
Table B.5 Compressive strength -trial 2 (35% FA-A)	136
Table B.6 Compressive strength -trial 3 (35% FA-A)	136
Table B.7 Compressive strength -trial 1 (50% FA-A)	137
Table B.8 Compressive strength -trial 2 (50% FA-A)	138
Table B.9 Compressive strength -trial 3 (50% FA-A)	138
Table B.10 Compressive strength -trial 4 (50% FA-A)	139
Table B.11 Compressive strength -trial 1 (35% FA-B)	140
Table B.12 Compressive strength -trial 2 (35% FA-B)	140
Table B.13 Compressive strength -trial 1 (35% FA-C)	141
Table B.14 Compressive strength -trial 2 (35% FA-C)	142
Table B.15 Compressive strength -trial 3 (35% FA-C)	142

Table C.1 Compressive strength –standard cure concrete cylinders-block (control mixture)	143
Table C.2 Compressive strength concrete cylinders-slab (control mixture).....	143
Table C.3 Compressive strength -concrete cylinders-block (35% FA-A).....	143
Table C.4 Compressive strength -concrete cylinders-block (50% FA-A).....	144
Table C.5 Compressive strength -concrete cylinders-slab (50% FA-A)	144
Table C.6 Compressive strength -concrete cylinders-block (35% FA-C)	144
Table D.1 Pullout force on 8 in. cube concrete specimen (control mixture).....	145
Table D.2 Pullout Force on 8in. cube concrete specimen (35% FA-A)	145
Table D.3 Pullout force on 8in. cube concrete specimen (50% FA-A)	146
Table D.4 Pullout force on 8in. cube concrete specimen (35% FA-C)	146
Table D.5 Pullout force on concrete block field-cured (control mixture)	148
Table D.6 Pullout force on concrete slab field-cured (control mixture).....	148
Table D.7 Pullout force on concrete block field-cured (35% FA-A)	148
Table D.8 Pullout Force on concrete block field-cured (50% FA-A).....	149
Table D.9 Pullout force on concrete slab field-cured (50% FA-A).....	149
Table D.10 Pullout force on concrete block field-cured (35% FA-C).....	149
Table E.1 Strength comparison between match cure and predicted strength	158
Table F.1 Strength comparison between various curing condition and predicted strength	165

Chapter 1 Introduction

The 2006 fly ash use survey conducted by the American Coal Ash Association (ACAA, 2006) indicates that 45% of the 72.4 million tons of fly ash produced was beneficially utilized. However, this still results in a majority of the fly ash (55%) to be disposed, typically in landfills. The 2006 survey also indicates that 59% of the beneficially used fly ash was used in cement and concrete applications. Since ready mixed concrete represents the single largest market for fly ash, it can offer the largest potential for increased fly ash utilization. Estimated ready mixed concrete production in the US in 2007 was 415 million cubic yards (NRMCA, 2008)

There is a large body of research and literature on the development and use of High-Volume Fly Ash (HVFA) concrete. In spite of that, the actual use of high-volumes of fly ash (> 30% of total cementitious materials content) in ready mixed concrete is limited. Surveys (PCA, and NRMCA 2000-2003, Obla et. al 2003) suggest that the average fly ash content in all ready mixed concrete is still about 10% (of total cementitious materials content) even though some producers may be using an average fly ash content as high as 30% in summer months and certain applications. To note that when fly ash is used in ready mixed concrete, the reported average according to the survey is actually 20%. Since only about half of all ready mixed concrete contains fly ash (37% contains only Portland cement and the rest contain Portland cement, slag and other supplementary cementitious

material blends, the average fly ash content in all ready mixed concrete effectively drops to 10%. *If the average fly ash content in all ready mixed concrete were increased to 20%, this would increase the overall fly ash utilization from 45% to 71% thereby far exceeding CBRC's 2010 goal of 50% fly ash utilization!* In order to achieve the average of 20% fly ash use in all ready mixed concrete all year around, it may be necessary to use 50% or more fly ash in certain applications. However, many contractors and producers cite the low rate of strength gain and delayed -setting times as the primary reasons for not using higher volumes of fly ash in concrete.

This research addresses one of the two major obstacles on the use of HVFA concrete - rate of strength gain. By using the maturity-based approach, it can be demonstrated that the HVFA concrete in the structural members has sufficient early-age strengths to allow for optimized construction scheduling, such as formwork removal and post-tensioning. The basic approach to this research is the premise that while the strength measured using laboratory or field-cured cylinders of HVFA concrete mixtures are low; the actual strengths in the structural members are likely to be higher. This is because the larger mass of most concrete structural members, compared to cylindrical specimens, allows for greater retention of heat of hydration that allows for a faster rate of strength gain. Essentially, HVFA concrete is penalized when construction operations such as formwork removal are not based on in-place strengths but on tests on field-cured cylinders.

The challenge is then to accurately estimate the concrete strength in the structure. The maturity method can be used for this purpose (Saul 1951, Freiesleben and Pederson 1977, Carino 1984). The in-place strength of concrete in the structure can be estimated by monitoring its temperature history over time, calculating the maturity, and by estimating the in-place strength from the pre-calibrated strength-maturity relationship. The maturity concept assumes that hydraulic cement concrete of the same maturity will have similar strengths, regardless of the combination of time and temperature yielding the maturity. Maturity concepts are well established for Portland cement concretes but have not been validated for HVFA concrete mixtures containing chemical admixtures (Schindler 2004, Carino 2004). The Arrhenius and Nurse-Saul maturity functions are most commonly used to calculate the maturity index. The Arrhenius maturity function is considered more accurate and was used in this research. The Arrhenius maturity function requires the use of mixture-specific activation energy to yield most accurate results. The activation energy quantifies the temperature sensitivity of the concrete mixture (Schindler 2004).

1.1 Research Objectives

The overall research objective was to examine one of the major issues that prevent the widespread application of HVFA concrete, the reduced early-age (less than 7 days) strengths. To deal with this issue, a science-based approach (maturity) was used, to demonstrate that HVFA concrete in the structures has sufficient early-age strengths to allow early form removal. The research identified a step-by-step guideline, which will

help the construction teams to use the maturity method for HVFAC to optimize construction scheduling. Below are the specific research objectives.

1.1.1 Maturity Modeling

1. Verify applicability of existing strength-age modeling for HVFAC mixtures.
2. Develop strength vs. age prediction models for HVFAC mixtures (F and C class fly ash with varying percentage of cement replacement).
3. Determine the effect of curing condition on the hydration rate for strength development.
4. Evaluate activation energy for various fly ash concrete mixes.

1.1.2 Setting Time of Mortar Mixes

1. Evaluate initial and final setting time of HVFA mortar mixes.
2. Compute activation energy using the setting time, which will help to evaluate AE during various hydration phases.
3. Compare activation energy computed from two different approaches (AE from strength-age data and from setting time).

1.1.3 Pullout Load vs. Strength Modeling

1. Develop a relationship between pullout force and compressive strength for these HVFA concrete mixtures.

2. Calibrate strength prediction models with field data on

- a) Concrete block members

- b) Pavement slabs

- 1.1.4 Evaluate Proposed Strength vs. Age Models from Field and Lab Data

1. Evaluate implications of match cure, lab and field cylinder strength prediction.

2. Compare strength gain models from lab and field samples

- 1.1.5 Effects of Different Lab and Field Monitoring Methods on Strength Measurements and Predictions

1. Match Cure Concrete Cylinders

2. Lab/Field Cure Concrete Cylinders

Thus, this research consisted of four different tasks:

The first task was the determination of the activation energy of each of the concrete mixtures using the procedure outlined in ASTM C1074. Various kinds of fly ashes (Class C and Class F fly ash meeting the standard ASTM C618) with multiple dosages (20% to 50% by mass of cementitious materials) were used and the activation energies of the resulting concrete mixtures were evaluated.

The second task was to develop strength-maturity relationships in the laboratory for the concrete mixtures. Ready mixed concrete from a concrete plant was used for this task. Concrete cylinders [10.2 cm x 20.3 cm (4 in. x 8 in.)] were cast and cured in lime-saturated water baths at a temperature of 23.0°C (73°F) and tested in compression at 1, 2, 4, 7, 14, and 28 days. Compressive strengths are plotted as a function of equivalent age at 23.0°C (73°F). The best-fit relationship of this strength versus maturity data is the strength-maturity relationship to be used for estimating in-place strength in the large-scale specimens made with that specific mixture. In addition compressive strength versus pullout load relationships were also developed. Approximately 20.32 cm (8 in.) concrete cubes were cast, with one pullout insert placed on each of the 4 side faces (barring top and bottom) of the cube. Pullout tests were conducted at the same time that cylinder compressive strengths were measured. The resulting data were used to establish the strength-pullout load relationships that was used to confirm the estimated in-place strength estimated from the maturity method.

The third task consisted of field validation where four concrete blocks and two concrete slabs were prepared in the field with multiple embedded temperature sensors during the period of October to December, when the ambient temperature ranged from 15.5°C (60°F) to 7.5°C (45°F). Ready mixed concrete from a concrete plant was used for this task. The temperature sensors inside the blocks and the slabs recorded the temperature as a function of age. Equivalent ages [relative to a reference temperature of 23.0°C (73°F)] can be calculated using the Arrhenius (Equivalent age) maturity function with the mixture-

specific activation energy determined in the previous tasks. From the equivalent ages and the previously established strength-maturity relationships, the in-place strength of the structural members was estimated. Pullout tests (ACI 228, 2003) were performed on the blocks and slabs and the data were analyzed statistically to arrive at reliable estimates of the in-place compressive strength. The match-cured cylinders were cured with a proprietary equipment to follow the temperature of the structural members, and subsequently test to obtain an estimate of the true in-place strength. The pullout tests and match-cured cylinder tests were used to confirm and validate the in-place strength predicted from the maturity method. Additionally, standard lab-cured and field-cured concrete cylinders were tested at specific ages and these strengths were compared to the in-place strengths estimated by the maturity method at those ages.

The fourth task consisted of developing thermal signatures of various HVFA concrete mixtures using Semi-Adiabatic Calorimetry. This portion of the research was conducted at Auburn University using the same materials in the other tasks. The results show the effect of the different fly ash contents on the rate of hydration, total heat of hydration, setting, and to some extent the degree of hydration. These results were useful to understand the heat evolution process of high-volume fly ash concrete mixtures. Additionally, the calorimetry results can also be used as input to simulation programs to estimate the in-place temperature development of concrete structural members with varying dimensions and boundary conditions. The Concrete Works program models the temperature profile in concrete members (see www.texasconcreteworks.com) and can be used to obtain an estimate of in-place temperature profiles and gradients of concrete members. The model

provides a visual 2-D animation temperature profile throughout the element as hydration progresses.

1.2 Description of Contents

This section briefly describe the structure of the dissertation and its content for each chapter.

Chapter 2. Background: This chapter provides a brief history of maturity modeling and the existing models for strength-age relationship of both control mix and high volume fly ash mixtures.

Chapter 3. Experimental Work – Mortar: This chapter describes the types of testing and concepts behind each testing carried out in this research. It also gives details on the types of materials used and the physical and chemical properties of cement, fly ash, aggregates, and chemical admixtures.

Chapter 4. Experimental Work – Concrete: This chapter provides details on the testing and experimental results (lab and field). This chapter unveils the concepts behind the strength-age methodology. It presents an initial evaluation of use of existing strength-age models with the experimental data, and then the development of new strength-age model for HVFA concrete mixtures. This chapter also presents a new approach to estimate activation energies for concrete mixtures.

- Chapter 5. Semi-Adiabatic Calorimetry Testing: This part of the research was done at Auburn University, Alabama with the help of Dr Anton Schindler. Semi adiabatic calorimetry was conducted to estimate activation energies using total hydration rate and degree of hydration.
- Chapter 6. Construction Team Guidelines: This chapter provides systematic guidelines to use the maturity method by the concrete industry for using high volume fly ash concrete. This section was written in cooperation with the NRMCA research team.
- Chapter 7. Conclusions: Summary and conclusion from the research results and outcomes are presented in this chapter.

Chapter 2 Background

Researchers in concrete materials have been using destructive methods to estimate properties of concrete, which helps to draw empirical correlations between different properties of concrete. Researchers have also used non-destructive methods to evaluate properties of concrete. One of the non-destructive testing methods to evaluate the in-place compressive strength of concrete is the maturity method described in ASTM C1074 (2004). The maturity method uses the hydration temperature-time profile over time to predict the compressive strength of concrete element for early ages (7 to 14 days), which can be further extended to determine long-term strength gain. The following sections will briefly discuss the strength vs. age and maturity modeling, and the use of maturity modeling for high volume fly ash concrete.

2.1 Strength-age Model

Bernhardt (1956) proposed a function for concrete strength gain as a function of temperature, Equation 1, which states, “The rate of strength gain at any time is a function of the current strength and the curing temperature.”

$$\frac{ds}{dt} = f(S) \times k(T)$$

Equation 1

where (ds/dt) = rate of strength gain at any age

$f(S)$ = function of strength

$k(T)$ = function of temperature

The author also suggested that compressive strength of a concrete mix at any age is a function of the limiting strength of that concrete mix and the rate constant. Rate constant affects the initial strength gain of concrete mixes. This can be mathematically written as Equation 2. The limiting Strength (S_u) is assumed independent of the curing temperature.

$$\left. \frac{dS}{dt} \right|_{s=0} = S_u K(T) \quad \text{Equation 2}$$

where: S_u = limiting strength (psi)

$K(T)$ = rate constant

Bergstrom (1953) summarized the maturity concept based on the Nurse-Saul maturity method, in which maturity is expressed as a product of temperature and time. It was concluded from the author that curing temperature and percentage of cement content have noteworthy effects on the strength gain of concrete. It was also concluded that the initial curing temperature of concrete has a significant effect on the later age strength of concrete.

Carino (1984) has successfully used the following hyperbolic Equation 3 for strength gain under isothermal curing up to equivalent ages of about 28 days at 22.8°C (73°F):

$$S(t) = S_u \frac{k(t) \times (t - t_o)}{1 + k(t) \times (t - t_o)} \quad \text{Equation 3}$$

where: $S(t)$ = compressive strength at time t ,

$K(T)$ = initial slope of age strength plot as a function of time,

t_o = time at which strength development begins,

S_u = ultimate compressive strength

2.2 Maturity Concept

It has been well-documented (Nurse 1949, Saul 1951, Carino 1991) that the strength of well-cured and consolidated concrete is a function of its age and curing temperature. The effects of time and temperature can be combined into one constant, called maturity, which is indicative of the concrete strength. In 1951, Saul concluded that the maturity concept could be effectively used to define the strength development of a concrete cured at any temperature above the datum temperature. Equation 4, commonly referred as Nurse-Saul function, is a simple mathematical function to define maturity with respect to a datum temperature. Datum temperature (T_o) be the lowest temperature at which strength gain in concrete is observed. Generally the value of the datum temperature is taken as -10°C (14°F), but for more precision it should be established for a particular concrete mixture. Equation 4 is used to convert the actual time temperature history to a maturity index also called the “Time Temperature Factor” (TTF). Saul (1951) presented the following principle, known as the maturity rule:

“Concrete of the same mix at the same maturity has approximately the same strength whatever combination of the temperature and time go to make up the maturity.”

$$M = \sum_0^t (T - T_o) \Delta t$$

Equation 4

where: M = maturity index, °C-hours (or °C-days),

T = average concrete temperature, °C, during the time interval Δt ,

T_o = datum temperature (usually taken to be -10 °C),

t = elapsed time (hours or days), and

Δt = time interval (hours or days).

The Nurse-Saul maturity function has gained widespread acceptance in the concrete industry, because of its simplicity in combining the effects of time and temperature to estimate strength development of hydraulic cement concrete. Apart from its simplicity the Nurse-Saul maturity has few drawbacks (Carino 2004); it is only valid provided the concrete temperature did not reach about 50°C (122°F) within 2 hours or about 100°C (212°F) within the first 6 hours after the concrete is mixed. The major deficiency of the Nurse-Saul maturity function is that the rate of strength gain is assumed a linear function of curing temperature, which has been shown to be invalid for a wide range of temperature (Carino 2004). Therefore, the Nurse-Saul maturity function can overestimate or underestimate the effect of temperature on the rate of strength gain.

Since the first breakthrough in maturity concepts, many other maturity functions have been developed and proposed. Freiesleben Hansen and Pedersen (1977) suggested another maturity function based on the concept of Arrhenius equation. The Arrhenius equation defines the chemical reaction between two reactants and is a function of activation energy and the reaction temperature. The activation energy is defined as the minimum energy necessary for a specific chemical reaction to occur. The Arrhenius approach is a sounder technical basis and experimental studies conducted have confirmed that it captures the time-temperature dependence of concrete more appropriately (Carino 2004).

Equation 5 represents the Arrhenius maturity function that can be used to compute the maturity index in terms of an equivalent age. Equivalent age represents the duration of the curing period at the reference temperature that would result in the same maturity when the concrete is cured at any other temperature. The exponential part of the Equation is an age conversion factor used to convert the actual temperature history to the temperature history at the reference temperature. The reference temperature values that have been used in Europe and the U.S. are 20°C (68°F) and 23°C (73°F), respectively.

$$t_e = \sum_0^t e^{\frac{-E}{R} \left(\frac{1}{T} - \frac{1}{T_r} \right)} \times \Delta t \quad \text{Equation 5}$$

where: t_e = the equivalent age at the reference temperature (hours),

E = apparent activation energy (J/mol),

R = universal gas constant (8.314 J/mol-K),

T = average absolute temperature of the concrete during interval Δt ,
(Kelvin),

T_r = absolute reference temperature, (Kelvin).

Δt = time interval (hours or days).

Much like the datum temperature in the Nurse-Saul approach, the activation energy is mixture specific and has to be established for a specific concrete mixture prior to using the Arrhenius maturity function for estimating in-place strengths. The equivalent age, maturity function, was opted in this research because it better captures the non-linear effect of temperature on the rate of strength development (Carino 2004).

ASTM C1074 provides procedures for both the Nurse-Saul and the Arrhenius approaches for computing the maturity index from the measured temperature history of the concrete. It also provides a technique for calculating the datum temperature as well as the activation energy from strength development data collected at various isothermal temperatures. Strength predictions using the maturity method should be validated by other in-place tests that measure the in-place compressive strength (Carino 2004). In this research pullout tests, (ASTM C900) and match-cured cylinder tests were conducted as the validation methods. (Upadhyaya et al. 2007).

2.3 Pullout Test

Pullout test is a non-destructive test method used to measure the pullout force required to displace a metal insert from a concrete structure (ASTM C900). The probe has an enlarged

head of, 2.54 cm (1 in.) diameter and is placed at a depth of 2.54 cm (1 in.) from the surface of the concrete specimen. The probe is pulled against a 5.5 cm (2.16 in.) diameter counter pressure disc applied on the surface as shown in Figure 2.1. A compression strut develops in the concrete between the enlarged head and the counter pressure disc during the process. A correlation is established between measured pullout force and compressive strength of cylindrical specimens in laboratory. The correlation is used to estimate the in-place concrete strength from the results of the pullout test. Pullout force can also be correlated to different uniaxial strength properties of concrete.

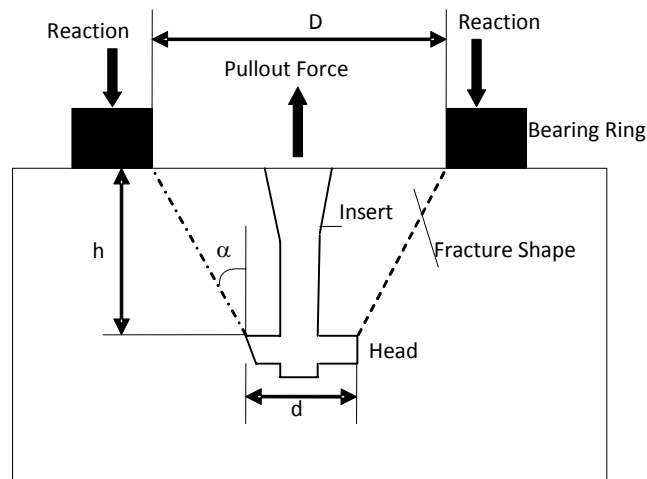


Figure 2.1 Pullout setup (Carino 2004)

2.4 Match Curing

It is well known that for members of larger mass the rate of hydration of concrete will be accelerated due to higher in-place temperatures, which will also lead to accelerated rate of in-place strength development. Field-cured cylinders do not provide reliable estimates of

the in-place compressive strength because of the mass effect. Match curing is therefore used to match the temperature curing history of molded cylinders to that of the in-place structural concrete member. The match curing system used in this research was called “Sure Cure”. The Sure Cure system consists of a micro-controller, the match cure cylinders and a Type-T thermocouple. The micro controller uses software that controls the temperature of the cylinders in the molds based on the temperature in the structure measured by the thermocouple. Thus, the concrete cylinders in the match cure molds experience the same temperature history as that of the structural member.

2.5 Pushout Cylinders

Pushout cylinder is a method that allows one to cure a molded cylinder in-place (ASTM C873), and they are pushed out of concrete element and tested in a compression testing machine. In-place cylinders are placed within the concrete structure to make sure they experience the same temperature and curing conditions as the structure. However, in some cases, these cylinders do not experience the same temperature history as the structure. In this research, a 15.24 cm (6 in.) diameter plastic mold was installed in the slab form work before the concrete pour. After the concrete was poured in the slab, 10.16 cm (4 in.) diameter concrete specimens were prepared in the plastic molds and kept in these 15.24 cm (6 in.) molds casted within the slab. The area between the 15.24 cm (6 in.) and 10.16 cm (4 in.) mold was filled with fine sand to allow some heat transfer between the slab and concrete cylinders. Push out were only used for 50% FA-A mixture slab because of the logistics.

2.6 Literature Review of HVFAC

Pinto and Hover (1999) conducted a study for estimating activation energy of a concrete mix based on the setting time approach. The study included 36 samples of control mix cured at five different temperatures. The setting time was measured in accordance to ASTM C403, and the analysis concluded that the apparent activation energy estimated with the setting time method is comparable to the activation energy values obtained from ASTM C1074 .

Brooks (2002) also developed a model to predict initial setting time of concrete based on theoretical initial spacing between the particles of unhydrated cementitious materials and rate growth of hydration products. The developed model was a function of water cement ratio, particle size distribution, temperature, specific gravity and chemical composition of the mixture. The basic assumption made by the author was that the initial setting time of a concrete (T_{IS}) is proportional to the ratio of the distance between unhydrated cement particles and the rate constant (k). Afterwards, a model was developed to predict initial setting time of cement pastes, Equation 6, incorporating, surface area of cement (S_c), specific gravity of cement (γ_c), rate constant (k) and water to cement ratio (w/c).

$$T_{IS} = \frac{3}{k\gamma_c S_c} \left[1.613 \left(1 + \gamma_c \frac{w}{c} \right)^{\frac{1}{3}} - 1 \right] \quad \text{Equation 6}$$

Atiş (2002) conducted a laboratory study to determine the heat development of HVFA concrete. Cement was replaced by 50 to 70% of low calcium fly ash (CaO=2.55%). A high range water reducer (Sikament 10) was used to maintain the workability of concrete. The author showed that the concrete with similar proportions would have same temperature rise regardless the use of super plasticizer. It was also concluded from the study that the increase in percentage of fly ash in concrete reduce significantly the amount of peak temperature compared to a “straight” Portland cement mix.

In 2003, Hun-Han et.al (2003) conducted a research to predict fly ash concrete compressive strength using apparent activation energy. A class F fly ash (CaO=3.6%) was used as a cement replacement (type II cement) ranging from 10 to 30% with varying water to cement ratio between 0.27-0.60. The research examined the long-term strength gain of fly ash concrete. One of the important findings was that the crossover effect for fly ash concrete was delayed with increasing fly ash content. In most of the cases, the crossover effect was observed at about 30 days of curing. This paper also summarized the activation energy for varying concrete mixtures; the results were quite interesting showing increase in activation energy with increase in fly ash content, which is noteworthy.

Maltais and Marchand (1997) investigated the effects of curing temperature [20°C (68°F) and 40°C (104°F)] on the cement hydration and compressive strength of fly ash mortar mixtures. Two kind of Class F fly ash (Cao = 7.32% and 18.10%) with varying percentage (10-30%) was used for the research. Compressive strength results show an interesting trend in strength gain for various concrete mixtures. Fly ash replacement of 10% of

cement showed a crossover effect at around 28 days of curing. Samples cured at higher temperature started to have lower strength compared to sample cured at lower temperature. On the contrary, 20% and 30% fly ash replacement do not show any crossover effect, and higher temperature tend to have higher strength till 72 days of curing. Important fact that is presented in the paper is for class F fly ash mixtures, the fly ash does not react before at least 28 days of curing.

Yazıcı et.al (2005) conducted an experimental research to see the effect of steam curing on the strength gain of high volume fly ash concrete made up with class C fly ash with 10-70% cement replacement. The authors showed that strength gain in HVFAC at 1 day for steam curing is higher compared to standard curing, and lower long-term strength for steam curing specimens.

Papayianni and Valliasis (2005) in their study used lignite fly ash (LFA) and ground fly ash (GFA). Lignite fly ash (LFA) had a CaO content of 36.70%. The research showed that the concrete containing fly ash is more sensitive to heating, and that the finesses of fly ash influence the degree of hydration..

Zang et.al. (1997) did a laboratory study to show the effects of high volume fly ash concrete on mechanical properties of concrete. In this study, cement replacement was about 50 to 60% with class C fly ash. The result showed that the high calcium fly ash concrete was increasing the compressive strength of concrete.

A laboratory investigation by McCarthy and Dhir (2005) showed that the compressive strength of high volume fly ash concrete mixtures have comparable strength to Portland cement mixtures. Their study also incorporated results of fresh concrete properties, strength, and durability assessment. It was reported, that both HVFA concrete and Portland cement concrete had comparable properties.

Chapter 3 Experimental Work – Mortar

Activation Energy is a key parameter for the equivalent age maturity model. To evaluate this parameter mortar testing was conducted. ASTM C1074 recommends preparation of 5.08 cm (2 in.) mortar cubes for evaluation of datum temperature and activation energy.

3.1 Materials

The following materials were used in the research for the mortar preparation at the NRMCA research laboratory

ASTM C150 Type I Portland cement, Lot# 8124

ASTM C618 Class C and Class F Fly Ash, Lot# 8125, Lot #8126

ASTM C33 Natural Sand, Lot # 8127

ASTM C33 No. 57 Crushed Limestone Coarse Aggregate, Lot #7998

ASTM C494/C494M: Polycarboxylate based Type F High Range Water Reducer, Lot # 8128

Table 3.1 lists the chemical properties of various cementitious materials used in this research. Fly ashes were selected that varied in terms of the percentage of the CaO content. The range of CaO was representative of that found in fly ash across the United States. The following three fly ashes were used:

1. Class F fly ash with a CaO content of 1.0%, identified as FA-A in this study,
2. Class F fly ash with a CaO content of 13.3%, identified as FA-B in this study, and

3. Class C fly ash with a CaO content of 23.44%, identified as FA-C in this study.

The following sources of fly ash and high-range water-reducing (HRWR) admixture were used:

- i) FA-A was supplied by STI, Baltimore, MD,
- ii) FA-B and FA-C were obtained by Boral Material Technologies Inc., and
- iii) HRWR admixture, (ViscoCrete 2100) supplied by Sika Corporation.

Table 3.2 includes the measured physical properties of the fine and coarse aggregates, The relative density (specific gravity), and absorption of coarse and fine aggregates were measured by ASTM C127 and ASTM C128 respectively; sieve analysis of both aggregates was measured by ASTM C136; bulk density (dry rodded unit weight) of coarse aggregate was measured by ASTM C29/C29M

Table 3.1 Chemical and physical properties of cement and fly ash (ASTM C 150, ASTM C618)

Item	Cement	FA-A	FA-B	FA-C
Silicon dioxide (SiO ₂), %	20.50	59.40	55.58	38.48
Aluminium dioxide (Al ₂ O ₃), %	5.00	30.30	18.96	20.64
Iron Oxide (Fe ₂ O ₃), %	3.30	2.80	4.52	5.46
Sum of SiO ₂ , Al ₂ O ₃ , Fe ₂ O ₃ , %	28.80	92.50	79.06	64.58
Calcium Oxide (CaO), %	62.70	1.00	13.29	23.44
Magnesium (MgO), %	3.80	-	3.01	4.10
Sulfur trioxide (SO ₃), %	2.90	0.10	0.53	1.69
Potassium Oxide (K ₂ O), %	-	0.64	0.83	0.61
Loss of Ignition, %	0.85	1.30	0.22	0.27
Insoluble Residue, %	0.29	-	-	-
Fineness 45mm sieve, % retained	8.2	26.40	23.75	10.75
Blaine (Specific Surface) m ² /kg	368	-	-	-
Specific Gravity	3.15	-	2.47	2.61
Setting Time-Vicat Initial (minutes)	130	-	-	-
Air Content %	7.50	-	-	-
Compressive strength, 3 days, psi	3790	-	-	-
Compressive strength, 7 days, psi	4910	-	-	-
Strength Activity Index with Portland Cement at 7 days, % Control	-	77.30	84.90	88.60
Strength Activity Index with Portland Cement at 28 days, % Control	-	78.30	84.10	94.60
Water Required, % Control	-	98.30	95.00	91.70
Autoclave Expansion %	0.14	-0.04	-0.01	-0.01
Available Alkali (as Na ₂ O), %	0.55	0.50	0.86	1.95
Tricalcium Silicate (C ₃ S), %	53.0%	-	-	-
Tricalcium Aluminate (C ₃ A), %	8.0%	-	-	-

Table 3.2 Gradation and properties of aggregates (ASTM C 136)

Sieve Sizes	Percentage Passing	
	Coarse Aggregate	Fine Aggregate
	No.57	-
1 ½	100.0	0.0
1	100.0	0.0
¾	92.0	0.0
½	49.0	0.0
3/8	28.0	100.0
No. 4	5.0	99.0
No. 8	1.0	84.0
No. 16	0.0	70.0
No. 30	0.0	52.0
No. 50	0.0	20.0
No. 100	0.0	3.0
No. 200	1.0	-
Fineness Modulus	-	2.73
Specific Gravity(SSD)	2.84	2.59
Absorption, %	0.3	1.3
Dry rodded unit weight, lb/ft ³	105.9	N/A

3.2 Mixing Mortar

ASTM C1074 recommends preparation of 5.08 cm (2 in.) mortar cubes for evaluation of datum temperature and activation energy. Four different temperatures (7.5°C (45°F), 21.0°C (70°F), 38.0°C (100°F), and 49.0°C (120°F)) were selected for mixing and curing the mortar cubes. Prior to batching, all the materials (cement, fly ash, fine aggregates, HRWR, and water) were preconditioned at their respective temperature, to assure that the mortars were maintained as close as possible to the desired curing temperature. Mortar mixtures were proportioned to match specific concrete mixtures according to ASTM C1074 Annex A1.

3.3 Mortar Testing

3.3.1 Fresh Mortar Tests

These tests were done for all the batches and curing conditions. Fresh mortar tests were conducted in accordance to the following ASTM Standards,

ASTM C1437: Flow test,

ASTM C185: Air content and density

ASTM C403/C403M Setting time by penetration resistance

For determination of setting time, mortar specimens were prepared and casted as specified in ASTM C403/C403M. After casting, specimens were submerged in water baths as recommended by ASTM C1074 Annex A1. The specimens were carefully removed from the water bath and excess water was removed before making the penetration measurements on the specimen in accordance to ASTM C403/C403M.

3.3.2 Hardened Mortar Tests

The primary objective of this portion of the research was to determine the activation energy of mixtures based on the type and quantity of fly ash. ASTM C1074 Annex A1 mentions that the activation energy can be obtained by analyzing compressive strength data obtained from 5.08 cm (2 in.) mortar cubes and the results are applicable to the concrete. Around 1000 5.08 cm (2 in.) mortar cubes were prepared and tested in

compression to consider all possible combinations of mixtures, testing temperatures and hydration ages included in this study. As per ASTM C1074, mortar cubes were molded and tested in compression in accordance with ASTM C109/C109M. Cube specimens were cured at four different isothermal curing conditions [7.5°C (45°F), 21.0°C (70°F), 38.0°C (100°F), and 49.0°C (120°F)]. For each batch, 20 mortar cubes were prepared and tested at six different ages. For each testing age three 5.08 cm (2-in.) mortar cubes were tested and the average value was recorded for the analysis. These cubes were tested in a 1334 kN (300-kip) capacity compression testing machine, which was setup at a maximum load range of 133 kN (30-kip) for compression testing.

After molding, the 5.08 (2-in.) mortar cubes were submerged in lime-saturated water baths maintained at the specified curing temperatures. Temperature sensors (iButton®), Figure 3.1, were cast in the center of two mortar cube for each condition during molding to record the temperature during the curing process. A wire was soldered at both ends of an iButton® to allow for interface with a computer using a RJ-11 connector, and coated with plastic dip to protect it from moisture. The iButton has an internal data logger, and information is transferred between the iButton and a PC with the program “One-wire Viewer.” The average temperature of two cubes was reported. These mortar cubes were not tested for strength.



Figure 3.1 Temperature sensor (iButton®)

3.4 Mixture Proportions

Six mortar mixtures were prepared. The mortar mixtures were proportioned so that the fine aggregate-to-cementitious materials ratio (by mass) is the same as the coarse aggregate-to-cementitious materials ratio of the concrete mixtures under investigation. This is consistent with the recommendations in Annex A1 of C1074. The concrete mixture proportions are provided in Table A.1 of Appendix A. Table 3.3 summarizes the mortar mixture proportions that correspond to the yield-adjusted concrete mixture proportions of Table A.1 of Appendix A (In this research the concrete testing was conducted prior to the mortar testing and therefore the yield-adjusted concrete mixture proportions were used to prepare the mortar mixtures).

Table 3.3 Mortar mixture proportions [5.08 cm (2-inch) cubes –ASTM C1074]

Item	Control Mixture	20% FA-A	35% FA-C	35% FA-B	35% FA-A	50% FA-A
Cement, gram (lb)	1876 (4.14)	1551 (3.42)	1357 (2.99)	1371 (3.02)	1199 (2.64)	1101 (2.43)
Fly Ash, gram (lb)	0.0	388 (0.85)	740 (1.63)	739 (1.63)	710 (1.57)	1066 (2.35)
Fine Aggregate, gram (lb)	7136 (15.73)	7110 (15.68)	7250 (16.00)	7185 (15.96)	7087 (15.77)	7036 (15.70)
Water, gram (lb)	1052 (2.53)	988 (2.38)	889 (2.15)	894 (2.05)	960 (2.17)	848 (1.89)
HRWR Admixture, ml (oz/cwt)	62.90 (2.1)	89.85 (3)	152.75 (5.1)	149.75 (5)	200.67 (6.7)	212.64 (7.1)
w/cm	0.56	0.51	0.42	0.43	0.51	0.39

Multiple trials were made for some of the mixtures because of unusual behavior in the measured compressive strength results of mortar cubes for those mixtures. Table 3.4 tabulates the list of trials and curing temperatures for those trials. Some of the trials were repeated for only two temperatures as indicated in Table 3.4. As described in ASTM C1074, at least three curing temperatures are needed to determine the activation energy (AE). Two approaches were used to group the data together to quantify AE values for mixtures as described below.

1. For the trial for which strength versus age data was not available at three temperatures, data from the other trials were used for the third temperature. For example: Mixture 50% FA-A Trial 3 has two curing temperatures and results for curing at a third temperature was not available, so data from Trial 2 was used to obtain at least three temperatures. These AE values are termed as “individual” AE values later in the report. For each trial, one AE value is reported. Example: control mix will have two AE values, one for each trial.

2. All the computed rate constants were grouped together for one particular mixture irrespective of which trial it belonged to and one AE value was calculated. These AE values are termed as “combined” AE values.

Table 3.4 Curing temperatures used for multiple trials

Mixture	Trial	Curing Temperature			
		7.5°C (45°F)	21.0°C (70°F)	38.0°C (100°F)	49.0°C (120°F)
Control	1	X	X	X	X
	2	X	X		X
20% FA-A	1	X	X	X	X
35% FA-A	1	X	X	X	X
	2	X	X		X
	3		X		X
50% FA-A	1	X	X	X	X
	2	X	X		X
	3		X		X
	4		X		X
35% FA-B	1	X	X	X	X
	2		X		X
35% FA-C	1	X	X	X	X
	2		X		X
	3		X		X

Note: X denotes the temperatures at which compressive testing was performed

3.5 Discussion of Test Results

3.5.1 Fresh Mortar Properties

Table 3.5 summarises the average recorded curing temperature for mortar cubes. Trials are marked as Trial 1 to Trail 4 depending on the number of trials for each mixture, as defined in. It can be observed that the isothermal conditions are closely matched for the 4

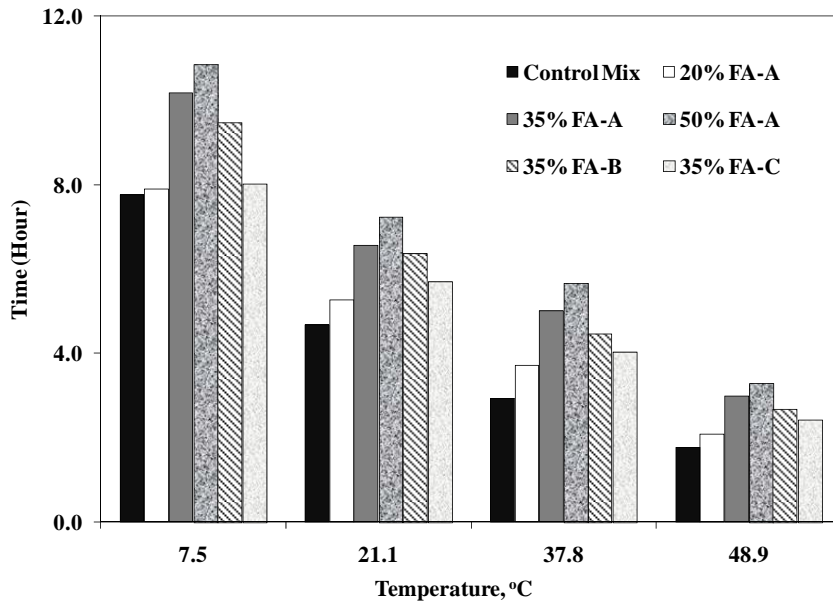
different curing conditions. Table 3.6 presents the initial and final setting times for the six mortar mixtures and these data are graphically presented in Figure 3.2. As expected, the figure clearly shows that the setting times decrease as the curing temperature increases for all the mixtures.

Table 3.5 Average curing temperature for mortar cubes

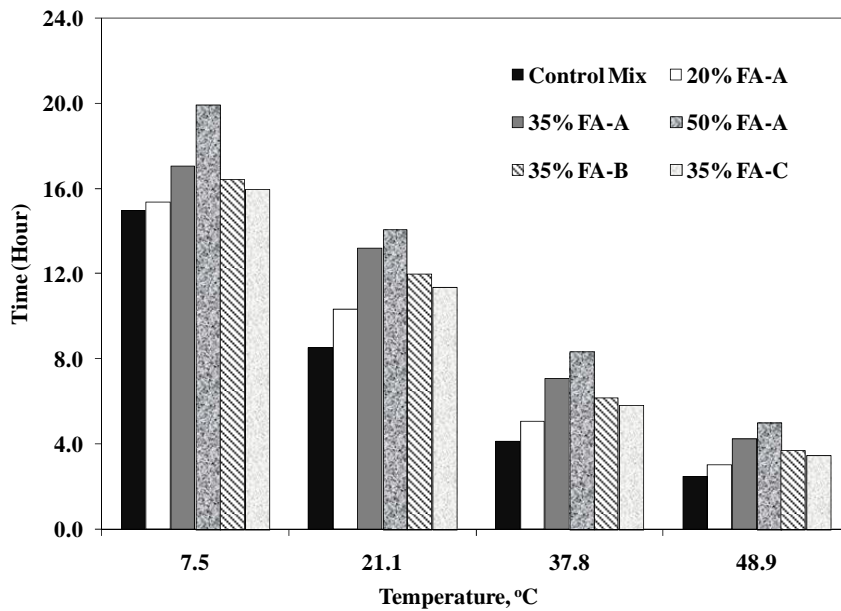
Mixture	Trial	Curing Temperature			
		7.5°C (45°F)	21.0°C (70°F)	38.0°C (100°F)	49.0°C (120°F)
Control	1	6.2 (43.2)	22.2 (72.0)	37.4 (99.3)	49.6 (121.2)
	2	6.3 (43.3)	24.0 (75.2)		49.6 (121.3)
20% FA-A	1	6.8 (44.3)	22.5 (72.5)	37.4 (99.4)	49.6 (121.2)
35% FA-A	1	6.8 (44.2)	22.2 (72.0)	36.3 (97.4)	48.9 (120.1)
	2	7.9 (46.2)	23.0 (73.4)		47.9 (118.2)
	3		21.8 (71.2)		49.7 (121.5)
50% FA-A	1	6.8 (44.3)	21.9 (71.4)	37.0 (98.6)	49.0 (120.2)
	2	5.9 (42.6)	24.2 (75.5)		50.0 (122.0)
	3		22.0 (71.6)		49.2 (120.6)
	4		21.7 (70.1)		49.4 (121.0)
35% FA-B	1	6 (42.8)	22.8 (72.1)	37.7 (99.8)	49.1 (120.3)
	2		23.7 (74.6)		48.3 (118.9)
35% FA-C	1	7.2 (45.0)	22.7 (72.9)	37.4 (99.3)	49.5 (121.1)
	2		23.8 (74.9)		48.6 (119.4)
	3		21.1 (70.0)		48.0 (118.4)

Table 3.6 Setting times for mortar mixtures (ASTM C403)

Mixture	Setting Time (hours)							
	T _c = 7.5°C (45°F)		T _c = 21.0°C (70°F)		T _c = 38°C (100°F)		T _c = 49.0°C (120°F)	
	Initial	Final	Initial	Final	Initial	Final	Initial	Final
Control Mixture	7.8	15.0	4.7	8.5	2.9	4.1	1.8	2.5
35%FA-C	8.0	16.0	5.7	11.4	4.1	5.9	2.4	3.5
35%FA-B	9.5	16.4	6.4	12.0	4.5	6.2	2.7	3.7
20% FA-A	7.9	15.4	5.3	10.4	3.7	5.1	2.1	3.0
35% FA-A	10.2	17.1	6.6	13.2	5.0	7.1	3.0	4.2
50% FA-A	10.9	19.9	7.3	14.1	5.7	8.4	3.3	5.0



(a-Initial setting time)



(b-Final Setting time)

Figure 3.2 Setting times of mortar mixtures

Table 3.7 to Table 3.10 present the flow results for the various mortar mixtures. It can be generally observed that the flow of the mixtures decreases as the mixing temperatures increase. At the higher temperature, the hydration reaction is faster compared to mixtures mixed at lower temperature, which means the free water will be bound faster and cause the workability of these mixtures to decrease.

Table 3.7 Flow results for mortar mixtures-trial I (ASTM C1437)

Mixture	Flow(%) - Trial I			
	T _c = 7.5°C (45°F)	T _c = 21.0°C (70°F)	T _c = 38°C (100°F)	T _c = 49.0°C (120°F)
Control Mixture	108	102	80	81
35%FA-C	100	96	112	109
35%FA-B	100	99	101	102
20% FA-A	102	98	99	98
35% FA-A	106	109	105	111
50% FA-A	100	103	101	101

Table 3.8 Flow results for mortar mixtures-trial II (ASTM C1437)

Mixture	Flow-Trial (%) II		
	T _c = 7.5°C (45°F)	T _c = 21.0°C (70°F)	T _c = 49.0°C (120°F)
Control Mixture	112.5	108	81
35%FA-C	-	113	92
35%FA-B	-	113.5	102
20% FA-A	-	-	-
35% FA-A	120	113.5	107.5
50% FA-A	119.5	102	98.5

Table 3.9 Flow results for mortar mixtures-trial III (ASTM C1437)

Mixture	Flow-Trial (%) III	
	T_c = 21.0°C (70°F)	T_c = 49.0°C (120°F)
35%FA-C	112	93
35% FA-A	111.5	105.5
50% FA-A	106	96.5

Table 3.10 Flow results for mortar mixtures-trial IV (ASTM C1437)

Mixture	Flow-Trial (%) IV	
	T_c = 21.0°C (70°F)	T_c = 49.0°C (120°F)
50% FA-A	104.5	99.0

The air content and density results for all trials are presented from Table 3.11 to Table 3.13. The interpretation of the tables shows that the density values of the mixtures increase as the mixing temperature increases and vice versa for the air content. At higher temperatures, air voids are less stable and hence the total air content values are expected to be slightly lower. Note that a 2% reduction in air in the mortar translates to about 1% reduction in air content for the concrete mixture.

Table 3.11 Air content and density for mortar mixtures-trial II (ASTM C185)

Mixture	Trial II					
	T _c = 7.5°C (45°F)		T _c = 21.0°C (70°F)		T _c = 49.0°C (120°F)	
	Density g/mL (lb/ft ³)	Air (%)	Density g/mL (lb/ft ³)	Air (%)	Density g/mL (lb/ft ³)	Air (%)
Control Mixture	131.1 (2.10)	6.99	131.7 (2.11)	6.76	132.3 (2.12)	5.93
35%FA-C	-	-	131.7 (2.11)	8.16	134.2 (2.15)	6.28
35%FA-B	-	-	131.1 (2.10)	8.78	134.2 (2.15)	6.13
20% FA-A	-	-	-	-	-	-
35% FA-A	128.0 (2.05)	8.49	129.9 (2.08)	7.78	130.8 (2.09)	6.49
50% FA-A	129.9 (2.08)	7.98	129.9 (2.08)	7.85	134.8 (2.16)	4.39

Table 3.12 Air content and density for mortar mixtures-trial III (ASTM C185)

Mixture	Trial III			
	T _c = 49.0°C (120°F)		T _c = 49.0°C (120°F)	
	Density g/mL (lb/ft ³)	Air (%)	Density g/mL (lb/ft ³)	Air (%)
35%FA-C	144.2 (2.31)	8.68	149.8 (2.40)	6.57
35% FA-A	131.1 (2.10)	8.10	144.8 (2.32)	6.63
50% FA-A	134.8 (2.16)	7.65	137.3 (2.20)	4.96

Table 3.13 Air content and density for mortar mixtures-trial IV (ASTM C185)

Mixture	Trial IV			
	T _c = 49.0°C (120°F)		T _c = 49.0°C (120°F)	
	Density (g/mL)	Air (%)	Density (g/mL)	Air (%)
50% FA-A	138.0 (2.21)	8.10	149.8 (2.40)	4.42

3.5.2. Compressive Strength

At each testing age the maturity was established based on the temperature history recorded by the temperature sensors. The testing ages of the cubes were selected based on the measured final setting time obtained for each specific mixtures. The first test age was selected such that the compressive strength of the mortar cubes was around 1.4 MPa-2.8 MPa (200 psi -400 psi). It was important to capture the strength development of the mixtures at early ages. After the age of the first test was obtained, subsequent tests were performed at twice the testing age of the previous test. The last testing age was selected to correspond to an equivalent age of 28 days at the reference curing temperature of 23°C (73°F) and was calculated by assuming an activation energy value. For example: for 49.0°C (120°F) curing temperature the last testing age was around 7 days, which corresponds to an equivalent age of 28 days at 23°C (73°F).

The average compressive strength values of 5.08 cm (2-in.) mortar cubes are reported in Appendix B from Table B.1 to Table B.15. These results include the test results obtained for all six mixtures cured at the four different isothermal curing temperatures of [7.5°C (45°F), 21.0°C (70°F), 38.0°C (100°F), and 49.0°C (120°F)]. From the results, it is observed that at elevated temperatures mortar cubes showed higher compressive strength at later ages compared to mortar cubes cured at lower temperatures, which is an unexpected behavior for cementitious mixtures. Figure 3.3 and Figure 3.4 show such behavior for the 35% FA-A mixture and 35% FA-C respectively. Carino (2004) describes

that concrete mixtures cured at elevated temperatures will have lower strength at later ages compared to the specimens cured at lower temperatures. This unexpected behavior was the reason for conducting several testing trials in order to verify this trend.

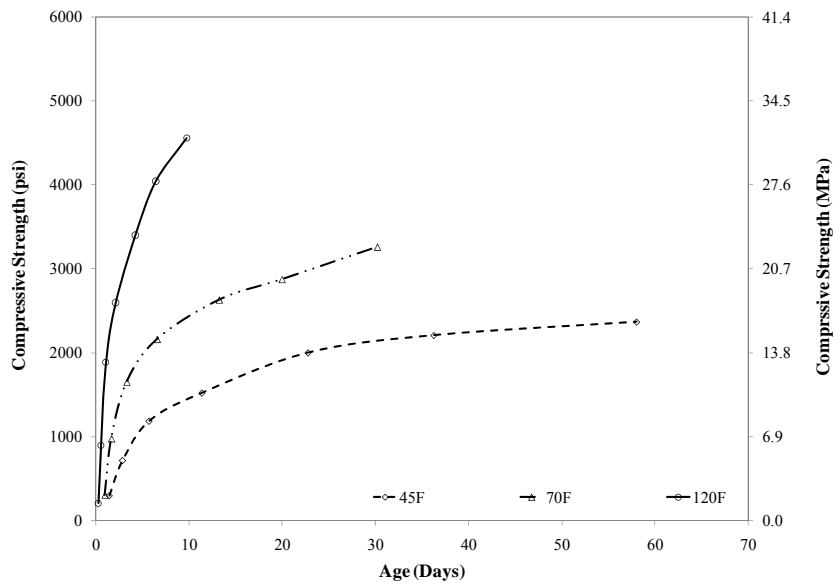


Figure 3.3 Compressive strength vs. actual age (35% FA-A mixture)

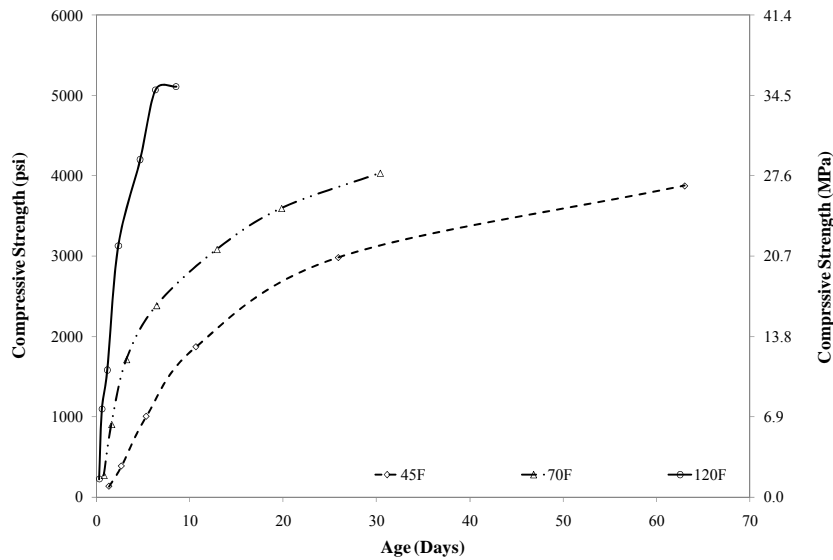


Figure 3.4 Compressive strength vs. actual age (35% FA-C mixture)

3.5.3. Calculation of Activation Energy

In order to calculate the activation energy values, the natural logarithms of rate constant values are plotted as a function of reciprocal of absolute temperature (curing temperature in Kelvin). The best-fit straight line is determined. The activation energy is the negative value of the slope divided by the universal gas constant. More details on how to calculate the activation energy is in ASTM C1074 Annex A1.

Activation energy (AE) was determined using strength-age data for the various mixtures. After the strength data for various mixtures were obtained, strength was plotted as a function of curing age for each curing temperature. In ASTM C1074, a hyperbolic model,

Equation 7, is suggested to characterize the compressive strength-age relationship. In this approach, t_0 was substituted with the final setting time measured for each batch of mortar:

$$S(t) = S_u(t) \frac{k(T) \times (t - t_{fs})}{1 + k(T) \times (t - t_{fs})} \quad \text{Equation 7}$$

where: $S(t)$ = compressive strength MPa (psi),
 $S_u(t)$ = limiting strength MPa (psi),
 $k(T)$ = rate constant (1/days),
 t = testing age (days), and
 t_{fs} = final setting time (days).

Least square regression analysis was used to determine the best-fit values for S_u , and $k(T)$. Table 3.14 summarizes the computed rate constants for the various trials and curing temperatures. Figure 3.5 to Figure 3.10 shows the graphical representation of rate constant versus curing temperature for all the mixtures and trials. The continuous line in each plot is the best fit curve for rate constant versus curing temperature from which the activation energy is calculated. The correlation coefficient (R^2) values are reasonably good with the exception for two mixtures that had R^2 values of 0.71 (35% FA-C), and 0.61 (35% FA-A). This suggests that the reaction rate for these mixtures may not fit Arrhenius theory, and a modified approach might be needed to capture this unusual effect for high-volume fly ash concrete. Figure 3.11 to Figure 3.16 illustrates the Arrhenius plots for all the mixtures and trials, from the figures it can be concluded that, the Arrhenius plot captures the

temperature sensitivity of all the mixes well. Within the same mixtures, variability can be observed in the plot for various trials. The reason for this is that, the reaction rate at early age is highly sensitive to initial curing temperature, a small variation in curing temperatures affects the strength of the mortar cubes at initial ages, which is reflected in the rate of reaction and temperature plot. Table 3.15 presents the computed apparent activation energy (AE) values for the various mixtures. The activation energies are summarized considering the data from each “individual” trial, as well as using the “combined” results of all trials. For the in-place strength estimation the activation energy of combined trials has been used as it is considered more accurate.

Table 3.14 Best fit regression constants

Mixture	Trial	Curing Temperature							
		7.5°C (45°F)		21.0°C (70°F)		38.0°C (100°F)		49.0°C (120 °F)	
		S _u MPa (psi)	k _t (day ⁻¹)	S _u MPa (psi)	k _t (day ⁻¹)	S _u MPa (psi)	k _t (day ⁻¹)	S _u MPa (psi)	k _t (day ⁻¹)
Control	1	29.9 (4329)	0.240	33.0 (4778)	0.636	31.2 (4517)	1.539	27.1 (3933)	2.450
	2	32.2 (4669)	0.203	29.1 (4216)	0.648			26.0 (3777)	1.973
20% FA-A	1	40.3 (5850)	0.093	36.8 (5336)	0.405	36.0 (5225)	0.928	37.3 (5409)	1.422
35% FA-A	1	18.4 (2662)	0.156	23.8 (3448)	0.410	32.1 (4652)	0.457	40.5 (5867)	0.404
	2	17.8 (2581)	0.161	23.7 (3435)	0.310			36.2 (5254)	0.542
	3			26.1 (3779)	0.290			40.3 (5849)	0.309
50% FA-A	1	37.0 (5358)	0.085	39.7 (5762)	0.175	56.0 (8125)	0.441	55.1 (7987)	0.677
	2	40.9 (5924)	0.096	39.7 (5762)	0.289			51.5 (7465)	0.772
	3			48.5 (7033)	0.133			51.5 (7473)	0.666
	4			44.3 (6423)	0.221			58.8 (8519)	0.343
35% FA-B	1	34.6 (5018)	0.117	34.1 (4945)	0.436	31.1 (4509)	0.459	34.4 (4992)	1.269
	2			34.3 (4972)	0.325			44.2 (6404)	0.686
35% FA-C	1	34.6 (5023)	0.056	36.2 (5256)	0.198	47.2 (6851)	0.138	62.2 (9015)	0.335
	2			31.6 (4580)	0.194			49.3 (7149)	0.335
	3			32.3 (4686)	0.013			48.4 (7021)	0.039

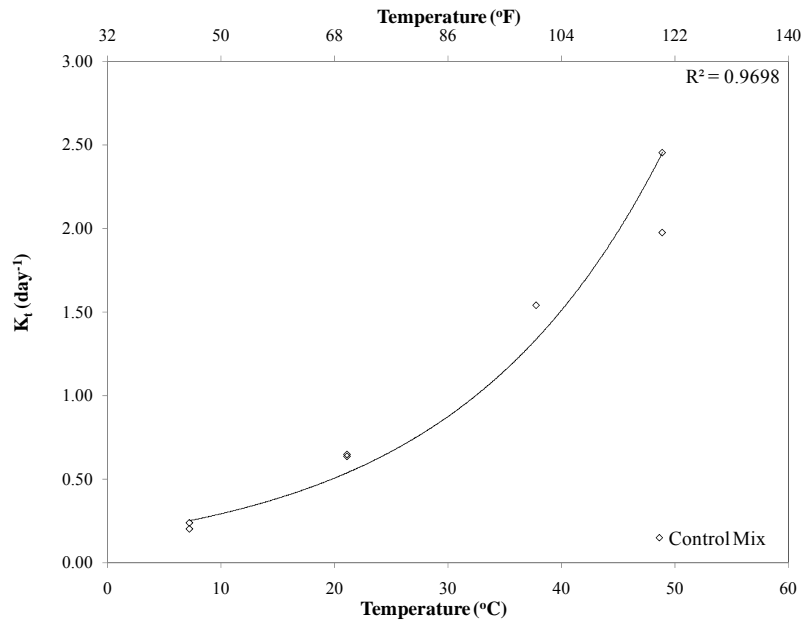


Figure 3.5 Rate constant vs. temperature-control mixture (AE-414001 J /mol)

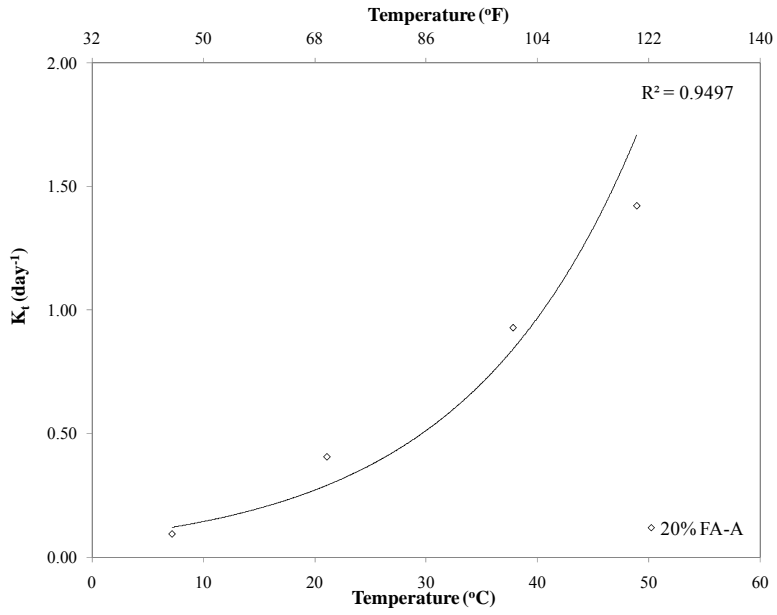


Figure 3.6 Rate constant vs. temperature-20% FA-A (AE-48100 J/mol)

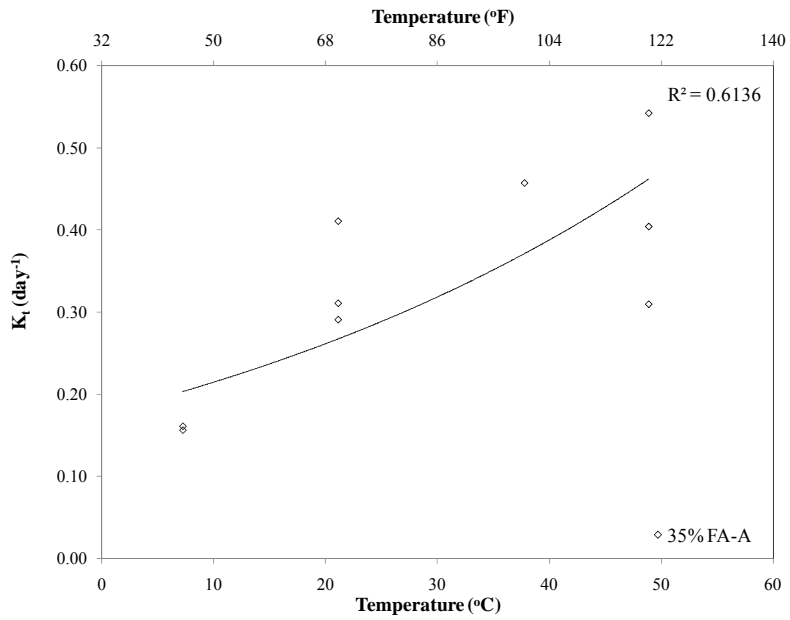


Figure 3.7 Rate constant vs. temperature-35% FA-A (AE-15600 J/mol)

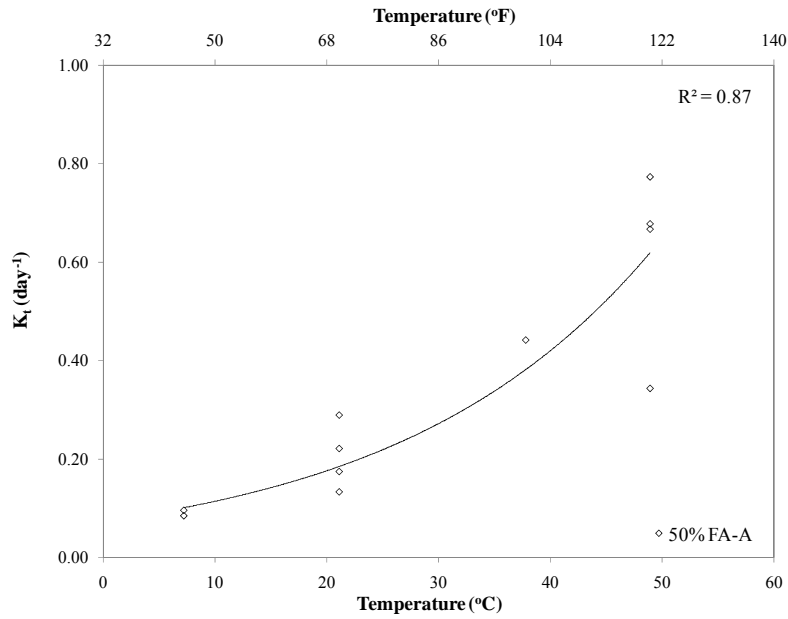


Figure 3.8 Rate constant vs. temperature-50% FA-A (AE-33400 J /mol)

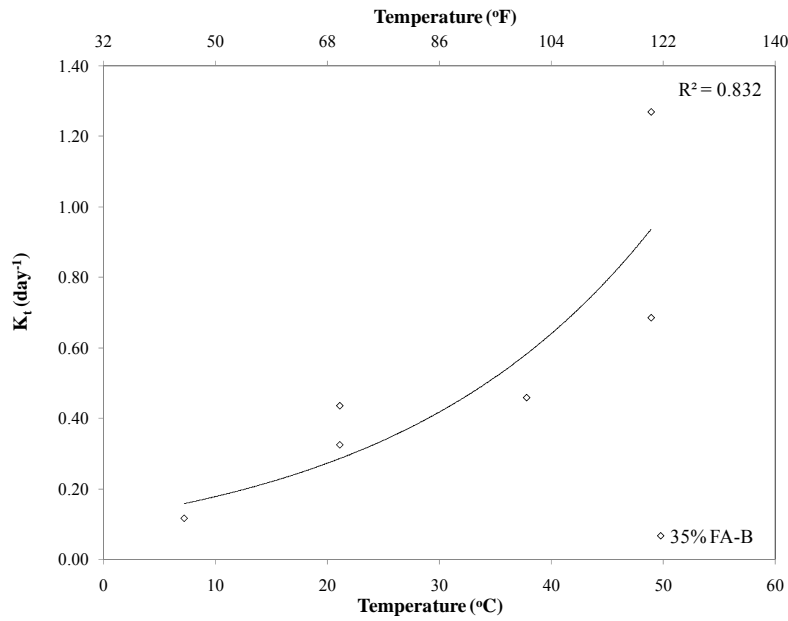


Figure 3.9 Rate constant vs. temperature-35% FA-B (AE-33000 J /mol)

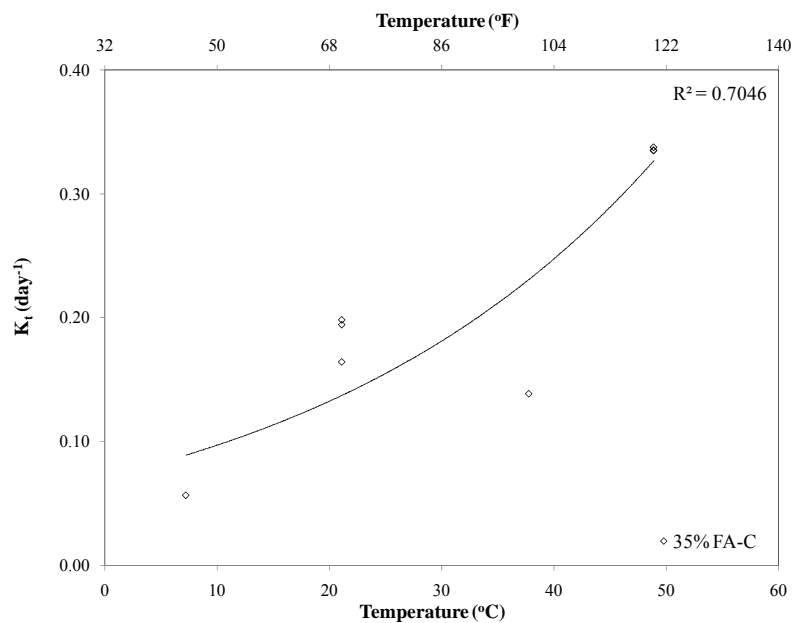


Figure 3.10 Rate constant vs. temperature-35% FA-C (AE-283001 J/mol)

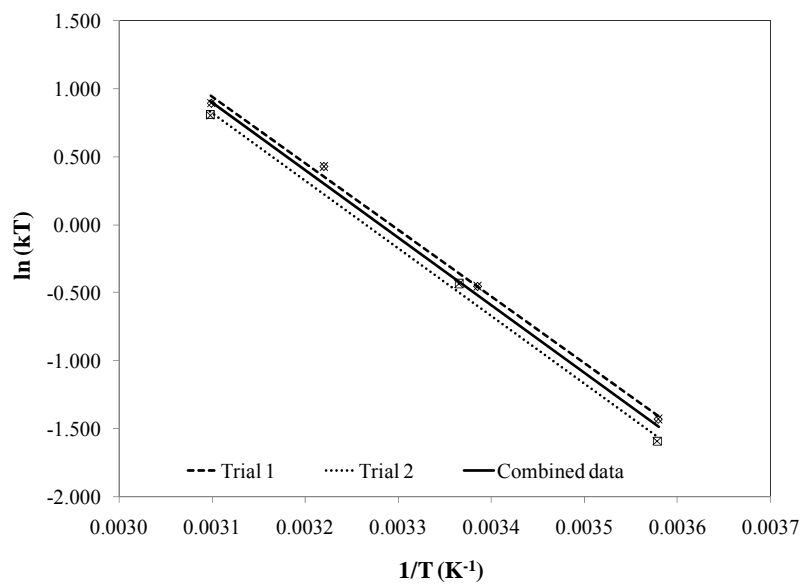


Figure 3.11 Arrhenius plot (Control mixture)

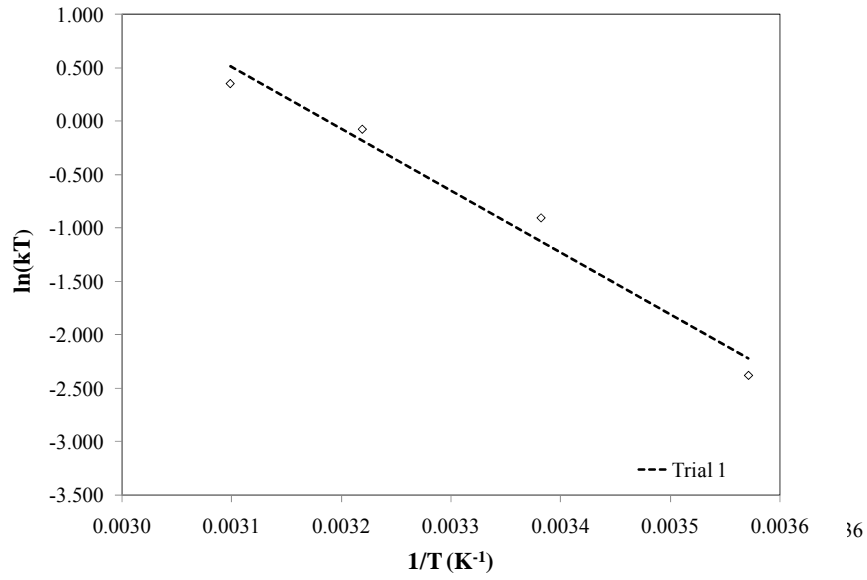


Figure 3.12 Arrhenius plot (20% FA-A)

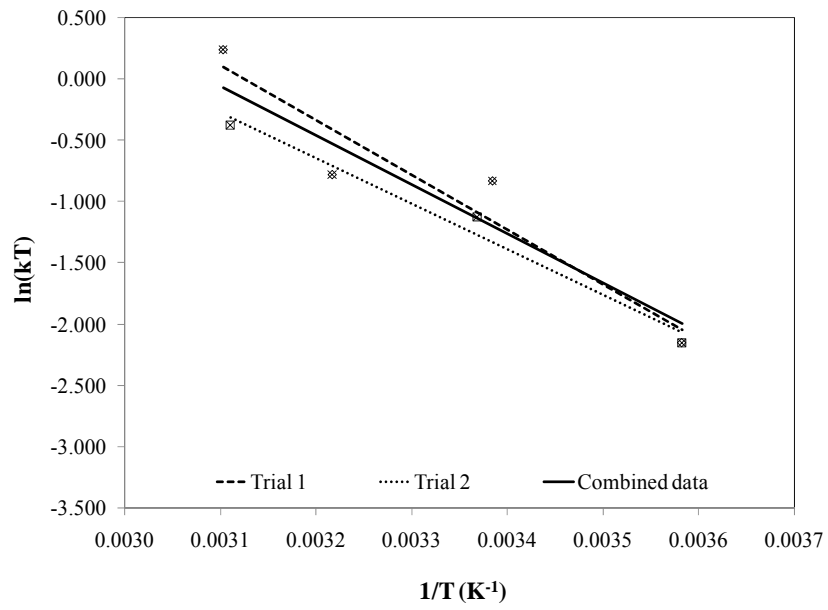


Figure 3.13 Arrhenius plot (35% FA-A)

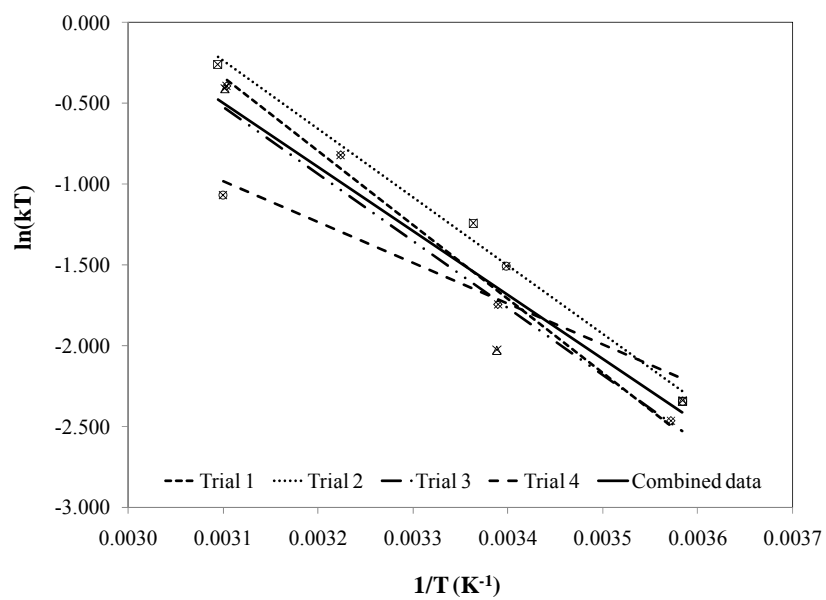


Figure 3.14 Arrhenius plot (50% FA-A)

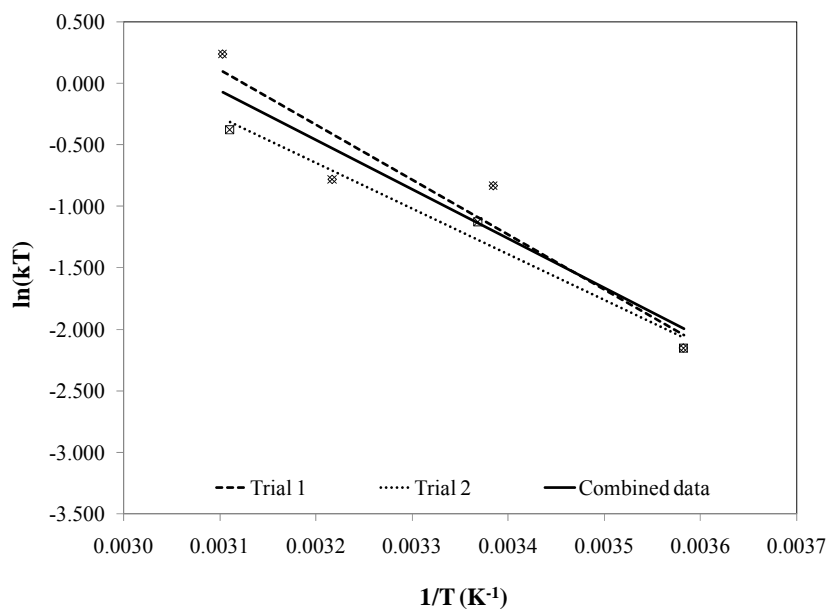


Figure 3.15 Arrhenius plot (35% FA-B)

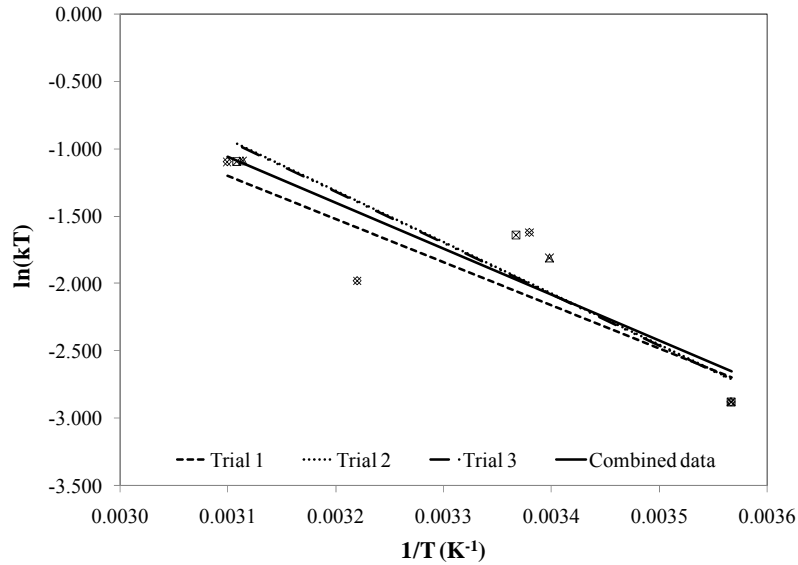


Figure 3.16 Arrhenius plot (35% FA-C)

Table 3.15 Calculated activation energies (ASTM C1074)

Mixture	AE (J/mol)	AE ₁ (J/mol)	AE ₂ (J/mol)	AE ₃ (J/mol)	AE ₄ (J/mol)
Control	41400	40900	41500		
20% FA-A	48100				
35% FA-A	15600	16900	22400	10700	
50% FA-A	33400	38000	35300	34500	21800
35% FA-B	33000	37100	31000		
35% FA-C	28300	26700	31700	31700	

AE= Activation Energy calculated based on combined data set

AE_i= Activation Energy calculated based for each of the trials, i = 1 through 4

It has been well documented that concrete cured at higher temperature tend to gain strength at early age, but on the other hand concrete cured at relative lower temperature tend to gain more strength at later age as compared to the higher temperatures. During this research this phenomenon was observed, and was true for the control mix only. The remaining cementitious materials showed an unusual behavior that contradicts the

conventional theory, the mixtures cured at higher temperatures gained higher strength even at later ages up to 28 days. Due to this unusual phenomenon, two new approaches were tried to model the effect of temperature on strength gain of high volume fly ash concrete. These two approaches were 1) Setting time method, and 2) Constant S_{uc} method.

3.5.3.1 Setting time method

This approach is based on the setting time of mortars for computing the activation energy. Setting of mortar or concrete is a gradual transition from liquid to solid, and the definition of any point at which the paste is considered set, is somewhat arbitrary (Pinto and Hoover, 2004). The hydration reaction starts from the instant when cementitious mixture is exposed to water. The hydration temperature tends to rise until final setting time of concrete and then starts to drop. Mortars used for this part of the research were representative of the concrete mixtures used in the field-testing. The mix proportions of mortar mixtures used are provided in Table 3.3. Setting time, is defined as the time interval between initial and final setting, Equation 8,

$$S_T = (F_s - I_s) \quad \text{Equation 8}$$

Where: S_T = Setting time (mins)

F_s = Final set time (mins)

I_s = Initial set time (mins)

Setting time of a cement paste is the function of the curing temperature, which means mortars cured at higher temperature will hydrate faster reducing the time of initial and

final set. That means that hydration reaction is an inverse function of setting time, Equation 9.

$$k_t = \frac{1}{S_T} \quad \text{Equation 9}$$

Where: K_t = hydration rate

Initial and final set times of the mortar were determined with penetration resistance testing in accordance to ASTM C403. Final setting of mortar relates to the point where stresses and stiffness start to develop in freshly placed concrete. It has been reported that the initial thermal gradient at setting (built-in curling) has a major impact on the long-term performance of concrete. Table 3.6 summarizes initial and final setting time for all the mixtures at four different isothermal curing conditions. Figure E.1 in Appendix E shows the Arrhenius plot for all the mortar mixtures, plotted based on the rate of reaction calculated using the setting time approach. The results show that the rate of reaction is highest for the control mix only, which results in a higher activation energy relative to all other mixtures. Table 3.16 summarizes the activation energy values computed based on the setting time approach. It is concluded that the activation energy of the mixtures reduces as the cement replacement increases. As the percentage of fly ash is increased, it alters the chemical properties of the cement matrix and reduces the hydration rate of the new cementitious mixture. As the hydration rate is decreased the energy required for the water and chemical to react is reduced, henceforth the cementitious mixtures with fly ash have low activation energy compared to the control mix. These computed activation energies were used to obtain a new strength-age maturity model, and to predict strength based on

the strength-age model at any given period of time. The results are provided in Figure E.2 to Figure E.11. The results clearly show that the match cure strength is always higher compared to other methods of prediction. It is also observed that strength using the maturity prediction models are close to match cure strength except the 35% FA-A mixture.

Table 3.16 Activation energy using setting time approach

Mix Type	AE (J/mol)
Control Mix	43200
35% FA-C	37800
35% FA-B	36400
20% FA-A	40000
35% FA-A	33200
50% FA-A	31400

3.5.3.2 Constant S_{uc} approach

The use of the strength-age model described in ASTM C1074 and used to estimate the rate constant and limiting strength. This approach results in varied ultimate strength for the same mixture when cured at different temperatures. Since the HVFA mixtures did not follow the temperature dependence in terms of the ultimate strength values, an alternative approach was considered in this research. This approach (constant S_{uc}) considers that there is one-limiting strength value for a mixture irrespective of the curing temperature. The best fit values for the constants, S_{uc} and $k(T)$ were estimated by keeping S_{uc} constant, which means one value of S_{uc} computed independently of the various curing temperatures, and thus calculating $k(T)$ for each curing temperature, as given by Equation 10. This

approach was used as some of the mixtures exhibited very different long-term strengths. Differences in long-term strengths will affect the best-fit rate constant associated with each curing temperature, as there is a relationship between the S_{uc} and k values. By using a constant S_{uc} value, this method also inherently matches the assumption of the maturity method in ASTM C 1074 in that the limiting strength value is assumed independent of temperature. Least square regression analysis was used to determine the best-fit S_u , and $k(T)$ values to minimize the sum of the square of the error between the estimated and measured strength values. Table 3.17 presents the best-fit limiting strength (S_{uc}) values and the rate constant ($k(T)$) for all the mixtures and trials. Table 3.18 summarizes the activation energies for all the trials. Figure F.1 in Appendix F shows the Arrhenius plots using the constant S_{uc} approach for all the cementitious mixtures. Figure F.2 (a-f) shows the comparison of Arrhenius plots for variable S_u and constant S_{uc} methods. The R^2 values for the best fit linear regressions are provided in Table 3.19, which clearly shows that the constant S_{uc} approach characterize the temperature sensitivity relatively well compared to the variable S_u approach for HVFA mixtures. It is been also observed from the plots that both methods have variability in characterizing the temperature sensitivity on rate constant.

$$S(t) = S_{uc} \frac{k(T) \times (t - t_{fs})}{1 + k(T) \times (t - t_{fs})} \quad \text{Equation 10}$$

where: $S(t)$ = compressive strength MPa (psi),

S_{uc} = constant limiting strength MPa (psi),

$k(T)$ = rate constant (1/days),

t = testing age (days), and

t_{fs} = final setting time (days).

Table 3.17 Best fit regression constants-Constant S_{uc}

Mixture	Trial	Curing Temperature				
		S_{uc} MPa (psi)	7.5°C (45°F) k_t (day ⁻¹)	21.0°C (70°F) k_t (day ⁻¹)	38.0°C (100°F) k_t (day ⁻¹)	49.0°C (120°F) k_t (day ⁻¹)
Control	1	31.3 (4534)	0.209	0.751	1.517	1.747
	2	29.2 (4232)	0.271	0.640		1.374
20% FA-A	1	31.5 (4562)	0.143	0.597	1.307	2.089
35% FA-A	1	28.3 (4103)	0.047	0.228	0.677	0.923
	2	29.8 (4324)	0.036	0.151		0.939
	3	28.1 (4070)	0.042	0.242		0.732
50% FA-A	1	53.2 (7711)	0.042	0.143	0.558	0.741
	2	46.6 (6761)	0.067	0.181		1.042
	3	50.0 (7245)	0.066	0.122		0.725
	4	28.1 (4070)	0.042	0.242		0.732
35% FA-B	1	33.5 (4859)	0.125	0.461	0.372	1.352
	2	39.7 (5751)	0.087	0.206		0.941
35% FA-C	1	42.7 (6185)	0.035	0.129	0.170	0.703
	2	41.0 (5939)	0.039	0.095		0.528
	3	44.5 (6447)	0.032	0.077		0.418

Table 3.18 Activation Energy computed based on constant S_{uc} approach

Mixture	AE (J/mol)	AE ₁ (J/mol)	AE ₂ (J/mol)	AE ₃ (J/mol)	AE ₄ (J/mol)
Control	33300	36800	28000		
20% FA-A	46000				
35% FA-A	53800	53100	59500	48100	
50% FA-A	44500	52400	45900	41400	37100
35% FA-B	38900	34300	43600		
35% FA-C	47100	47500	46800	46200	

Table 3.19 R square values for best fit linear fit

Mixtures	R ² (%)	
	Variable S _u	Constant S _{uc}
Control mix	99.23	92.94
20% FA-A	97.42	97.81
35% FA-A	64.21	94.63
50% FA-A	88.36	95.01
35% FA-B	87.51	87.42
35% FA-C	82.1	96.51

Figure F.3 to Figure F.8 shows the plots of predicted strength based on the activation energy computed using the constant S_{uc} approach and other methods. From the plots, it is observed that there is quite variability between match cure strength and maturity predicted strength. It is also clear from the plots that the constant S_{uc} approach predicts strength well for fly ash mixtures compared to the control mixture. Table 3.20 shows the percent difference between predicted strength based on the three approaches and maturity strength. It can be observed that there is lot of variability between all the methods. However, the constant S_{uc} method predicts better the strength of fly ash mixtures. On the other hand, the variable S_u approach estimated better the strength of the control mixture. In the case of the HVFA concrete mixtures, strength computed based on the constant S_{uc}, was 8 to 24% lower compared to the match cure method. However, such a difference is less than the other two approaches. Thus, the constant S_{uc} approach may be better for predicting strength of the HVFA concrete mixtures. Additional investigation is thus needed to confirm the unusual behavior of strength gain for the fly ash mixtures, and validate the reliability of the constant S_{uc} approach. The variable S_u method is further discussed at later sections of this study.

Table 3.20 Percent difference between predicted strength and maturity method

Mixtures		Variable S_u	Setting Time	Constant S_u
Control	Block	-16.0	-17.7	-25.5
	Slab	-42.1	-73.3	-71.1
35% FA-A	Block	-37.3	-41.7	-24.0
50% FA-A	Block	-14.3	-17.4	-13.2
	Slab	-4.6	-5.0	-8.5
35% FA-C	Block	-20.2	-16.6	-9.19

Chapter 4 Experimental Work – Concrete

4.1 Materials

The same materials were used for concrete and mortar batches; the physical and chemical properties of the materials used for concrete field and laboratory testing are presented in Table 3.1 and Table 3.2 in Chapter 3.

4.2 Mixing Concrete

These non-air-entrained concrete mixtures had a target slump of 12.7 to 17.8 cm (5 to 7 in.) Type F HRWR was used in the concrete mixture to achieve the target slump. The concrete was mixed in a dry batch ready mixed concrete plant, which means all the materials were batched into the concrete truck mixer and mixed in the truck mixer. The concrete was delivered to the NRMCA research facility which was located about 20 minutes from the concrete plant. The plant only stored Fly ash FA-A, which required that Fly ash FA-C be added to the ready mixed concrete truck at the NRMCA laboratory followed by additional mixing. HRWR was also added as needed at the laboratory to attain target slump.

4.3 Concrete Testing

Concrete tests were conducted in accordance with ASTM standards. The NRMCA Research Laboratory participates in proficiency sample testing of the Cement and Concrete Reference Laboratory (CCRL), is inspected biannually for conformance to the

requirements of ASTM C1077, and maintains its accreditation under the AASHTO Laboratory Accreditation Program.

4.3.1 Fresh Concrete Tests

All concrete batches were tested in accordance with ASTM standards for slump (ASTM C143/C143M), air content (ASTM C231), density (ASTM C138/C138M), and temperature (ASTM C1064/C1064M).

4.3.2 Hardened Concrete Tests

Compressive Strength Tests:

Compressive strength tests for concrete mixtures were conducted in accordance with ASTM C39/C39M. Specimen size used was 10.2 x 20.3 cm (4 x 8 in.) cylindrical specimens. Neoprene caps in accordance with ASTM C1231/C1231M of 70 durometer hardness were used to cap the test specimens. Three types of curing were followed:

1. Standard-cured test specimens were transferred to the 100% humidity room [23°C (73 °F)] as soon as they were cast, demolded at 24 hours and cured until the test age. Cylinders were tested at an age of 1, 2, 4, 7, 14, and 28 days. Strength test results reported are the average of 3 test cylinders tested at the same age. Temperature sensors were placed in two of the concrete cylinders. The average temperature data were used to establish the strength-maturity relationship for each mixture.

2. Field Cured cylinders were also tested at an age of 2, 4, and 7 days. Compressive strength test results reported are the average of 3 test cylinders for field-cured cylinders tested at the same age. Two additional concrete cylinders were casted with temperature sensor (iButtons) at the center, to compare the temperature development with that structure. These concrete specimens with temperature sensors were not tested for compressive strength, and were only used to recording temperature.

3. Match-cured cylinders were also tested at an age of 2, 4, and 7 days. The match curing process used is shown in Figure 4.1. Compressive Strength test results reported are the average of 2 test cylinders tested at the same age. Two additional concrete cylinders were cast with a temperature sensor (iButton) at the center, to compare the temperature development with that structure. These concrete specimens with temperature sensors were not tested for compressive strength.

Pullout Tests:

Wooden 20.32 cm (8 in.) cube molds shown in Figure 4.2 were used for developing the correlations between pullout load and compressive strength of companion cylinders.

Testing was conducted at six ages (1, 2, 4, 7, 14, and 28 days). Early stripping inserts were used in the 20.32 cm (8 in.) concrete cubes, one pullout insert was used in each side of the four faces to eliminate the possibility of any radial cracking propagation affecting the results during the pullout test (Figure 4.3). A LOK-test machine was used to perform the

pullout test, as shown in Figure 4.4. Pullout force test result reported is the average of 8 pullout test at same age from 2 cubes. An additional cube was made to record the temperature of these specimens; therefore, 13 cubes were prepared for each mixture. Temperature sensors (iButtons) were placed in one of the cubes at a height of 2.54 cm (1 in.) from the bottom surface of the cube at the center of the surface. The temperature data were used to compare the temperature development of the cubes and cylinders. These molds were fabricated with wood and were coated with waterproofing paint and varnish. Before filling the concrete, the wooden cube molds were coated with form oil to prevent the concrete from adhering to the molds. A correlation between the pullout load and compressive strength was determined for each mixture. This correlation was used to estimate the in-place strength at locations where the pullout test on the concrete members was performed.



Figure 4.1 Match cure system showing 8 match-cured cylinder molds connected to a micro-controller computer



Figure 4.2 Custom 20.32 cm (8 in.) cube mold



Figure 4.3 Cube molds with pullout inserts at the centers of the 4 side faces



Figure 4.4 Pullout Equipment

Concrete Blocks:

Concrete blocks of dimension 0.6 x 0.6 x 1.8 m (2 × 2 × 6-ft) were used to simulate the in-place strength development of HVFA mixtures under field conditions. The 0.6 x 0.6 x 1.8 m (2 × 2 × 6-ft) wooden forms, shown in Figure 4.5, were designed to incorporate 12 pullouts inserts on each side of the longer faces (24 total). The minimum distance between 2 inserts was kept in accordance to ASTM C900, which states that the minimum clear distance between two inserts should be eight times the head diameter, and the minimum clear distance between the edge and the insert should be four times the head diameter. Inserts were installed at 145 mm (5.7 in.) clear distance center to center, and 115 mm (4.5 in.) from the edge, to eliminate any potential effects of radial cracking from one test to the next. The inserts extended a distance of 2.54 cm (1 in.) into the concrete surface. The

blocks were also designed to allow the research team to perform very early pullout tests before the forms were removed. This was done by creating a small access window on specific locations of the block mold as shown in Figure 4.5.



Figure 4.5: Field block with pullout inserts and temperature sensors

Four 0.6 x 0.6 x 1.8 m (2 × 2 × 6-ft) concrete blocks were prepared, one for each of the four different concrete mixtures. Temperature sensors (iButtons) were installed in eight different locations in each concrete block. Appendix A, Figure A.3 shows the locations of the temperature sensors. Temperature of concrete elements should be measured at critical locations within a structure since a variable temperature gradient may be observed in relation to the specific location, Appendix G shows the plots for temperature profile within the block. One thermocouple was also installed at 2.54 cm (1 in.) from the surface of the block, which was needed for the match cure cylinders to replicate the same thermal

profile as the block. The temperature profile from the iButton (denoted by P4 in Figure A.3) located at a depth of 2.54cm (1 in) from the surface was used to calculate the equivalent age of the block. Whenever maturity is used to perform critical formwork removal operations it is customary for the temperature sensor to be placed at a depth of 2.54 cm (1 in.) from the concrete surface. It should be observed that the temperature sensor for the maturity (P4 in Figure A.3), the thermocouple for match-cured cylinder tests, and the pullout inserts extended to a depth of 2.54cm (1 in) from the concrete surface. The blocks were placed in two lifts with each layer being consolidated using an internal vibrator. As soon as the blocks were struck off, they were covered with a plastic sheet. A commercially used black curing blanket about 20-mil-thick was used to cover the blocks. The curing blanket was kept over the plastic sheet in order to provide some additional insulation to the blocks during the curing process. Figure 4.6 shows the concrete block being cured.

The pullout test on the concrete blocks was conducted in accordance to ASTM C900, at three different concrete ages (2, 4, and 7 days). Testing at an age of 2 days was conducted with the side forms still on the blocks, so access for the pullout test was obtained through a 100 mm (3.9 in.) diameter opening in the form as shown in Figure 4.5. The formwork of each block was removed at a concrete age of 3 days. After the forms were removed, the block was cured using plastic sheeting and curing blankets. At each testing age, eight pullout tests were conducted at randomly selected locations on the block, with the requirement that four tests be performed on each of the two longer faces of the block. This approach was used to eliminate the effect of variability due to different curing conditions

and hydration that the sides of the block may experience. The average of these eight tests was calculated and used to estimate the in-place compressive strength at that age using the pre-determined pullout load versus strength correlation.



Figure 4.6 Concrete block curing in field.

The pullout tests and match-cured cylinder test results were used to validate the in-place strengths predicted by maturity. Field-cured cylinders were also tested as a point of comparison since this approach is currently the most commonly used technique to determine the in-place compressive strength.

Slab tests:

In addition to the concrete blocks, two $2.4 \times 2.4 \times 0.18$ m (8 ft \times 8 ft \times 7 in.) slab (Figure 4.7), were prepared for the control (Portland cement mixture) and the 50% fly ash mixtures. The slabs had 24 floating inserts and 5 temperature sensors at different

locations. The sensor for maturity calculation (denoted by P4, in Figure of Appendix) was located at a depth of 5.08 cm (2 in.) from the top surface around the middle third of the slab. This sensor was located 5.08 cm (2 in.) below the surface to have the same depth below the surface as the average depth of concrete tested when a floating pullout insert is tested. Refer to Figure A.4 in Appendix A for detailed geometry of the slab and the location of iButtons and the thermocouple used to drive the match cure cylinders. For the 50% FA-A mixture the in-place cylinders were used in lieu of the match-cured cylinders, due to logistics issues. For the 50% FA-A mixture concrete block and slab were casted at the same day so the match cure system was used for the block. Figure 4.8 illustrates the test slab with the floating inserts and cast-in-place cylinders. The pullout test was conducted in accordance with ASTM C900 at three ages (2, 4, and 7 days) by testing eight pullout inserts at each age. The compressive strength of the field-cured and match-cure cylinders was also evaluated at the same three ages as for the slab pullout testing, and using three replicates. For the control mixture, the match cure system was used to evaluate the in-place strength. On the other hand, for the 50 % FA-A mixture, two cast-in-place cylinders were tested at each age and the average value was recorded. The temperature data were also recorded in order to compute the maturity development at various locations. With the calculated maturity and the predetermined strength-maturity relationship, the in-place strength development could be estimated.



Figure 4.7 Concrete slab with cast-in-place cylinders and temperature sensors



Figure 4.8 Slabs with cast-in-place cylinders, floating inserts and field cure cylinders
Note: red marking are the pullout inserts; field-cured cylinders placed outside the slab; cast-in-place cylinders are within the slab.

The concrete blocks and slabs were cast at NRMCA research facility in ambient exposure conditions during the period of October to December. Table 4.1 tabulates the placement dates and average ambient temperature during the first 96 hours after placing the concrete in the block. The block and slab of the control mixture were cast on different dates, Figure G.1 in Appendix G shows the plot of ambient outside temperature for the first 96 hours during the curing process.

Table 4.1 Placement of concrete for blocks and slabs- over the first 96 hours

Mixtures	Block	Slab	Placement Date	Average Ambient Temperature °C (°F)
35% FA-C	X		10-05-2006	15.0 (59.0)
35% FA-A	X		10-26-2006	10.0 (50.0)
Control	X		11-03-2006	5.6 (42.0)
Control		X	11-20-2006	6.1 (43.0)
50% FA-A	X	X	11-28-2006	12.7 (55.0)

4.4 Mixture Proportions

All the concrete mixtures were non-air-entrained and the Type HRWR dosage was adjusted to attain a target slump of 12.7 to 17.8 cm (5 to 7 in). The yield adjusted concrete mixture proportions used are summarized in Table 4.2. The water and cementitious contents were generally accurate except for Mixture 35%FA-A which had a much lower cementitious materials content and higher water content presumably due to a batching error at the concrete plant. To achieve sufficient strength at early ages for fly ash concrete, the water-cementitious materials ratio (w/cm) was decreased and a HRWR was added to achieve desired workability.

Table 4.2 Yield adjusted concrete mixture proportions

Item	Control Mixture	35% FA-C	35% FA-A	50% FA-A
Cement, kg/m³ (lb/yd³)	302.6 (510)	215.4 (363)	196.4 (331)	182.7 (308)
Fly Ash, kg/m³ (lb/yd³)	0	117.5 (198)	116.3 (196)	176.8 (298)
Coarse Aggregate, kg/m³ (lb/yd³)	1151.0 (1940)	1151.0 (1940)	1160.4 (1956)	1167.0 (1967)
Fine Aggregate, kg/m³ (lb/yd³)	770.1 (1298)	783.7 (1321)	752.3 (1268)	769.5 (1297)
Water, kg/m³ (lb/yd³)	169.7 (286)	141.2 (238)	157.2 (265)	140.6 (237)
HRWR Admixture ml/45 kg (oz/cwt)	62.9 (2.1)	152.7 (5.1)	200.7 (6.7)	140.6 (7.1)
w/cm	0.56	0.42	0.50	0.39

4.5 Discussion of Test Results

4.5.1 Fresh Concrete Properties

Fresh concrete properties are reported in Table 4.3

Table 4.3 Fresh concrete properties

Parameter	Mixture ID				
	Control (Block)	Control (Slab)	35%FA-A (Block)	50%FA-A (Block & Slab)	35%FA-C (Block)
Slump, cm (in.)	15.2 (6.0)	15.2 (6.0)	21.0 (8.25)	21.6 (8.5)	20.3 (8.0)
Concrete Temp, °C (°F)	12.8 (55)	14.4 (58)	12.8 (55)	13.9 (57)	22.2 (72)
Total Air Content (%)	2.4	3.4	1.1	1.1	1.7
Density, kg/m³ (lb/ft³)	89.0 (149.8)	89.1 (150.1)	88.9 (149.8)	90.8 (153.0)	85.0(143.3)

4.5.2 Standard Cured Strength Results and Strength-Maturity Relationship

Compressive strength testing of standard-cured 10.2 x 20.3 cm (4 x 8 in.) concrete cylinders was performed to develop the strength-maturity relationship for the four

mixtures listed in Table 4.3. Table C.1 to Table C.6 in Appendix C summarizes the compressive strength results for the standard-cured cylinders. The equivalent age maturity function was used to compute the maturity index. The activation energies used to convert the actual ages to equivalent age at the reference temperature of 23°C (73°F) for each mixture are average AE values (labeled as AE) of the corresponding mixtures and are provided in Table 3.15. Table 4.4 to Table 4.7 tabulate the compressive strength results of standard-cured cylinders for all the four concrete mixtures. These tables also show the computed equivalent age based on the measured temperature profile of the concrete cylinders. Resulting strength versus equivalent age relationships were plotted and the best-fit hyperbolic functions are shown in Figure 4.9 to Figure 4.12.

Table 4.4 Compressive strength control mixture

Age (Days)	Eq. Age @23°C (73°F) (Days)	Strength MPa (psi)
1	0.84	7.1 (1023)
2	1.64	11.8 (1714)
4	3.25	16.9 (2449)
7	5.81	18.6 (2692)
14	12.26	23.9 (3470)
28	24.96	30.2 (4378)

Table 4.5 Compressive strength 35% FA-A mixture

Age (Days)	Eq. Age @23°C (73°F) (Days)	Strength MPa (psi)
1	0.95	4.8 (699)
2	1.90	7.1 (1034)
4	3.78	9.7 (1402)
7	6.62	12.6 (1820)
14	13.05	18.0 (2609)
28	26.54	24.2 (3505)

Table 4.6 Compressive strength 50% FA-A mixture

Age (Days)	Eq. Age @23°C (73°F) (Days)	Strength MPa (psi)
1	0.98	7.2 (1039)
2	1.94	11.5 (1662)
4	3.80	16.4 (2372)
7	6.59	19.5 (2832)
14	12.79	25.3 (3668)
28	25.33	33.2 (4811)

Table 4.7 Compressive strength 35% FA-C mixture

Age (Days)	Eq. Age @23°C (73°F) (Days)	Strength MPa (psi)
1	0.98	5.6 (807)
2	1.94	12.3 (1781)
4	3.88	19.5 (2822)
7	6.79	24.2 (3503)
14	13.29	28.3 (4104)
28	26.15	35.9 (5212)

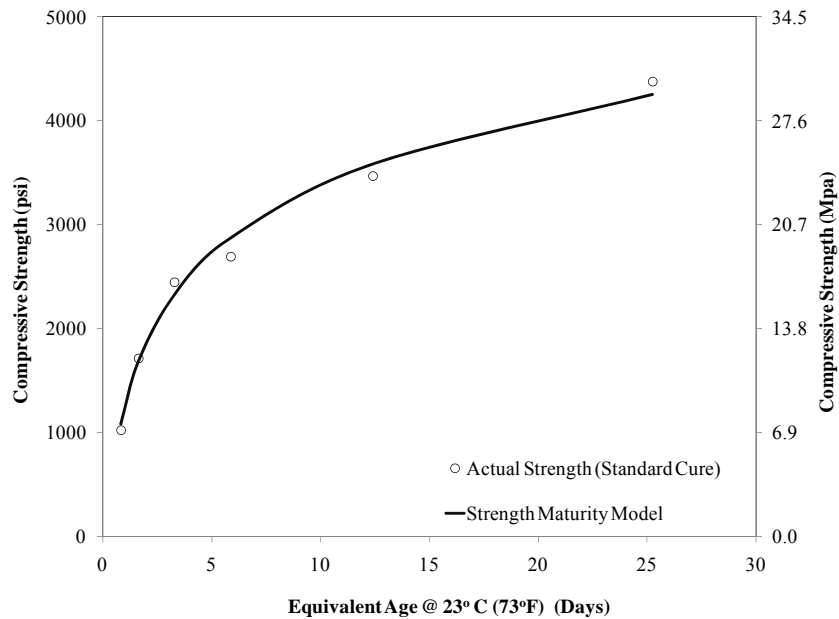


Figure 4.9 Maturity model- control mixture

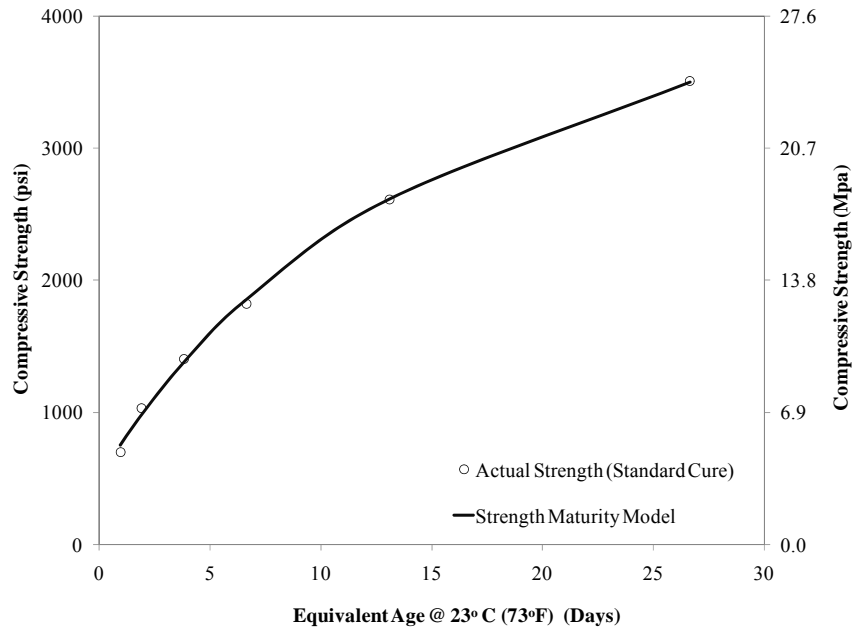


Figure 4.10 Maturity model- 35% FA-A mixture

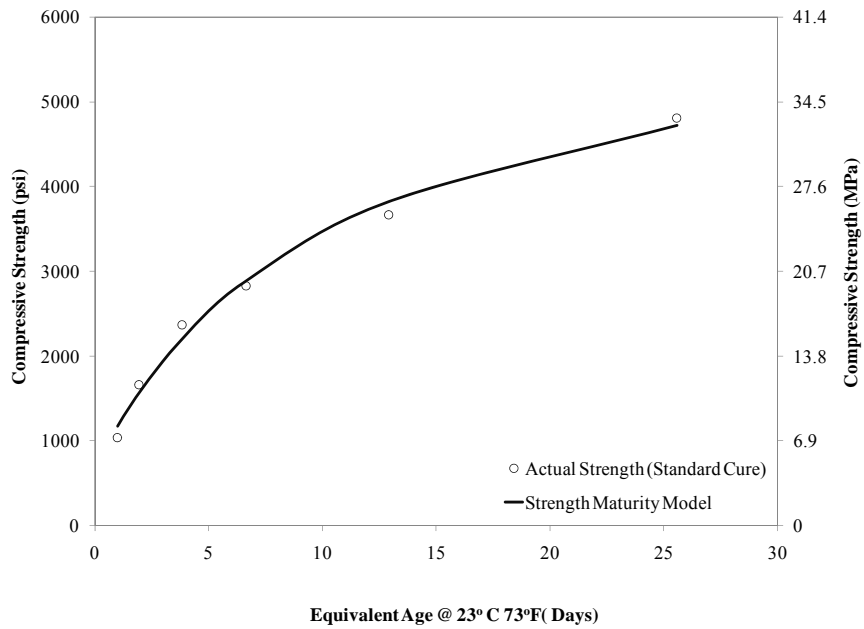


Figure 4.11 Maturity model- 50% FA-A mixture

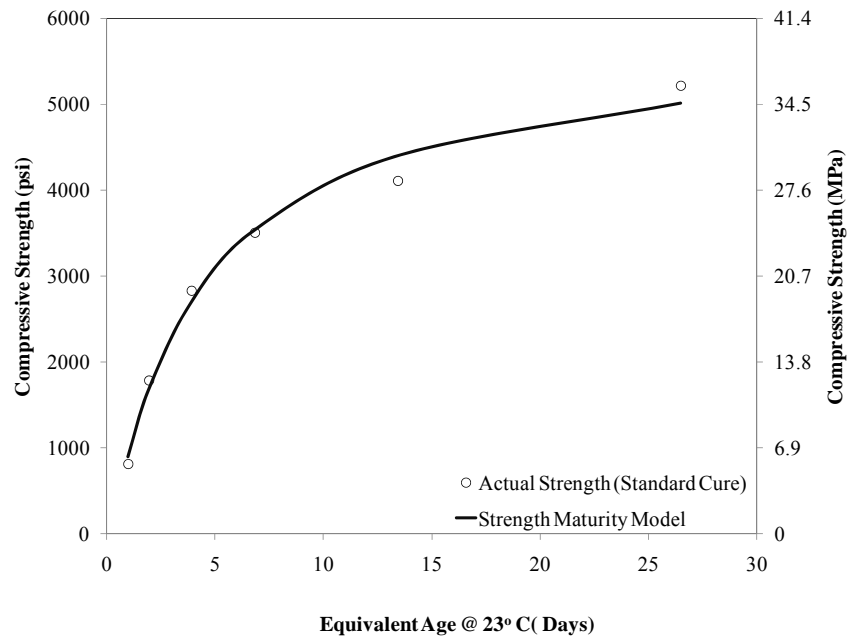


Figure 4.12 Maturity model- 35% FA-C mixture

The hyperbolic function accurately characterized the strength-maturity relationship for all mixtures. Strength-Maturity plots shown in Figure 4.9 to Figure 4.12 are later used to estimate the in-place compressive strengths of the concrete blocks and slabs that were constructed with the same mixtures placed under field conditions.

4.5.3 Pullout force test results and pullout force versus strength correlation

The pullout test is used during construction to evaluate the in-place compressive strength of concrete structural elements at any given time. This section details the pullout test results and correlations with compressive strength for the different mixtures used in this

research. Appendix D summarizes the pullout results for laboratory and field cure specimens. Pullout force results of standard cure cubes are tabulated in Table D.1 to Table D.10 in Appendix D, and these results are used to develop a correlation between pullout force and compressive strength. The compressive strength and pullout force plots are presented in Appendix D from Figure D.1 to Figure D.4. It is noted that the compressive strength increases as an exponential function of the pullout force. This relationship can be described by Equation 11, where a and b are regression constants (ACI 228.1R-03).

$$C = a \times P^b \quad \text{Equation 11}$$

Equation 11 can also be rewritten in a log transformation, as shown in Equation 12, which when plotted on log-log axes will provide a straight line relationship:

$$\log(C) = \log(a) + b \times \log(P) \quad \text{Equation 12}$$

Where: C = Compressive strength MPa (psi),

P = Pullout force (kN), and

a, b = Regression constants, a (MPa, psi)

Figure D.1 to Figure D.4 Appendix D contain the plots of compressive strength versus the pullout force for all the concrete mixtures. In each graph is also shown the data scatter for the pullout test results for each testing age. The strength-pullout force relationships are based on the average pullout force (from eight measurements) and the average

compressive strength. The strength relationship constants are tabulated in Table 4.8 for each mixture.

Table 4.8 Regression constants for strength relationship

	a MPa (psi)	b	R² (%)
Control	0.59 (85.63)	1.20	99.5
35% FA-A	0.42 (60.73)	1.30	99.5
50% FA-A	0.32 (46.72)	1.36	99.1
35% FA-C	0.58 (84.21)	1.22	98.4
Combined	0.46 (67.14)	1.24	97.4

From Figure D.1 to Figure D.4 it is observed that there is a good correlation between compressive strength and pullout force for individual mixtures. Further investigation was conducted to explore the possibility of having a single strength relationship for all mixtures. This new relationship, calibrated for all the mixtures tested in this research, is shown in Equation 13 and had an R² of 97.4%.

$$C = 67.14 \times P^{1.24} \quad \text{Equation 13}$$

Where: C = Compressive strength, (psi)

Equation 14 is the relationship recommended by the manufacturer of the pullout testing apparatus to obtain the compressive strength from a known pullout force. This relationship was also used to estimate the compressive strength and compare them with pullout-strength correlation developed in this research.

$$C = 100 \times P^{1.12} \quad \text{Equation 14}$$

Where: C = Compressive strength, psi

P = Pullout Force, kN

Figure 4.13 to Figure 4.16 shows the estimated versus measured strength plots for each concrete mixture. In each plot the compressive strength is estimated from the pullout load using the above three equations. It is clearly observed from the figures that the manufacturer's recommended equation does not provide a good estimate of the compressive strength. The correlation developed for each specific mixture provides a more accurate estimate of the measured compressive strength, and is subsequently used to estimate the strength of field-cured concrete element.

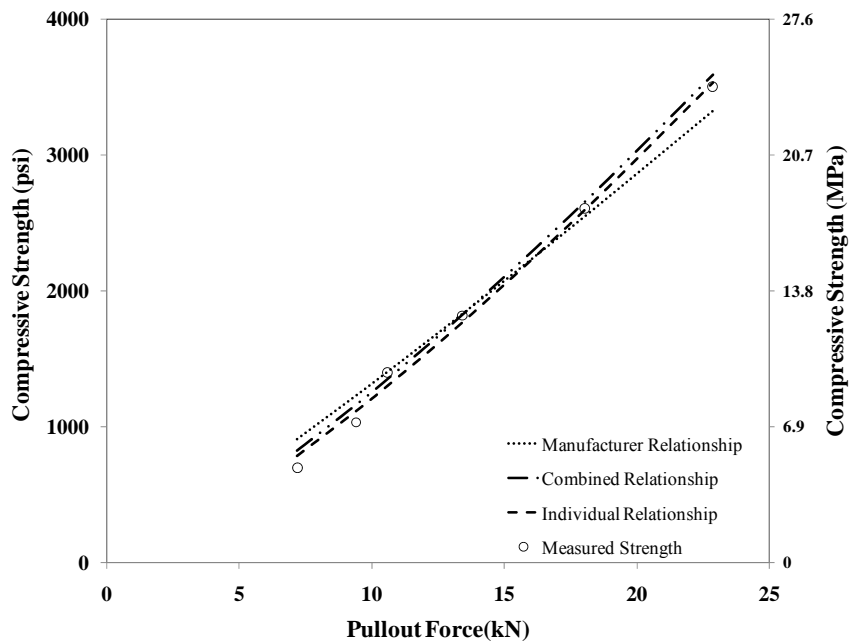


Figure 4.13 Compressive strength vs. pullout force relationship-Control mixture

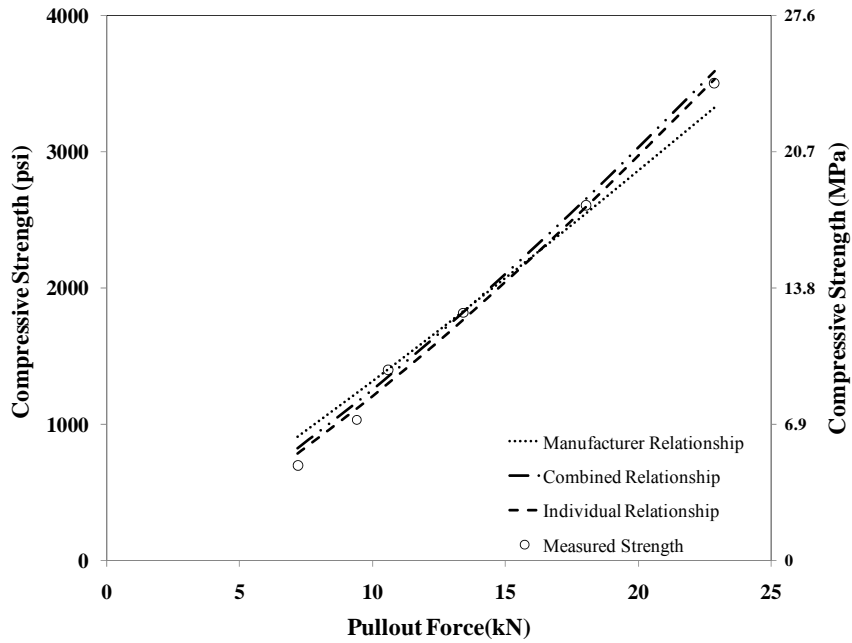


Figure 4.14 Compressive strength vs. pullout force relationship-35% FA-A mixture

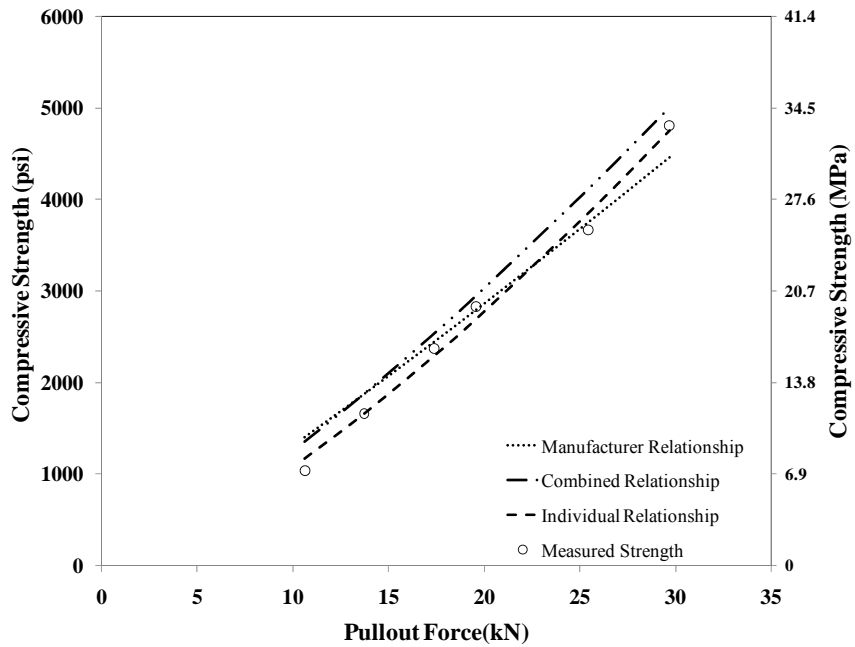


Figure 4.15 Compressive strength vs. pullout force relationship-50% FA-A mixture

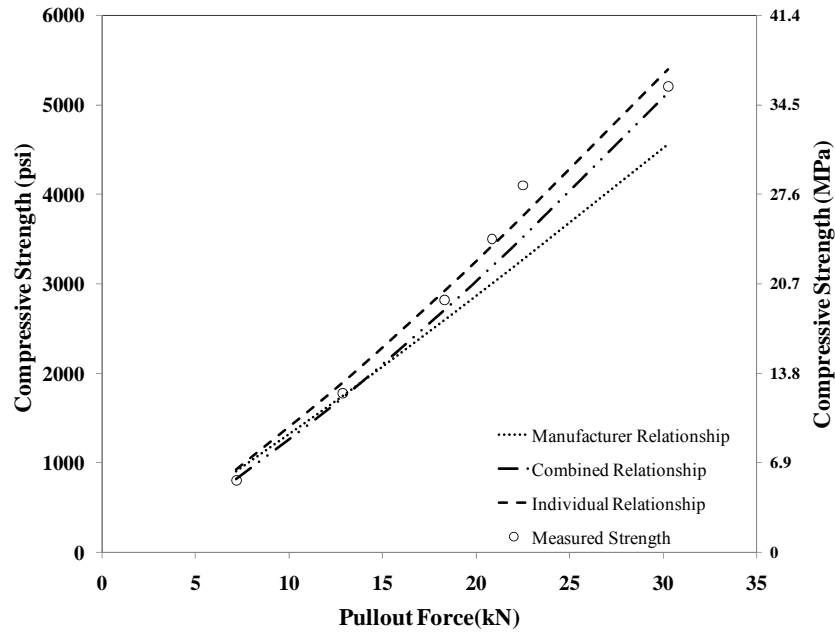


Figure 4.16 Compressive strength vs. pullout force relationship-35% FA-C mixture

4.5.4 In-Place Strength Estimates Based on Field-Cured and Match-Cured Cylinder Strengths

It is well known that concrete cured at higher temperature will gain early-age strength more rapidly than when it is cured at lower temperatures. Higher temperature means faster rate of chemical reaction and thus faster rate of strength gain. Figure G.2 to Figure G.11 in Appendix G show the temperature profile based on different curing conditions. As it can be observed from, the temperature profiles the match cure cylinders, which replicate the actual temperature profile of the structural element (block and slab) experience higher temperatures compared to the field-cured and standard-cured cylinders.

Figure 4.17 to Figure 4.21 show the compressive strength plots for the various curing conditions of the four mixtures, including the data from the block and slab concrete elements. From the data collected from the comparative experiments it can be concluded that compressive strength measured using field or standard-cured cylinders do not accurately represent the conditions of the block and slabs and thus underestimate the in-place compressive strengths of the structural concrete elements.

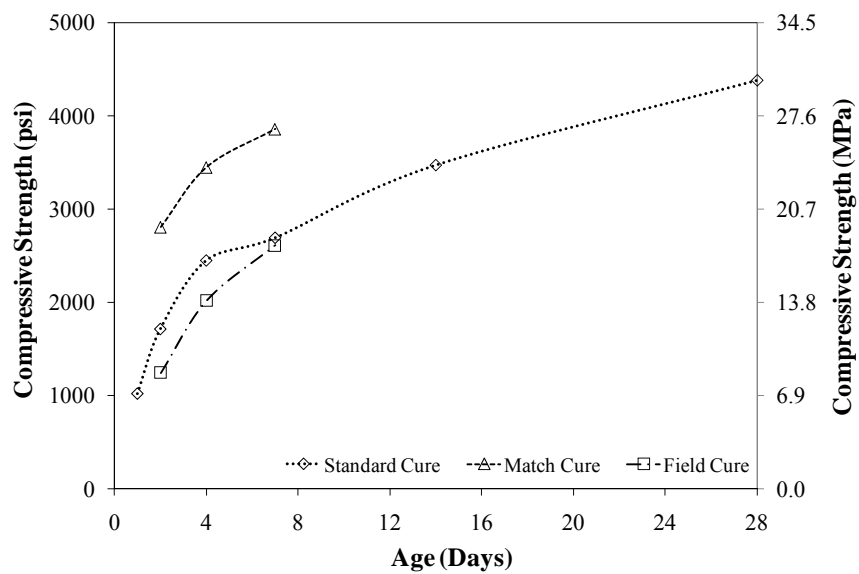


Figure 4.17 Compressive Strength vs. age for different curing conditions (control mixture-block)

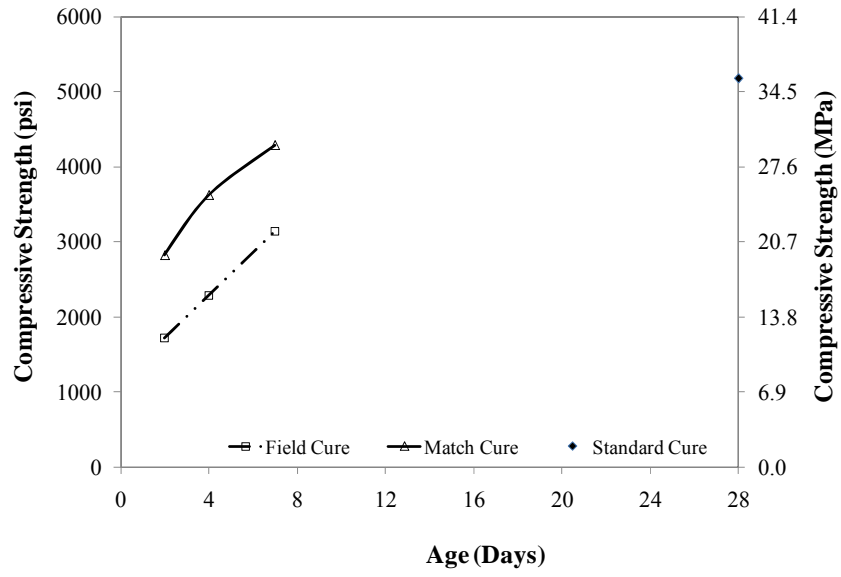


Figure 4.18 Compressive Strength vs. age for different curing conditions (control mixture-slab)

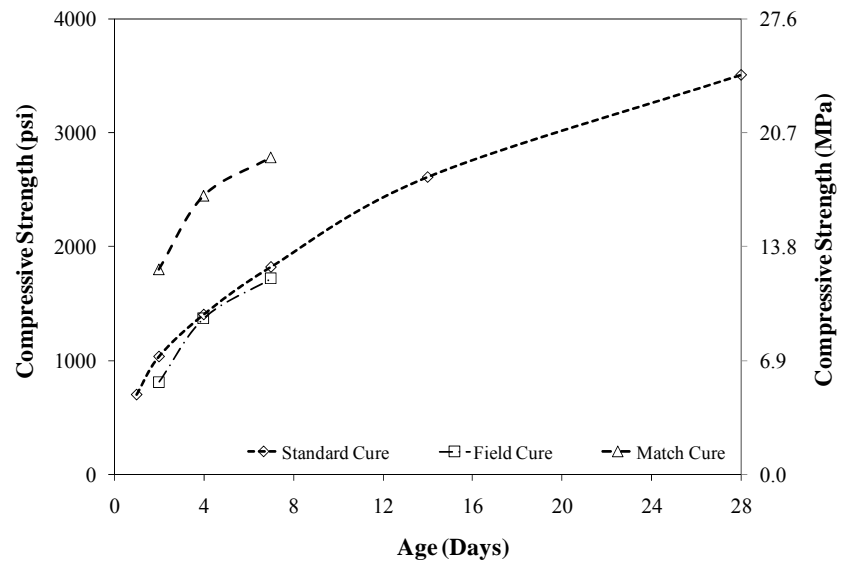


Figure 4.19 Compressive Strength vs. age for different curing conditions (35% FA-A mixture-block)

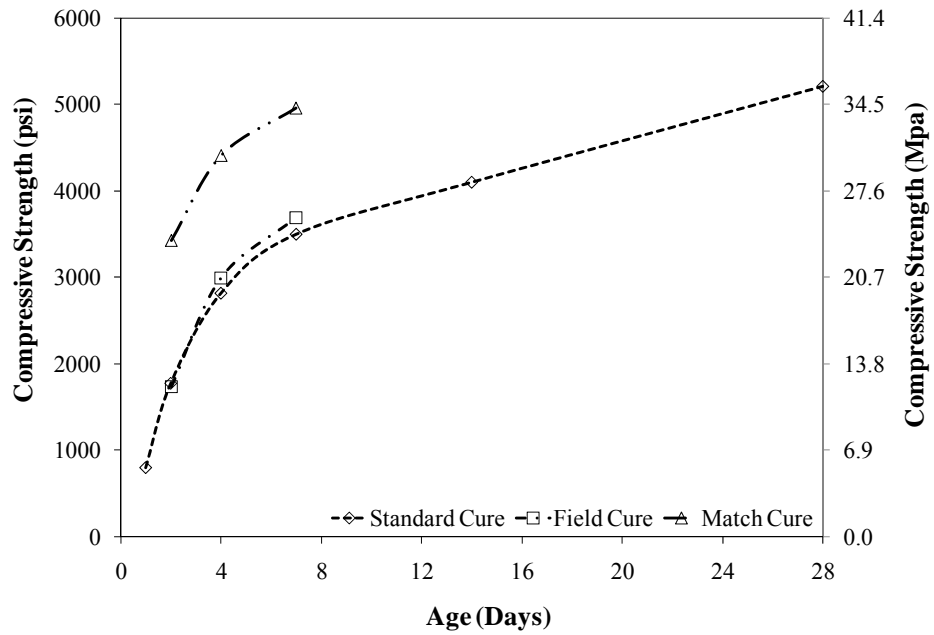


Figure 4.20 Compressive Strength vs. age for different curing conditions (35% FA-C mixture-block)

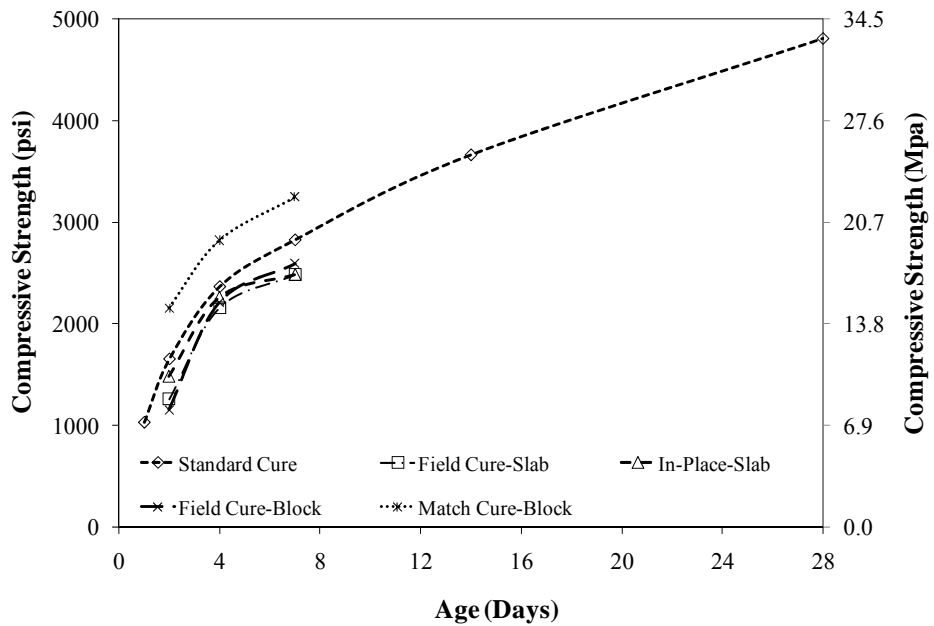


Figure 4.21 Compressive Strength vs. age for different curing conditions (50% FA-A mixture-slab and block)

4.5.5 In-Place Strength Estimates Based on Pullout and Maturity

The maturity method and the pullout test were used to estimate the in-place strengths of the concrete in the field block specimens and the field slabs. These estimates were compared with the strengths of match-cured cylinders, which were assumed to represent the best estimates of actual in-place strength. The strengths of the field-cured cylinders were also included in this comparison.

In-place temperature histories (see Appendix G) were recorded using iButton temperature data loggers located 1 in. from the block surface (Sensor P4 in Figure A.3) and 5.08 (2 in.) from the slab surface (Sensor P4 in Figure A.4). These measured temperature histories were converted to equivalent age using Equation 5 and the computed activation energies for each specific mixture. After equivalent age was calculated, the predetermined strength-maturity relationships (Figure 4.9 to Figure 4.12) were used to estimate the in-place strength at the location of the iButton data loggers at test ages of 2, 4, and 7 days. The measured average pullout loads were converted to estimates of in-place compressive strengths using the pullout-strength correlations developed earlier for each mixture (see Figure 4.13 to Figure 4.16).

Table 4.9 shows the equivalent ages at each test age and the estimated in-place strengths based on the maturity method and the pullout test. Table 4.10 compares the strengths of the match-cured cylinders with the strengths of the field-cured cylinders and with the

estimated strengths based on the maturity method and pullout test. The values in the parentheses are the percentage difference in strength compared with the corresponding strength of the match-cured cylinders. Figure 4.22 to Figure 4.25 show these strength comparisons for the four blocks and

Figure 4.26 and Figure 4.27 show the comparisons for the two slabs. Table 4.11 summarizes the average percent difference between the match-cured cylinders and in-place strength estimations by field-cured cylinders, maturity method, and pullout tests.

In general, the estimated strengths based on the pullout test and the maturity method were lower than the strengths of the match-cured cylinders by 15 to 20%. The field-cured cylinders, on the other hand, resulted in 20 to 50 % lower strengths in most cases. The lower strengths of the field-cured cylinders can be explained by their lower in-place temperatures compared with the temperatures recorded by the iButton data loggers in the block.

Estimated strengths from pullout tests and maturity were generally in good agreement. It was noted that the thermocouple was used to drive the match-cured cylinders, the temperature history recorded by the iButton data loggers at the same location were close to the thermocouple values. Thus, the iButton data were used to calculate the equivalent age for the maturity method. Since overall the thermocouple temperatures were consistently higher, the match-cured cylinders were therefore at a higher equivalent age than what was used to estimate the strength from the strength-maturity relationship. This

may account for some of the consistently lower estimated strengths based on maturity.

Other factors for the differences are proposed in the following discussion of the results for each mixture.

Control mixture—For the slab, the estimated strengths based on the maturity method were considerably lower (40 %) than the match-cured cylinder strengths. The slab was cast from a different batch than the block. The 28-day standard-cured cylinder strength for the slab concrete was 35.71 MPa (5180 psi) compared with 30.2 MPa (4380 psi) for the block concrete (see Table C.1). Thus, the slab concrete was stronger than the block concrete. In estimating the in-place strength of the slab, the strength-maturity relationship for the block was used. This result reinforces the known limitation of the maturity method, which is that it is not able to account for batching errors. Another observation is that at the test age of 7 days, the equivalent age of the slab was only 4.5 days because of the low in-place temperature. For the block, at 7 days the equivalent age of the block was 8.5 days. This can explain why at 7 days, the estimated strengths of the block and slab based on the pullout test were similar even though the potential strength of the slab concrete was higher. At the test age of 7 days, the strength of the match-cured cylinders was 3860 psi, which is greater than the 14-day strength of 23.9 MPa (3470 psi) for the standard-cured cylinders (see Table 4.4). Thus, the match-cured cylinders may have systematically greater strength than the standard cylinders after accounting for the effects of maturity. This premise requires additional investigation.

35 % FA-A mixture—At the test age of 7 days, the equivalent age of the block was 7.1 days. The 7-day strength of the standard-cured cylinder was 12.5 MPa (1820 psi) (see Table 4.5). The estimated strength for the maturity method (13.3 MPa, 1925 psi) is consistent with this value, but the match-cured strength is significantly higher at 19.2 MPa (2790 psi). A possible explanation may be related to the maximum in-place temperature in the block, which was about 33.3°C (91°F). The mortar tests discussed in Chapter 3 showed that when mortar cubes were cured at 37.8°C (100 °F), the estimated long-term strength was greater than for room-temperature curing. This apparent strength enhancement due to higher early age temperature in the fly ash mixtures may explain why the match-cured cylinders were stronger than estimated from the strength maturity relationship. However, this does not explain why the estimated strength based on the pullout test was lower [12.4 MPa (1800 psi) at 7 days]. A possible effect may be related to the thermal strains introduced in the surface layer after formwork was removed at 3 days. More research is needed to confirm this suggestion.

50 % FA-A mixture—At test ages of 2, 4, and 7 days, the computed equivalent ages of the block specimens were 2.4, 4.6 and 6.6 days, while for the slab the corresponding values were 1.6, 3.2, and 5.1 days. Thus, the slab temperatures were lower than standard temperature. For the block, the match-cured cylinder strengths were considerably greater than the estimated strengths based on the maturity method. This may again be attributed to the strength-enhancing effect of the higher early-age temperature in the block, which reached 33.3°C (91°F). At the 7-day test age, the match-cured cylinder strength was 22.4 MPa (3250 psi). On the other hand, the 7-day standard-cured strength was 19.51 MPa

(2830 psi) (see Table 4.6). For the slab, because the in-place temperatures were not above the standard temperature, the strength-enhancement due to high temperature was absent. As a result, there was reasonable agreement between the match-cured cylinder strengths and the estimated strength based on maturity (see Table 4.10). The estimated strengths based on the pullout test were in good agreement with the strengths of the match-cured cylinders at the 2-day test age. At 4 and 7 days, the estimated strengths from pullout were considerably less than the match-cured cylinders. Again, this could be related to thermal strains that reduce the pullout resistance in the surface layer, but this premise needs to be studied further.

35 % FA-C mixture—The in-place temperature used to calculate equivalent age of the block reached a maximum value of 43.9°C (111°F). At test ages of 2, 4, and 7 days, the equivalent ages for the block were 3.7, 6.4, and 9.6 days. The standard-cured cylinder strength at 7 days was 24.1 MPa (3500 psi), while the match-cured cylinder strength at an equivalent age of 6.4 days was 30.3 MPa (4400 psi). Thus, the enhancing effect of high temperature on long-term strength appears to be present, and this would explain why the estimated strengths based on maturity are consistently lower than the match-cured cylinder strengths. At the 2-day test age, the estimated strength from the pullout test is close to the match-cured cylinder strength. At 4 and 7-day test ages, however, the estimated strengths from the pullout test are considerably lower than the match-cured cylinders. This is consistent with the behavior in all the other cases.

Summary—Figure 4.22 to Figure 4.27 compare the various estimates of in-place strength as a function of the equivalent age at the time of testing based on the iButton data and the activation energies of the various mixtures. In general, the field-cured cylinders resulted in the lowest strengths because of their lower in-place temperatures. The match-cured cylinder strengths were assumed the best estimates of in-place strength, but these strengths were consistently higher than the estimates based on the maturity method or the pullout test. Two factors have been suggested for this behavior:

1. There may be a systematic effect related to the nature of the match-cured specimens (degree of consolidation and drying effect) that results in a higher apparent strength.
2. The higher in-place temperature of the match-cured cylinders may have introduced the strength enhancing effect that was observed in the mortar specimens cured at elevated temperatures.

Both of these proposed factors require additional research. Finally, the lower estimated strengths based on the pullout test might be related to tensile strains introduced into the surface concrete due to thermal gradients and moisture gradients. This suggestion also requires additional research

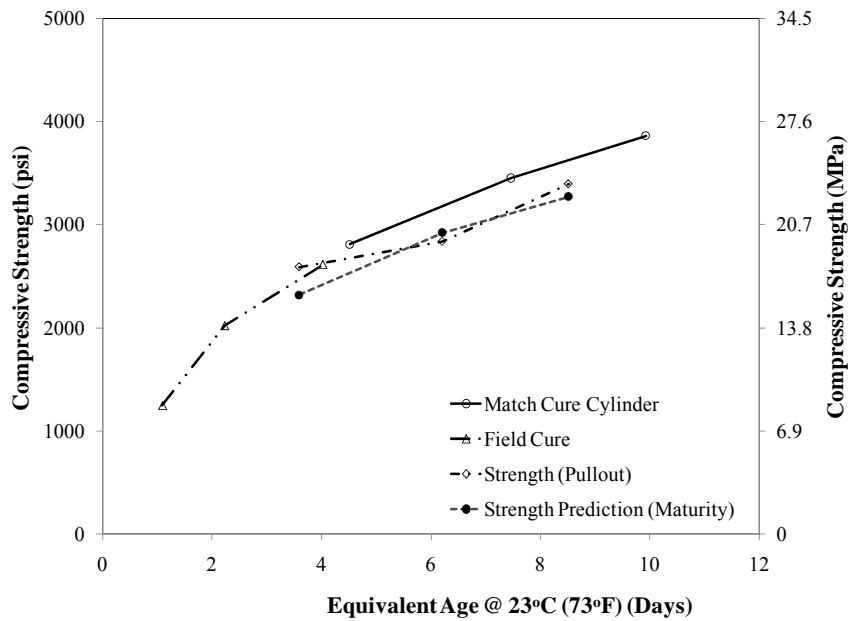


Figure 4.22 Comparison of strength obtained from various methods vs. equivalent age (control-mixture block)

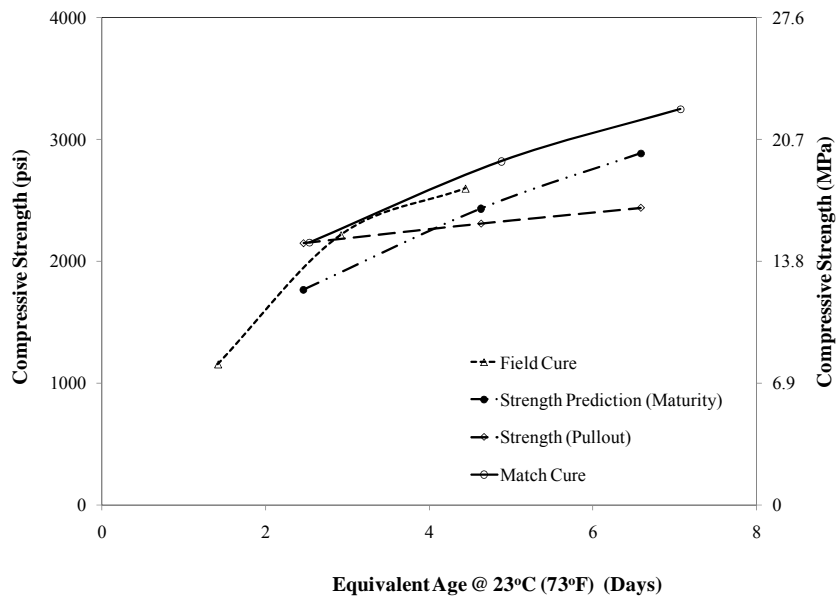


Figure 4.23 Comparison of strength obtained from various methods vs. equivalent age (50% FA-A block)

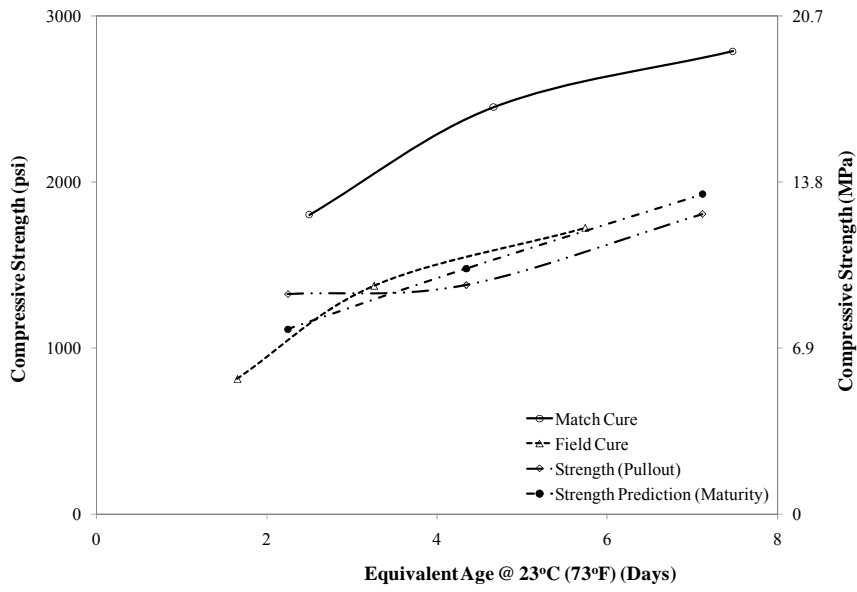


Figure 4.24 Comparison of strength obtained from various methods vs. equivalent age (35% FA-A block)

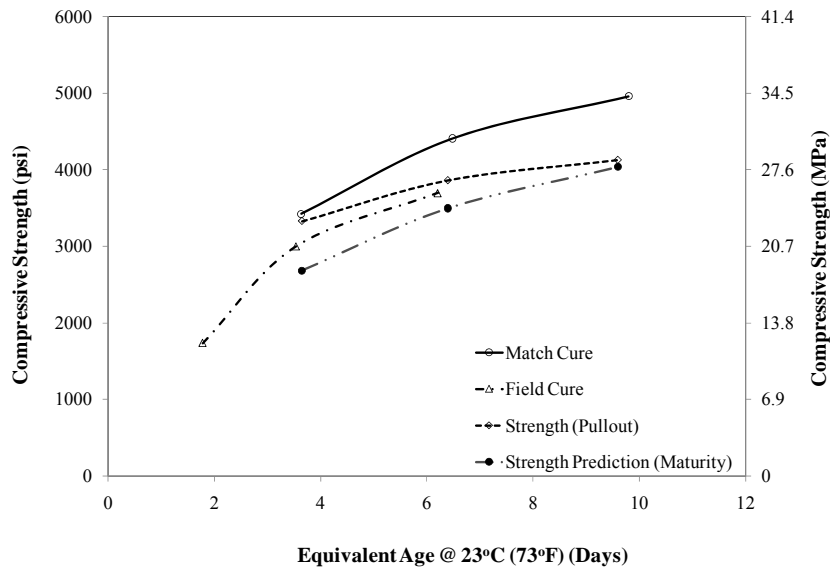


Figure 4.25 Comparison of strength obtained from various methods vs. equivalent age (35% FA-C block)

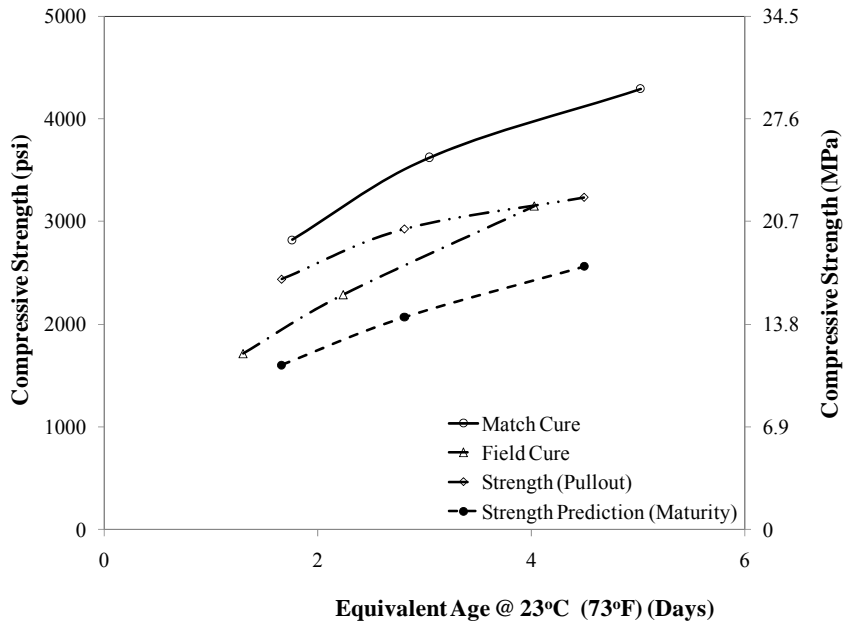


Figure 4.26 Comparison of strength obtained from various methods vs. equivalent age (control mixture-slab)

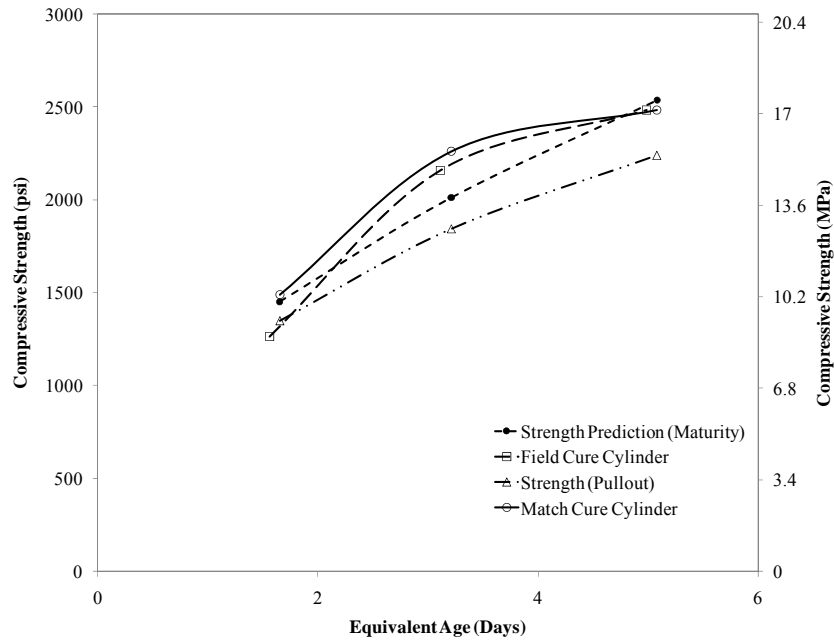


Figure 4.27 Comparison of strength obtained from various methods vs. equivalent age (50% FA-A-slab)

Table 4.9 Strength prediction using maturity and pullout correlation

Mixture	Concrete Element	Actual Age (Days)	Equivalent Age (23°C, 73°F) (days)	Strength Prediction Maturity Method MPa (psi)	Pullout Load (kN)	Strength Prediction Pullout Correlation MPa(psi)
Control Mixture	Block	2	3.60	16.0 (2322)	17.2	17.9 (2590)
		4	6.21	20.2 (2922)	18.5	19.6 (2836)
		7	8.51	22.6 (3271)	21.5	23.4 (3395)
	Slab	2	1.7	11.1 (1605)	16.3	16.8 (2437)
		4	2.8	14.3 (2069)	19.0	20.2 (2928)
		7	4.5	17.7 (2561)	20.7	22.3 (3237)
35% FA-A	Block	2	2.2	7.3 (1058)	10.8	9.1 (1325)
		4	4.3	10.2 (1477)	11.1	9.5 (1379)
		7	7.1	13.3 (1925)	13.6	12.4 (1804)
50% FA-A	Block	2	2.4	12.2 (1769)	16.6	14.8 (2151)
		4	4.6	16.8 (2434)	17.5	15.9 (2311)
		7	6.6	16.8 (2887)	18.2	16.8 (2441)
	Slab	2	1.6	10.0 (1448)	11.8	9.3 (1349)
		4	3.2	13.9 (2014)	14.8	12.7 (1844)
		7	5.1	17.6 (2550)	17.1	15.4 (2240)
35% FA-C	Block	2	3.7	18.5 (2685)	20.4	22.9 (3325)
		4	6.4	24.1 (3496)	23.0	26.6 (3858)
		7	9.6	27.8 (4035)	24.3	28.4 (4123)

Table 4.10 Strength comparison between various curing condition and predicted strength

Mixture	Concrete Element	Actual Age (Days)	Match Cure Strength MPa (psi)	Strength Prediction Maturity Method MPa (psi)*	Strength Prediction Pullout Correlation MPa (psi)*	Field Cure MPa (psi)*
Control Mixture	Block	2	19.4 (2810)	16.0 (2322) (-17.4)	19.9 (2590) (-7.8)	8.6 (1249) (-55.6)
		4	23.7 (3452)	20.2 (2922) (-15.4)	19.6 (2836) (-17.8)	13.9 (2021) (-41.5)
		7	26.6 (3861)	22.6 (3271) (-15.3)	23.4 (3395) (-12.1)	18.0 (2615) (-32.3)
	Slab	2	19.5 (2825)	11.1 (1605) (-43.2)	16.8 (2437) (-13.7)	11.8 (1717) (-39.2)
		4	25.0 (3625)	14.3 (2069) (-42.9)	20.2 (2928) (-19.2)	15.8 (2288) (-36.9)
		7	29.6 (4289)	17.7 (2561) (-40.3)	22.3 (3237) (-24.5)	21.7 (3148) (-26.6)
35% FA-A	Block	2	12.4 (1802)	7.3 (1058) (-41.3)	9.1 (1325) (-26.5)	5.6 (813) (-54.9)
		4	16.9 (2450)	10.2 (1477) (-39.7)	9.5 (1379) (-43.7)	9.5 (1374) (-43.9)
		7	19.2 (2786)	13.3 (1925) (-30.9)	12.4 (1804) (-35.2)	11.9 (1722) (-38.2)
50% FA-A	Block	2	14.9 (2156)	12.2 (1769) (-17.9)	14.8 (2151) (-0.2)	8.0 (1155) (-46.4)
		4	19.5 (2823)	16.8 (2434) (-13.8)	15.9 (2311) (-18.1)	15.3 (2216) (-21.5)
		7	22.4 (3251)	19.9 (2887) (-11.2)	16.8 (2441) (-24.9)	17.9 (2599) (-20.1)
	Slab	2	10.3 (1491)	10.0 (1448) (-2.9)	9.3 (1349) (-9.5)	8.7 (1263) (-15.3)
		4	15.6 (2262)	13.9 (2014) (-11.0)	12.7 (1844) (-18.5)	14.9 (2159) (-4.6)
		7	17.6 (2545)	17.6 (2550) (0.2)	15.4 (2240) (-12.0)	17.1 (2485) (-2.4)
35% FA-C	Block	2	23.6 (3422)	18.5 (2685) (-21.5)	22.9 (3325) (-2.8)	11.9 (1732) (-49.4)
		4	30.4 (4405)	24.1 (3496) (-20.6)	26.6 (3858) (-12.4)	20.7 (2998) (-31.9)
		7	34.2 (4953)	27.8 (4035) (-18.5)	28.4 (4123) (-16.8)	25.5 (3695) (-25.4)

* values in the second brackets are strength percent difference between match cure and that column

Table 4.11 Average percent differences between match cured and various other in-place strength prediction techniques

Mixture	Concrete Element	Maturity Method, % (based on standard Cure Cylinders)	Pullout, %	Field Cure
Control	Block	-16.0	-12.6	-43.1
	Slab	-42.1	-19.1	-34.2
35% FA-A	Block	-37.3	-35.1	-45.7
50% FA-A	Block	-14.3	-14.4	-29.3
	Slab	-4.6	-13.3	-7.4
35% FA-C	Block	-20.2	-10.7	-35.6
Average		-22.4	-17.5	-32.6

Chapter 5 Semi-Adiabatic Calorimetry Testing

The curing temperature of the concrete is arguably the variable that has the most significant effect on the rate of hydration. In this section, the maturity method is used to account for the effect of temperature and time on the rate of hydration. The equivalent age maturity function shown in Equation 15, as developed by Freiesleben and Pedersen (1977), is widely accepted as the most accurate maturity formulation.

$$t_e(T_r) = \sum_0^t \exp\left(\frac{E}{R}\left(\frac{1}{273+T_r} - \frac{1}{273+T_c}\right)\right) \cdot \Delta t \quad \text{Equation 15}$$

- where: $t_e(T_r)$ = equivalent age at the reference curing temperature (hours),
 Δt = chronological time interval (hours),
 T_c = average concrete temperature during the time interval, Δt , ($^{\circ}\text{C}$),
 T_r = constant reference temperature ($^{\circ}\text{C}$),
 E = activation energy (J/mol), and
 R = universal gas constant (8.3144 J/mol/K)

The hydration reaction of Portland cement is an exothermic process, and the total amount of heat generated may affect the in-place performance of some structures. The total heat released during hydration is a function of the composition of cementitious materials, amount of cementitious

materials, and the water-cementitious material ratio of the mixture. In the remainder of this section, models to quantify the total heat of hydration, degree of hydration, temperature sensitivity, and the temperature associated with the hydration of concrete are presented.

5.1 Quantifying the Total Heat of Hydration of the Cementitious Materials

The total heat of hydration (at 100% hydration) can be estimated directly from the cement chemistry (Bogue 1947). Each of the cement constituents have been found to have a unique heat of hydration and the total heat of hydration of the cement at complete hydration (H_{cem}) can be quantified as shown in Equation 16.

$$H_{cem} = 500 p_{C_3S} + 260 p_{C_2S} + 866 p_{C_3A} + 420 p_{C_4AF} + 624 p_{SO_3} + 1186 p_{FreeCaO} + 850 p_{MgO}$$

Equation 16

where: H_{cem} = total heat of hydration of the cement (J/g), and
 p_i = weight ratio of i-th compound in terms of the total cement content.

The calcium oxide (CaO) of the fly ash has been used as an indicator of its cementitious characteristics and the amount of heat that it may contribute during hydration with Portland cement (Schindler and Folliard 2005). With knowledge of the total cementitious materials content (C_c), and the heat of hydration (H_u) per unit weight of all the cementitious materials, the ultimate heat of hydration (H_T) for combinations of cement and fly ash at 100% hydration can be modeled as shown in Equations 17 and 18.

Equation 17

$$H_T = H_u \cdot C_c$$

where: H_T = total ultimate heat of hydration of the concrete (J/m^3),

C_c = cementitious materials content (g/m^3), and

H_u = total heat of hydration of cementitious materials at 100% hydration (J/g),

defined as follows:

Equation 18

$$H_u = H_{cem} \cdot p_{cem} + 1800 \cdot p_{FACaO} \cdot p_{FA}$$

where: p_{cem} = cement weight ratio in terms of total cementitious content,

p_{FA} = fly ash weight ratio in terms of total cementitious content, and

p_{FACaO} = fly ash CaO weight ratio in terms of the total fly ash content.

5.2 Quantifying the Degree of Hydration Development

The degree of hydration (α) is a measure of the extent of the hydration reactions between the cementitious materials and the water, and is defined as the ratio between the quantity of hydrated cementitious material and that total hydrated amount on complete hydration of the original cementitious material. The degree of hydration is a function of time, with α varying between 0%, at the start of hydration, and 100% when hydration is fully completed. In reality, not all of the cementitious material always hydrates, and a degree of hydration of 100% may never be reached

(Mills 1966). The degree of hydration versus equivalent age relationship is used to characterize the hydration behavior of a specific concrete mixture at the reference temperature (T_r).

In this research, the indirect method of estimating the degree of hydration based on the heat development that occurs during hydration is used. It has been shown that the heat released divided by the total heat available provides a good measure of the degree of hydration (Van Breugel 1997), and this is mathematically express as follows:

$$\alpha(t) = \frac{H(t)}{H_T} \quad \text{Equation 19}$$

where: $\alpha(t)$ = degree of hydration at time, t , and

$H(t)$ = cumulative heat of hydration released at time, t , (J/m^3).

Once test data of the degree of hydration development have experimentally been determined, the data can be represented by a best-fit mathematical model. The exponential formulation shown in Equation 20 has been shown to accurately represent the s-shape of the hydration development (Schindler and Folliard 2005)

$$\alpha(t_e) = \alpha_u \cdot \exp\left(-\left[\frac{\tau}{t_e}\right]^\beta\right) \quad \text{Equation 20}$$

where: $\alpha(t_e)$ = the degree of hydration at equivalent age, t_e ,

- τ = hydration time parameter (hours),
- β = hydration shape parameter, and
- α_u = ultimate degree of hydration.

5.3 Temperature Sensitivity of Cementitious Materials

In the equivalent age maturity method, the activation energy defines the temperature sensitivity of a concrete mixture. By using the equivalent age maturity approach, the rate of hydration at any specific temperature can be determined from a known rate of hydration at the reference temperature. It has been shown that the activation energy (E) for strength and hydration prediction purposes may be very different. Schindler (2004) evaluated the temperature sensitivity of the hydration process over a temperature range of 4.4°C to 40.6°C and developed the activation energy model shown in Equation 21.

$$E = 22,100 \cdot p_{C_3A}^{0.30} \cdot p_{C_4AF}^{0.25} \cdot Blaine^{0.35} \cdot \left(1 - 1.05 \cdot p_{FA} \cdot \left(1 - \frac{p_{FACaO}}{0.40} \right) \right) \quad \text{Equation 21}$$

- where: p_{C_3A} = weight ratio of C_3A in terms of the total cement content,
- p_{C_4AF} = weight ratio of C_4AF in terms of the total cement content, and
- $Blaine$ = Blaine value, specific surface area of cement (m^2/kg).

5.4 Modeling the Heat Generation and Temperature Associated with Hydration

The temperature development in a concrete specimen curing under adiabatic conditions (where there is no heat transfer to the environment) can be determined with Equation 22 (Jonasson et al. 1995).

$$\frac{dT}{dt} = \frac{Q_H}{\rho \cdot c_p} = \frac{dH}{dt} \left(\frac{1}{\rho \cdot c_p} \right) \quad \text{Equation 22}$$

where: T = temperature of the concrete ($^{\circ}\text{C}$),
 ρ = concrete density (kg/m^3),
 c_p = concrete specific heat capacity ($\text{J}/\text{kg}/^{\circ}\text{C}$),
 Q_H = rate of heat generation (W/m^3), and
 H = heat of hydration of the concrete (J/m^3), equal to $H_T \cdot C_c \cdot \alpha$.

The rate of heat generation heat, Q_H , is dependent on the degree of hydration. The degree of hydration is a function of the time and temperature history, which can be characterized by the equivalent age maturity function. With this approach, the adiabatic temperature rise of the concrete specimen can be evaluated at discrete times after batching. By using the equivalent age maturity method and the exponential formulation to quantify the degree of hydration (Equation 20), the rate of heat generation, at time t , can be determined as shown in Equation 23 (Schindler and Folliard 2005).

$$Q_H(t) = H_u \cdot C_c \cdot \left(\frac{\tau}{t_e}\right)^\beta \cdot \left(\frac{\beta}{t_e}\right) \cdot \alpha(t_e) \cdot \exp\left(\frac{E}{R} \left(\frac{1}{273+T_r} - \frac{1}{273+T_c}\right)\right) \quad \text{Equation 23}$$

5.5 Experimental Work

Semi-adiabatic calorimetry was used in this research to quantify the hydration development of various cementitious systems. There is currently no standardized ASTM test method for semi-adiabatic calorimetry; however, the test was performed based on the draft test procedure of RILEM TCE-119 (1998). Tests were performed on six mixture proportions—as listed in Table 5.1, and each test was performed over approximately a six-day period. These six mixture proportions match those used during the field work performed during this research. A standard cement source was chosen, and the type and dosage level of the SCMs used with the cement were changed. The following three fly ashes were used: 1) low-lime Class F fly ash, 2) intermediate-lime Class F fly ash, and 3) Class C fly ash. These three fly ashes are identified by the letter A, B, and C, respectively, in Table 5.1.

Table 5.1: Mixture proportions used for semi-adiabatic testing

Item	Mixture ID					
	Control	20%FA-A	35%FA-A	50%FA-A	35%FA-B	35%FA-C
Cement, kg/m ³ (lbs/yd ³)	302.6 (510)	251.5 (424)	196.4 (331)	182.7 (308)	220.1 (371)	215.4 (363)
Fly Ash, kg/m ³ (lbs/yd ³)	0	62.9 (106)	116.3 (196)	176.8 (298)	118.7 (200)	117.5 (198)
Water, kg/m ³ (lbs/yd ³)	169.7 (286)	160.2 (270)	157.2 (265)	140.6 (237)	143.6 (242)	141.2 (238)
Coarse Agg. SSD, kg/m ³ (lbs/yd ³)	1154.4 (1,946)	1156.9 (1,950)	1164.0 (1,962)	1170.5 (1,973)	1156.9 (1,950)	1154.5 (1,946)
Fine Agg. SSD, kg/m ³ (lbs/yd ³)	782.5 (1,319)	772.4 (1,302)	755.2 (1,273)	730.9 (1,232)	792.0 (1,335)	812.2 (1,369)
Target Total Air Content, %	3	3	3	3	3	3
HRWR Admixture, ml /ft ³ (oz/yd ³)	245.2 (10.7)	364.3 (15.9)	808.8 (35.3)	985.2 (43.0)	653.0 (28.5)	655.3 (28.6)
w / cm	0.56	0.51	0.51	0.39	0.43	0.43
Fly ash ID	-	FA-A	FA-A	FA-A	FA-B	FA-C
Fly ash CaO Content (%)	-	1.2	1.2	1.2	13.3	23.4

The batch size was 0.02 m³ (1.5 ft³) and the concrete was made under laboratory conditions. The following tests were performed on each batch to ensure that the concrete was acceptable: slump, fresh concrete temperature, total air content, fresh concrete unit weight, and the 28-day compressive strength. Three, moist-cured, cylinders were tested at 28 days to verify the concrete's strength potential.

With semi-adiabatic calorimetry, a small amount of heat loss is allowed to occur over time. Therefore, the temperature development is not as high as it would be under fully adiabatic conditions. Due to the elevated temperatures reached during hydration, most of the hydration is completed in a short period of time (7 days). A disadvantage of the semi-adiabatic test method is that the true adiabatic heat development has to be calculated from the test results, and losses associated with the test have to be accounted for. Once the test data are collected, the degree of hydration can be computed based on heat transfer principles and with the heat of hydration model previously document in Equations 18, 20, 21, and 23. The result can thus be affected by inaccurate assumptions of activation energy (temperature sensitivity) and material properties such as thermal conductivity, specific heat, and density. These results will show the effect of all the mixture proportions on the rate of hydration, total heat of hydration, setting, and to some extent the degree of hydration. These results will be useful to show how the addition of various amounts and types of fly ashes alter the hydration process of these mixtures.

5.6 Test Data and Discussion of Results

The concrete quality control tests that were performed on each batch are summarized in Table 5.2. Note that all fresh properties were acceptable and similar for the six batches. It can also be seen from Table 5.2, that the 28-day strength of Mixture 35%FA-B was more than 8.3 MPa (1200 psi) lower than that of Mixtures 35%FA-A and 35%FA-C. It is unusual that the strength of Mixture 35%FA-B is lower than that of Mixture 35%FA-A, simply since mixture 35%FA-B had a lower w/cm than that of 35%FA-A mixture.

Table 5.2: Quality control data collected for batches produced for semi-adiabatic testing

Parameter	Mixture ID					
	Control	20%FA-A	35%FA-A	50%FA-A	35%FA-B	35%FA-C
Slump (in.)	7.5	7.5	6	8	6.5	6
Concrete Temp. (°F)	74	74	72	73	71	74
Total Air Content (%)	2.25	2.5	2	2	2	2
Unit Weight (lb/ft ³)	150.4	152.5	154.6	154.5	155.2	154.8
28-day Comp. Strength (psi)	5,190	5,370	6,260	6,070	4,970	6,550

Table 5.3 provides a summary of the best-fit hydration parameters that were obtained from the semi-adiabatic test data. The activation energy values listed in Table 5.3 were determined with the activation energy model shown in Equation 19. A reference temperature of 22.8°C (73°F) was used during the back-calculation of the hydration parameters. The hydration parameters are of the expected order of magnitude, except for the ultimate degree of hydration for Mixture 35%FA-B; this is also the mixture that exhibited a lower than expected 28-day compressive strength. The ultimate degree of hydration for a mixture made with these materials and proportions should be in the range of 0.75 to 0.90. The increase in the hydration time parameter, τ , for Mixture 35%FA-C

relative to any of the other mixtures indicates that a retardation of the hydration reaction has occurred. This retardation would correspond to an increase in initial and final setting times, which is typical for Class C fly ash mixtures. The hydration parameters listed in Table 5.3 can be used to model the in-place temperature development with a heat transfer model that is appropriate for the specific member size and boundary conditions.

Table 5.3: Best-fit hydration parameters obtained from semi-adiabatic testing ($T_r = 22.8^\circ\text{C}$)

Parameter	Mixture ID					
	Control	20%FA-A	35%FA-A	50%FA-A	35%FA-B	35%FA-C
E-value for Hydration (kJ/mol)	46.1	36.4	28.1	22.3	29.2	29.1
Total Heat of Hydration (J/kg)	488	394	314	258	401	464
Slope Parameter, β	0.785	1.024	1.000	1.100	0.990	0.899
Time Parameter, τ (hours)	17.8	13.3	13.7	13.4	13.0	24.6
Ultimate DOH, α_u	0.913	0.854	0.770	0.837	0.579	0.855

The semi-adiabatic calorimetry test results are summarized in Figure 5.1 to Figure 5.4. Figure 5.1 and Figure 5.2 can be used to evaluate the effect that changes in fly ash A proportions and w/cm will have on the hydration behavior. The proportions of these mixtures do not allow one to only evaluate the effect of an increase in the dosage of fly ash A. This is because an increase in w/cm was required to achieve realistic rates and levels of compressive strength gain. It may be seen in Figure 5.1 that there is a significant reduction in cumulative heat of hydration as the replacement level of fly ash A is increased. This trend is true even though in general the w/cm was decrease as the replacement level of fly ash A was increased. It is also significant to note that the mixtures made with fly ash A all have 28-day strengths that exceed that of the control mixture, yet they generate much less heat and this would be advantageous in mass concrete applications. It can be

seen from Figure 5.1 that the cumulative heat of hydration development of Mixture 35%FA-A and 50%FA-A are very similar. These mixtures also had similar strength levels. The rate of hydration for Mixture 35%FA-A and 50%FA-A are very similar, as shown in Figure 5.2. This would be an indication that the decrease in w/cm to change from a 35% to a 50% replacement level produced mixtures with very similar hydration kinetics.

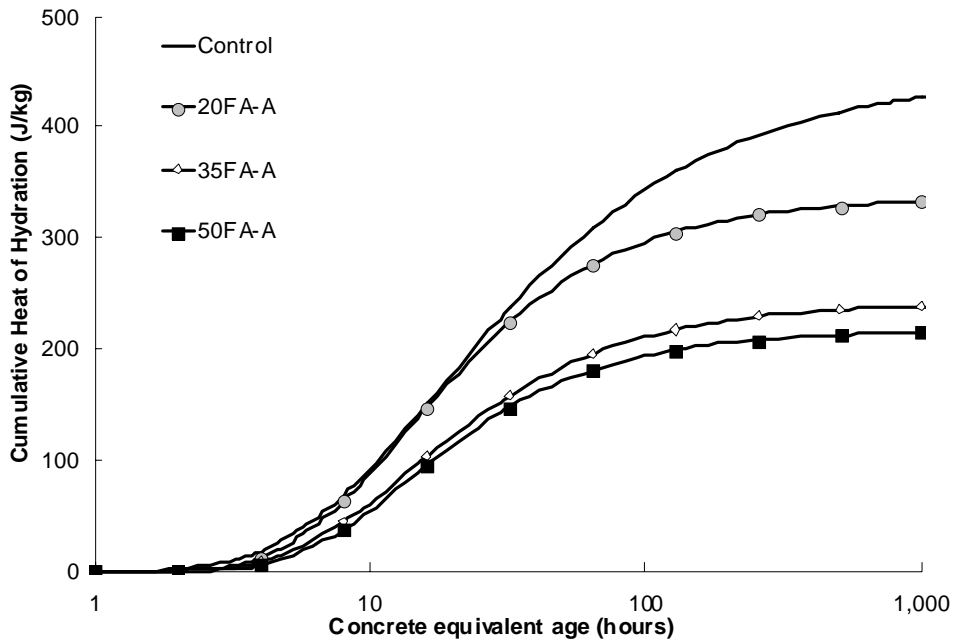


Figure 5.1 Effect of change in fly ash proportions and w/cm on cumulative heat of hydration development

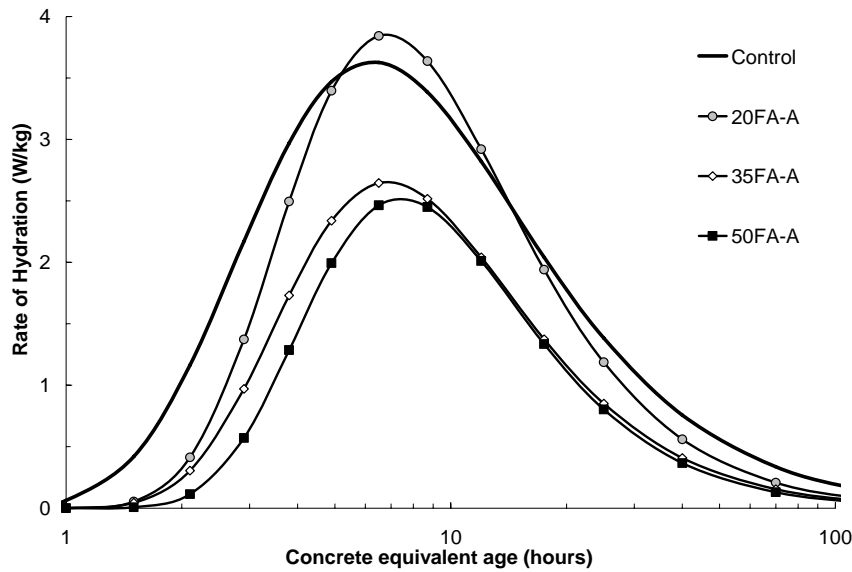


Figure 5.2 Effect of change in fly ash proportions and w/cm on rate of hydration

Figure 5.3 and Figure 5.4 can be used to evaluate the effect that a change in fly ash type and w/cm will have on the hydration behavior. A comparison of the cumulative heat of hydration of the Control mixture and Mixture 35%FA-C as shown in Figure 5.3 reveals that the Class C fly ash retarded setting of the mixture and it only slightly reduced the cumulative heat of hydration. The retardation effect when the Class C fly ash (35%FA-C) is used, can clearly be seen on the rate of hydration graph shown in Figure 5.4. Fly ash A and B did not retard setting much and both significantly reduce the cumulative heat of hydration. The cumulative heat of hydration of Mixture 35%FA-B appears to be lower than expected; and this issue was mentioned when the hydration parameters were discussed. The data shown in Figure 5.3 and Figure 5.4 show that the total heat of hydration of the cementitious system is significantly reduced with the use of a replacement of 35%

Class F. The data in Figure 5.3 indicates that Class F fly ash has little contribution to the early-age heat development.

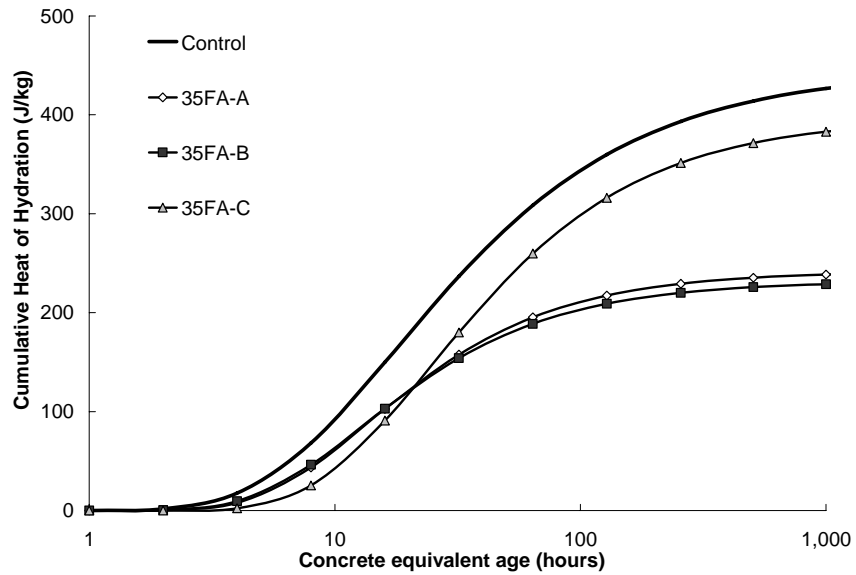


Figure 5.3 Effect of change in fly ash type and w/cm on cumulative heat of hydration development

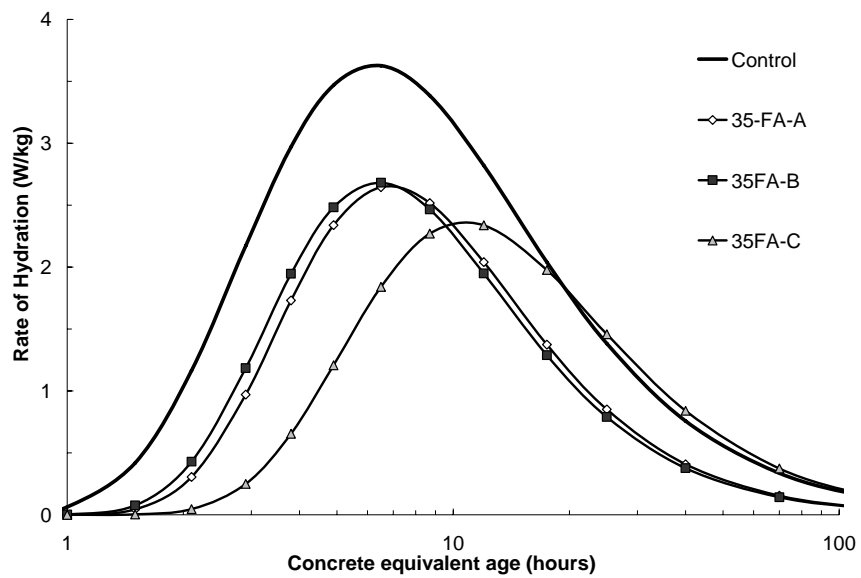


Figure 5.4 Effect of change in fly ash type and w/cm on rate of hydration

Chapter 6 Step by Step Procedure for Optimizing the Design of HVFA Mixtures

This chapter provides the systematic guidelines developed with NRMCA (Obla et. al. 2008) for the construction team (contractor, concrete producer, and engineer) and provides recommendations on the application of the maturity method to support the use of optimized HVFA concrete mixtures by providing a simple method to estimate in-place strength development. The optimized HVFA mixture proportions will allow to evaluate the lowest total cementitious materials contents and highest water-cementitious materials ratio (w/cm) that can be permitted for durability concrete that can still attain the early-age strengths required for a specific application.

6.1 Step-by-Step Approach

The following approach is suggested in the application of the maturity method to facilitate the use of optimized higher volume fly ash (HVFA) concrete mixtures while accounting for their effect on the early-age strength gain and the resulting impact on construction operations. The approach consists of three phases:

Phase I—Develop the HVFA concrete mixture proportions and determine the strength maturity relationship of that concrete.

Phase II—Carry out computer simulations of the construction process to determine whether the proposed HVFA mixture will meet the early-age strength requirements under anticipated field temperature conditions.

Phase III—Use the maturity method to estimate in-place concrete strength development during construction.

This procedure is described next:

6.1.1 Strength Requirement for Structural Application

It is important that the design professional establish an appropriate early-age strength requirement for a specific application (such as form removal, application of prestressing, early in service opening of pavements, etc.) of HVFA concrete. Standard practice followed by the construction industry before the application of any load on structural elements is that, concrete should attain at least 70% of the specified 28-day strength. It is important to determine the specific early-age strength level that is required based on the structural design and the anticipated loads applied at these early ages, for example, a requirement of 19.3 MPa (2800 psi) in 72 hours. The reason for this is the slower rate of HVFA early-age strength development compared to conventional concrete.

6.1.2 Mix Design of HVFA Concrete

The purpose of this phase is the selection of appropriate concrete ingredient materials and the establishment of HVFA concrete mixture proportions that will achieve the required early-age strength and other performance requirements.

Material Selection:

Early age strength is critical for some applications; it is practical to select appropriate materials that can attain the required early-age strengths. It is necessary to be careful in selecting the type of material to be used for HVFA concrete. It may not be possible to use some of the suggested materials due to material availability and conflicts with other performance criteria.

It is recommended to select a cement source with a higher rate of strength gain. Cements with higher alkali content have been shown to accelerate pozzalonic reactivity; however, such cements may increase the tendency for alkali-silica reactions with susceptible aggregates.

Therefore, it is necessary to conduct alkali silica reactivity test in order to identify any potential problem using high alkali cement. Fly-ash properties such as higher fineness can be used to select fly-ash sources. A HRWR admixture is often necessary to attain the low w/cm and maintain the required workability. Some admixture suppliers are manufacturing HRWR admixtures tailored specifically for HVFA concrete mixtures that reduce the water demand significantly, increase the early-age strength, and reduce the setting time of concrete. A high range water-reducing (HRWR) admixture that does not increase the setting time of concrete at high dosages should be used.

Water to Cementitious material ratio (w/cm) selection

HVFA concrete mixtures, particularly those designed to attain high early-age strength, should have lower w/cm than conventional concretes. While a w/cm as low as 0.27 has been used in some applications (Sivasundaram et al. 1989), in most situations a w/cm of about 0.40 may be

adequate. When proportioning a HVFA mixture to attain high early-age strength, a w/cm of 0.40 is a good starting point. The low w/cm is typically attained by decreasing the mixing water content as much as possible. The lowest value of mixing water content should be in the range of 118.7 to 142.4 kg/m³ (200 to 240 lb/yd³) but this depends on the characteristics of local materials (primarily aggregate size, shape, and texture). Higher water contents may be necessary for slab-type applications that require a trowel finish, since finishability is an important criterion for such applications. Low water content may detract from attaining good finishability even when HRWR admixtures are used.

Cementitious Materials Content

The total cementitious materials content can be determined by dividing the selected mixing water content by the required w/cm . HVFA concrete mixtures typically have a total cementitious materials content that is higher than mixtures containing lower fly ash contents or no fly ash. Typically, the total cementitious materials contents of normal-strength [$f'_c < 4.1$ MPa (6000 psi)]. HVFA concrete mixtures are less than 356 kg/m³ (600 lb/yd³), and usually less than 415.2 kg/m³ (700 lb/yd³).

Adjustment to Cementitious Materials Content

The suitability of a chosen cementitious materials content can be assessed by ensuring that the $w/(c+kf)$ value of the HVFA mixtures is equal to or slightly below the $w/(c+kf)$ value of a control

mixture. That has been found to meet the performance criteria; where k = efficiency factor and w , c , and f are the masses of water, cement, and fly ash, respectively. The efficiency factor of fly ash vary from 0.25 to 0.45, which means that 0.45 kg (1 lb) of fly ash is equivalent to 0.11 kg (0.25 lb) to 0.20 kg (0.45 lb) of cement in terms of early-age strength development. In this research, the efficiency factor was calculated as 0.38 based on similar early-age, standard cured cylinder strengths for the control mixture without fly ash and the mixtures with 35% of the high-lime fly ash (FA-C) and with 50% of the low-lime fly ash (FA-A). It may be necessary to increase slightly the total cementitious materials content of the HVFA mixture to ensure that the $w/(c+kf)$ of the HVFA mixture is slightly below the $w/(c+kf)$ of the control mixture. This process for adjusting the cementitious materials content is illustrated by the following example:

- a. Assume that the concrete supplier has selected appropriate local materials to produce HVFA mixtures.
- b. Assume that the control mixture contains 20% fly ash with a total cementitious material content of 296.6 kg/m^3 (550 lb/yd^3) and a w/cm of 0.50. The goal is to develop a HVFA mixture containing 50% fly ash with an early-age (2 to 4 days) strength that will match that of the control mixture.
- c. Choose a w/cm of 0.40 as a starting point for the HVFA mixture.
- d. Assume that the lowest mixing water content that can be used with local materials is 130.5 kg/m^3 (220 lb/yd^3). This low water content will most likely require the use of a Type F HRWR to attain the desired workability.

- e. The total cementitious materials content is calculated as 130.5 kg/m^3 (220 lb/yd^3)/ $0.40 = 296.6 \text{ kg/m}^3$ (550 lb/yd^3).
- f. Assuming that $k = 0.38$, the calculated value of $w/(c+kf)$ for the control mixture is 0.57. The calculated value of $w/(c+kf)$ for the HVFA mixture is 0.58. Increasing the total cementitious materials content of the HVFA mixture to 296.6 kg/m^3 (562 lb/yd^3) will reduce $w/(c+kf)$ to 0.57, which is the same as the control mixture.
- g. The final HVFA trial mixture is as follows: Cement = 166.7 kg/m^3 (281 lb/yd^3), fly ash = 166.7 kg/m^3 (281 lb/yd^3), and water = 130.5 kg/m^3 (220 lb/yd^3).

6.1.3 Selection of an Activation Energy

In order to determine the maturity index (equivalent age) of the concrete from its temperature history, it is necessary to use the appropriate value of the activation energy (AE). The activation energy defines the temperature dependence of early-age strength development and its value depends primarily on the cementitious materials and mixture proportions that are used. Table 6.1 provides the activation energies for the six mixtures tested in this project. Alternatively, the activation energy for the selected cementitious materials can be determined in accordance with the Annex of ASTM C1074. In calculating the equivalent age at a reference temperature (T_r), such as 23.3°C (73°F), an exponential equation known as the Arrhenius equation is used. The equation requires that temperature be expressed using the absolute temperature scale. So if inch-pound units are used, temperature needs to be converted to the Rankine scale ($^\circ\text{R}$) by adding 459.7 to the temperature in $^\circ\text{F}$. If SI units are used, temperature needs to be converted to the Kelvin scale (K) by adding 273.2 to the temperature in $^\circ\text{C}$. Activation energy is measured in

units of energy per mole and is reported typically in SI units, that is, J/mol, where J stands for joules and "mol" stands for mole. The Arrhenius equation uses the parameter activation energy divided by the universal gas constant (R), and the quotient is often called Q. In SI units, R has a value of about 8.31 J/(K mol), where K stands for degrees Kelvin (note that the degrees symbol is not used with K). When the activation energy is divided by the gas constant, the units are K. For example, if the activation energy is 40,000 J/mol (or 40 kJ/mol), the Q value is 40,000/8.31 (K) or about 4,800 K. The Q values for the six mixtures tested in this project are shown in Table 6.1. Thus, Q-values in units of K need to be multiplied by 1.8 to obtain the value in units of °R. The last column of Table 1 gives the Q-values in terms of °R.

Table 6.1 Activation energies for mixtures

Mixture	w/cm	Activation Energy (kJ/mol)	Q-Value (K)	Q-Value (°R)
Control	0.56	41.4	4890	8960
20% FA-A	0.51	48.1	5790	10410
35% FA-A	0.50	15.6	1880	3380
50% FA-A	0.39	33.4	4020	7230
35% FA-B	0.42	33.0	3970	7140
35% FA-C	0.42	28.3	3400	6130

6.1.4 Develop Strength Maturity Relationship

For the development of the strength-maturity relationship, prepare a trial batch of the HVFA concrete mixture in accordance with ASTM C192/C192M and cast seventeen 4 by 8 in. concrete cylinders. The cylinders should be standard cured in a moist room immediately after they are molded. Two cylinders should have embedded temperature sensors to measure concrete temperature. The sensors are connected to maturity meters or data loggers. Test three cylinders according to ASTM C39/C39M at each age of 1, 3, 7, 14, and 28 days. Temperature data should be collected every half hour or less for the first 48 hours and may be collected at more extended intervals for later ages as specified in ASTM C1074. The strength versus equivalent age data are fitted to an equation that will be used for estimating in-place strength in the actual structure based on measured in-place temperatures. Several equations can be used for this purpose. The ConcreteWorks program uses the following exponential equation, Equation 24:

$$f_c = f_{cu} e^{-\left(\frac{\tau}{t_e}\right)^\beta} \quad \text{Equation 24}$$

Where: f_c = compressive strength (psi);

t_e = equivalent age (hours);

f_{cu} (psi), τ (hours), and β = best fit parameters (maturity constant)

6.1.5 Hydration Parameters for HVFA Concrete

The hydration parameters are used by the thermal analysis program to model the development of heat of hydration. Table 5.3 lists the hydration parameters for the six mixtures tested in this the cementitious materials and mixture proportions have been selected.

6.1.6 Thermal Analysis using ConcreteWorks Thermal Modeling Software

Evaluate whether the selected HVFA mixture will meet the early-age strength requirements. A thermal analysis computer program, such as ConcreteWorks, should be used to verify whether the selected HVFA mixture would meet the early-age strength requirements. The hydration constants and maturity constants of the mixture and construction related parameters are provided as input and the program calculates the temperature histories within the structure. Construction related information would include the specific geometry of the structural member, the location of the structure, the date and time of the placement, and form insulation. Data on the location of the structure and when the concrete will be placed are used to access a database of likely ambient temperatures during construction. Based on the predicted temperature development and the strength-maturity relationship, the program estimates strength development at different locations in the structure. The corner of a member, where two edges meet, will generally be the coldest location and will result in the lowest strength. The center of a member will generally have the highest temperature and highest strength. For traffic opening decisions for concrete pavements,

the in-place strength at the center of the pavement can be estimated. For removal of forms from columns, the estimated strength at 1 in. from the column face can be used. The strength at this location is similar to the average strength predicted by the ConcreteWorks program. The project engineer can decide to use the HVFA mixture if the estimated in-place strengths exceed the early age strength requirements. If the requirements are not met, the HVFA concrete mixture proportions can be modified or alternative formwork insulation methods can be evaluated to increase the internal temperature and strength development. For example, it may be decided to reduce the w/cm by increasing the total cementitious materials content or by adding HRWR admixture, or both, as follows:

Trial B – 50% fly ash, total cementitious materials = 610 lb/yd³, w/cm = 0.36, Type F HRWR admixture; Trial C – 50% fly ash, total cementitious materials = 326.3 kg/m³ (550 lb/yd³), w/cm = 0.40, Type F HRWR admixture specially formulated for HVFA concrete that reduces setting time and enhances early-age strength gain. If a new HVFA mixture is selected, a new strength-maturity relationship needs to be developed.

6.1.7 In-Place Strength Predictions

For reliable estimates of the in-place strength, the value of the activation energy and the strength maturity relationship have to be determined for the materials and mixture proportions used in the

project. However, this is not always possible, especially for small projects. At a minimum, a strength-age curve has to be developed from testing standard-cured cylinders in the laboratory (step 4). In that case, the strength versus age curve is a good approximation of the strength versus equivalent age relationship, provided the temperature of the concrete specimens is maintained within 21.1°C (70°F) to 24.4°C (76°F). Prior to performing critical operations, such as formwork removal or post-tensioning, strengths estimated from the maturity method have to be verified with other tests to ensure that the concrete in the structure has a potential strength that is similar to that of the concrete used to develop the strength-maturity relationship. This is because the maturity method is based on measuring only the in-place temperature, and this measurement cannot detect batching errors. When the maturity method indicates adequate in-place strength, verification tests using the pullout test can be done on the structure in accordance with ASTM C900. This would require embedding pullout inserts in the concrete during placement. Alternatively, early-age tests of field cast cylinders can be used to estimate the potential 28-day strength. This can be done in accordance with ASTM C918/C918M.

Chapter 7 Conclusions

The following conclusions were obtained from this research:

- 1) Compressive strength measured from field-cured and standard-cured cylinders does not provide reliable estimates of in-place strengths for concrete structures. To this regard, match-cured cylinders better estimate the actual field in-place strength of structural members.
- 2) Match-cured strength test data has clearly demonstrated that HVFA concrete in actual structures has much higher early-age strengths than the strengths measured by testing cylinders that were cured under standard laboratory conditions. This means that concrete mixture proportions may be further optimized (use of lower total cementitious contents, increase the quantity of fly ash and/or higher w/cm) without negative effects on construction operations.
- 3) Pullout test results can be correlated to compressive strength results of HVFA concrete mixtures. Since pullout test results are dependent on many factors, (eg: aggregate type, and other concrete composition parameters) these relationships need to be determined for every specific mixture considered.

- 4) Estimated strength based on maturity method and the pullout test method was 15 to 20% lower as compared to match-cured cylinder strengths at identical actual early ages of 2 to 7 days. However, they were much more accurate than field-cured cylinders, which were about 20 to 50% lower.

- 5) Mortar cubes of HVFA mixtures have shown increased long-term strengths when cured at higher temperatures as compared to cubes cured at lower temperatures. Further investigation is needed to better understand this unusual observation and improve the strength estimation by maturity.

- 6) Extensive age strength maturity modeling was conducted using a variety of alternatives for predicting ultimate concrete strength. The results show that the variable S_u and Constant S_{uc} provide the best predictions for HVFA mixtures. Further analysis revealed that the constant S_{uc} models estimated reliable strength for supplementary cementitious mixtures, while the variable S_u method predicts better concrete strength for straight Portland cement mixtures.

- 7) Alternative methods for estimating the activation energy of concrete mixtures were examined. It was shown that the method based on the setting time approach has a significant potential for doing so. Such alternative method is particularly useful since it

requires less time and effort, providing yet reliable activation energy for cementitious mixtures.

8) A step by step methodology was developed providing recommendations on the application of the maturity method to support the use of optimized HVFA concrete mixtures. This methodology provides the procedure to estimate in-place strength. Objective of this approach is to optimize HVFA mixture proportions to provide the lowest total cementitious content and the highest water-cementitious ratio (w/cm) meeting acceptable concrete durability and attaining the required early-age strength.

9) Even though this experimental study included a variety of fly ash types and content in concrete mixtures, further research is needed to extend and validate the results.

Appendix A

Appendix A summarizes the details of the testing plan adopted for this research.

The HVFA concrete mixtures included in this research are shown in Table A.1.

Table A.1 Mixture Proportions

Item	Control	20%FA-A	35%FA-A	50%FA-A	35%FA-B	35%FA-C
Type I cement, kg/ m ³ (pcy)	296.6 (500)	251.5 (424)	220.1 (371)	178.0 (300)	220.1 (371)	220.1 (371)
Fly ash, kg/ m ³ (pcy)	0	62.9 (106)	118.7 (200)	178.0 (300)	118.7 (200)	118.7 (200)
Total Cementitious	296.6 (500)	314.4 (530)	338.8 (571)	356.0 (600)	338.8 (571)	338.8 (571)
Fly ash (%)	0%	20%	35%	50%	35%	35%
Water, kg/ m ³ (pcy)	172.1 (290)	160.2 (270)	143.6 (242)	128.1 (216)	143.6 (242)	143.6 (242)
w/cm	0.58	0.51	0.42	0.36	0.42	0.42
w/c	0.58	0.64	0.65	0.72	0.65	0.65
Type A WR, ml/45 kg (oz/cy)	119.8 (4)	119.8 (4)	119.8 (4)	119.8 (4)	119.8 (4)	119.8 (4)
Type F HRWR, ml/45 kg (oz/cy)	0	0	Adjust	Adjust	Adjust	Adjust
Lab-Concrete	X		X	X		X
Field-Block	X		X	X		X
Field-Slab	X			X		
Lab-Mortar	X	X	X	X	X	X

The target slump will be 10.2 to 15.2 cm (4 to 6 in.)

Task 2. Activation Energy (ASTM C1074).

Objectives:

- Establish the activation energy of the different cementitious systems.
 - Examine whether there is a relationship between the activation energy and the amount of fly ash.
- a. Mixtures:

Six (6) mortar mixtures will be used for this research

- i. Portland cement only
 - ii. Class F fly ash at 3 levels (20, 35, 50 % of total cementitious material)
 - iii. Intermediate (10%) and high (25%) lime Class C fly ash at 35% only
- b. Fly ash concrete mixtures are proportioned so that early strength at 3 and 7 days will be comparable to that of the Portland cement control mixture. The target strength value for the control mixture will be between 27.6 to 34.5 MPa (4000-5000 psi). The mortar mixtures will be proportioned so that the ratios of FA/C are the same as the ratios of CA/C in the corresponding concretes, as recommended in Annex A1 of ASTM C1074.
- c. Mortars will be mixed and cured at 4 temperatures [7.2°C (45°F), 21°C (70°F), 37.8°C (100°F), and 48.9°C (120°F)]. The mortar cubes will be cured in lime-saturated water baths.
- d. Mortar cubes will be tested for compressive strength at 6 different ages. These ages are equivalent ages based on curing at 23°C (73°F), the ages are 1, 2, 4, 7, 14, and 28 days.

Table A.2 Initial Activation Energy

Mixture Proportion	Initial activation energy
Control: Portland Cement Only	40,000 J/mol
20% Class F Ash	38,000 J/mol
35% Class F Ash	32,000 J/mol
50% Class F Ash	28,000 J/mol
35% Class C Ash (Cao=10%)	34,000 J/mol
35% Class C Ash (Cao=25%)	36,000 J/mol

- e. Total of sixteen (24) 5.08 cm (2 in.) cubes will be made per batch
 - i. 3 cubes for each age ($3 \times 6 = 18$)
 - ii. 2 cubes with one I-buttons sensor each will be prepared to record mortar temperature.
 - iii. 4 extra cubes
- f. Cube temperature will be recorded with an I-Button sensor at 60-min interval.
- g. Cubes will be tested for compressive strength at each age in accordance with ASTM C109.
- h. Strength-age relationship will be determined by regression analysis.
- i. Determine k values by fitting the following equation to the strength-age data for each curing temperature.

$$S(t) = S_u \frac{k(T) \times (t - t_o)}{1 + k(T)(t - t_o)}$$

$S(t)$ = Compressive strength at age t

$k(T)$ = Initial slope of strength-age curve divided by S_u (the rate constant for initial strength development)

t_o = Age when strength development is assumed to begin

S_u = Limiting strength

j. Regression analysis will be used to calculate best-fit values for S_u , t_o , and k .

k. Plot the natural logarithm of the k -values as a function of the reciprocal absolute temperature (degrees Kelvin). Determine the best-fitting straight line through the four points. The negative of the slope of the line is the value of the activation energy divided by the gas constant.

$$\ln k(T) = \ln(a) - E_a/RT$$

Task 3. Strength-Maturity (Equivalent Age) Relationship and Pullout Test Strength Relationship.

Objectives:

- Establish the strength-maturity relationships for each concrete mixture.

- Establish the relationship between pullout strength and cylinder strength for each concrete mixture.
 - a. Four mixtures will be tested to establish the strength maturity relationship at standard temperature. (Table 1)
 - i. Portland cement mixture
 - ii. 35 and 50% Class F fly ash mixture
 - iii. 35% Class C fly ash (25% lime) mixture
 - b. 10.2 cm by 20.3 cm (4 in. by 8 in.) concrete cylinders will be prepared and cured in accordance with ASTM C192/C192 M.
 - c. Three (3) cylinders will be tested at each age (1, 2, 4, 7, 14, 28 days). Two cylinders in each mixture will have embedded sensor (mid-depth) to obtain the temperature-age relationship (for use in calculating equivalent age).
 - d. Cylinders will be cured in lime-saturated water bath at 23°C (73°F). Specimen will be put in the water bath immediately after casting.

- e. Perform compressive strength tests at ages of 1, 2, 4, 7, and 14, and 28 days according to ASTM C39/C39M. Test three specimens at each age and compute the average strength. Unbounded neoprene pads will be used to cap the specimens.
- f. Plot the average compressive strength as a function of equivalent age at 23°C (73°F). The activation energy values obtained in Task 1 and the measured temperature histories will be used to calculate the equivalent ages at each test age.

Pull out Test Correlation (ASTM C900)

- a. 8-in. concrete cubes will be cast with four pullout inserts per cube, one on each of the 4 vertical faces (Figure A.1).
- b. Four mixtures will be used to obtain the relationship between pullout strength and cylinder compressive strength (Table A.1)
 - i) Portland cement mixture
 - ii) 35 and 50% Class F fly ash mixtures
 - iii) 35% Class C fly ash (25% lime) mixture
- c. 8 pullout tests (2 cubes) will be performed at the same time as the cylinder compressive strength tests (1, 2, 4, 7, 14, 28 days). 12 cubes per mixture will be

- prepared. One I-Button sensor 1 in. from the bottom of the mold (at the center of the horizontal plane of the cube) will be embedded in each of the two 28-day cubes. The average of these two will be used for our comparison/maturity calculations.
- d. Cure the cubes in the same water bath as the cylinders. Pullout mold will be put into bath right after casting. Strip molds 24 hours after casting¹.
 - e. When compressive strength tests are performed in step (c), perform 8 pullout tests at the same time.
 - f. Results from these tests will be used to establish the strength relationship for the pullout test. The procedures in ACI 228.1R will be used to obtain the strength relationship.
 - g. The pullout strength relationships will be examined to determine whether there is a unique relationship applicable to all mixtures, or if each mixture requires a unique relationship. Compare the relationships with the manufacturer's recommended relationship.

¹We will do a 50% trial mix and see if strength at 24 hours is adequate for stripping. If yes, we will strip; If Not we will skip 1 day test for that mix and start at 2 days.

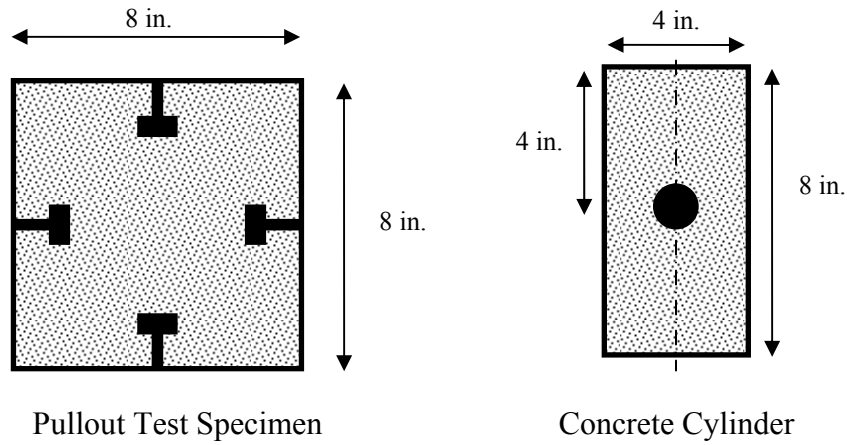


Figure A.1 Specimens for task 3

Task 4. Field Testing

Objectives:

- To simulate the use of maturity method and pullout test to estimate early-age in-place strength of HVFA mixtures.
- To compare estimated strengths by maturity and pullout testing with strength based on temperature-matched curing (Figure A.2).
- To demonstrate that in-place strength development of HVFA mixtures will be greater than that of standard-cured cylinders.

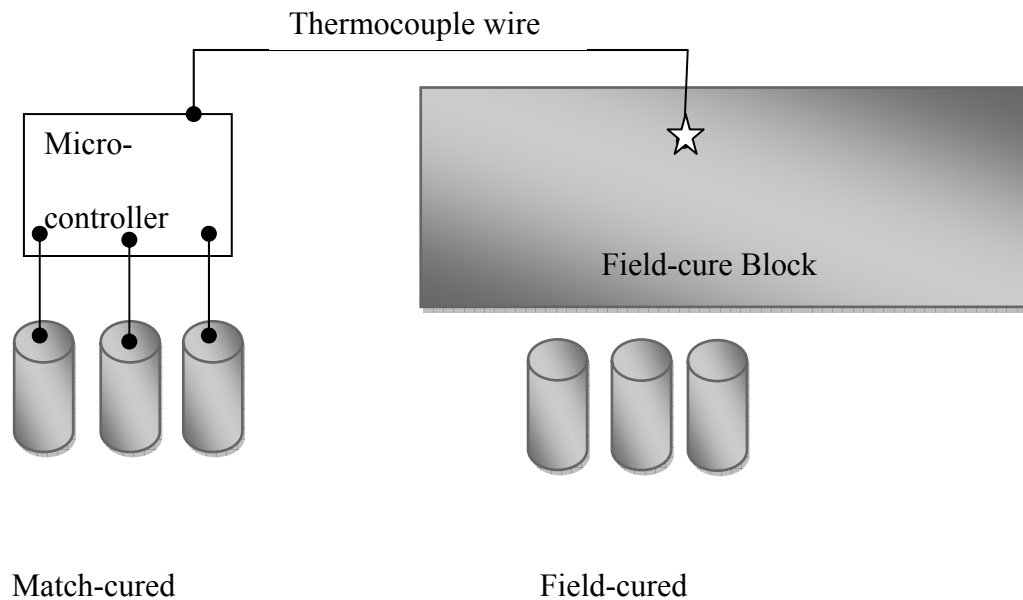


Figure A.2 Schematic of field testing

Part 1: Concrete block (mass concrete)

- a. One 0.6 m x 0.6 x 1.8 m (2 ft by 2 ft by 6 ft) block will be cast for each mixture with seven temperature sensors inside each block (Figure A.3). Thermocouple sensor will be used to drive a temperature-matched curing system.

- b. A temperature-matched curing system will be used to obtain the best-estimate of the actual in-place compressive strength at different ages. Eight cylinders will be prepared for temperature-matched curing. At actual ages of 2, 4, and 7 days, six (6) temperature-matched cylinders will be tested. We will need to test 2 cylinders at each age. One cylinder will have an I-Button sensor to measure the concrete

temperature. This cylinder should not be tested for strength. We will thus have one spare that could be tested at an age where the two breaks are not close to each other. The average cylinder strength will represent the actual in-place strength.

- c. Ten additional 10.2 x 20.3 cm (4 in. by 8 in.) cylinders will be prepared when each block is cast. Nine cylinders will be field-cured according to ASTM C31/C31M and three replicates will be tested at each age of 2, 4, and 7 days. One cylinder will be cast with an I-button sensor at mid-depth to monitor temperature of field cure cylinder.
- d. Twenty four pullout inserts will be cast at the mid-depth of block mold in accordance to ASTM C900. Eight pullout tests/age will be performed exactly at the same age at which the match-cured and field-cured cylinders are tested. All pullout inserts will be randomly placed at the same elevation.
- e. Two days pullout strength will be tested through the access panels while the form work is still attached, to simulate the actual field test (Early stripping). Block molds will be stripped after 3days to do a pullout test using conventional way for other 2 ages (4 and 7 days). Block will be cured using waterproof cover and curing blanket all the time to provide good curing of the concrete.

- f. Four mixtures will be used for the field concrete blocks along with field companion cylinders
- i. Portland cement mixture
 - ii. 35 and 50% Class F fly ash mixture
 - iv. 35% Class C fly ash (25% lime) mixture
- g. Eight I-Buttons will be placed in each concrete block to monitor temperature of the specimen with age (Figure A.3). The temperature-matched cured cylinders will follow the temperature history of the thermocouple sensor with 1.0 in. cover and placed at mid-depth of the block, as shown in Figure A.3 (denoted by a star).

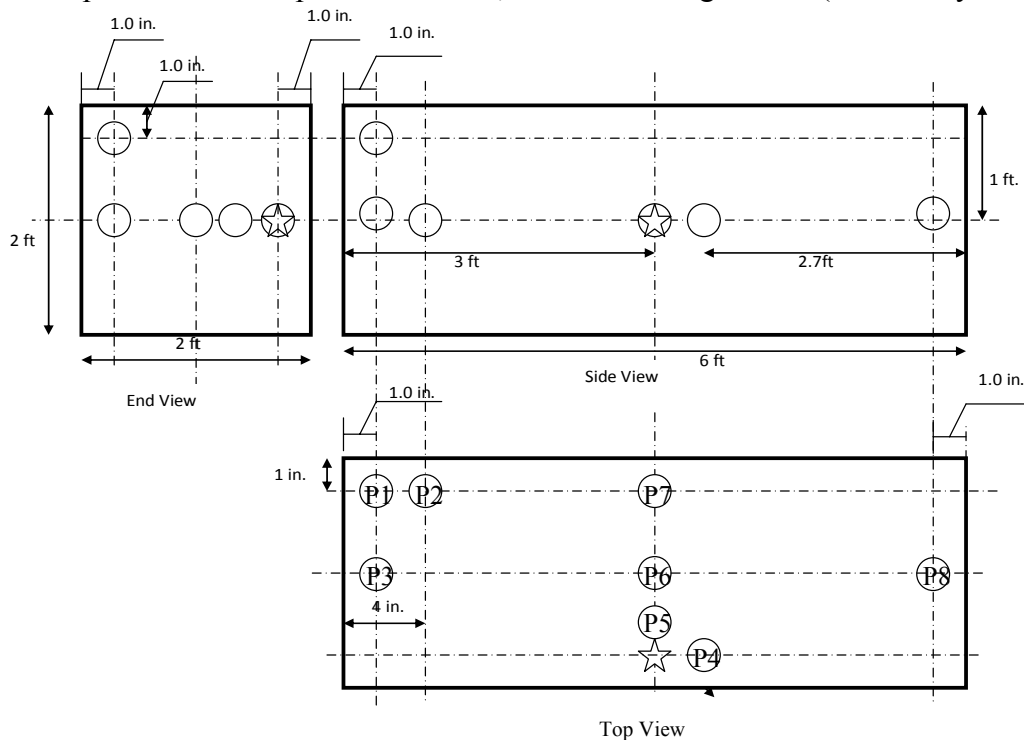


Figure A.3 Concrete block and temperature sensor locations

(P4 is used for maturity calculations)

- h. Use the strength-maturity relationship and the pullout strength relationship to estimate the in-place concrete strength and compare with the strength of the temperature-matched cured cylinders.

Part 2: Concrete slab (pavement)

- a) One concrete slab of size 2.4 m x 2.4 m x 0.2 m (8 ft. by 8 ft by 7 in.) for each of the two mixtures shown in Table A.1 will be cast.
 - i. Portland cement mixture
 - ii. 50% Class F fly ash mixture
- b. Concrete cylinders will be prepared for temperature-matched curing, field curing, and standard curing as was done for the concrete block tests.
- c. Twenty four pullout test inserts will be floated into the top of each slab with accordance to ASTM C900.
- d. Five I-buttons shown in Figure A.4 will be used in each slab to record temperature of the slab. Two temperature sensors will be placed at mid depth, and other two sensors will be embedded at 5.08 cm (2 in.) from the top surface. The thermocouple sensor will be used to drive the temperature-matched curing system.

- e. At actual ages of 2, 4, and 7 days, cylinders (field-cured and match-cured) will be tested for compressive strength. At the same ages, 8 pullouts tests will be conducted. Concrete strength estimated based on the strength maturity relationship and the pullout test strength relationship would be compared with the measured compressive strength of the match-cured cylinders.

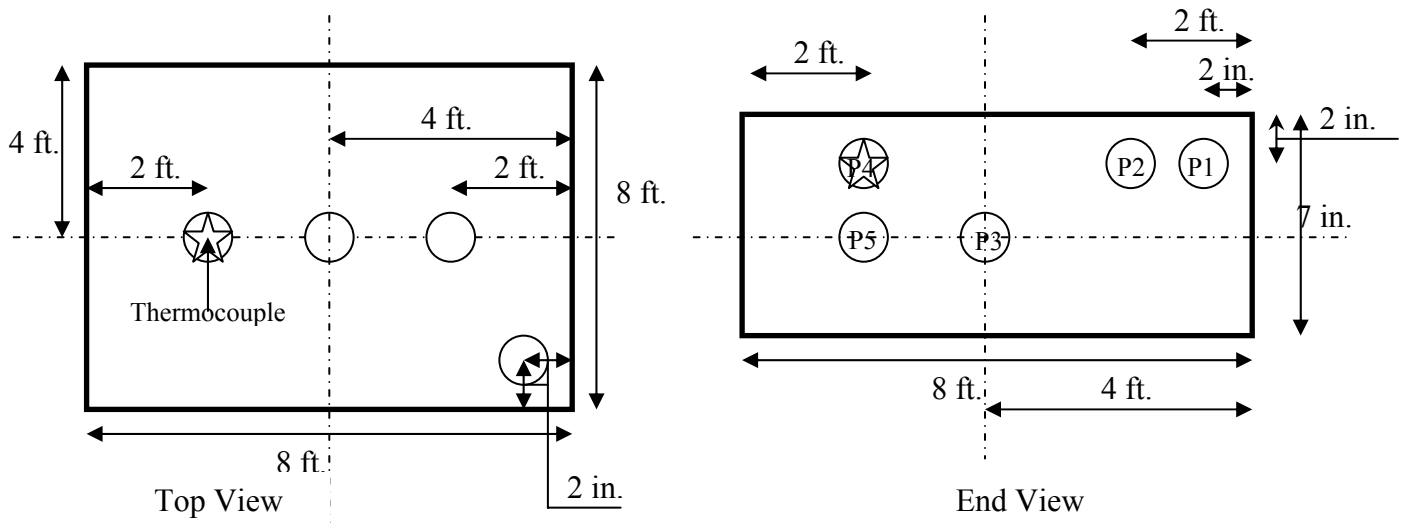


Figure A.4 Concrete slab and temperature sensor locations

(P4 is used for maturity calculations)

Appendix B

Appendix B summarizes the average compressive strength results of three, 5.08 cm (2 in.)mortar cubes at each curing age.

Table B.1 Compressive strength -trial 1 (control mixture)

Temp °C (°F)	Age (Days)	Strength MPa (psi)	COV(%)
7.5 (45)	1.25	6.3 (915)	5.4
	2.5	9.9 (1442)	1.3
	4.99	14.6 (2117)	3.9
	9.98	19.7 (2863)	0.7
	26.24	24.5 (3555)	1.3
	69	29.7 (4302)	0.6
21.0 (70)	0.71	7.6 (1100)	0.5
	1.42	13.9 (2021)	2.3
	2.84	19.8 (2872)	1.9
	5.69	24.2 (3513)	0.9
	13.21	27.0 (3919)	1
	30.7	34.2(4953)	2.4
38.0 (100)	0.34	6.9 (1006)	2.5
	0.69	15.1 (2188)	5.8
	1.37	19.6 (2846)	1.4
	2.75	23.1 (3354)	0.5
	5.92	27.4 (3975)	2.2
	12.77	27.4 (3975)	2.2
49.0 (120)	0.21	3.6 (523)	3
	0.41	13.3 (1931)	0.2
	0.82	17.5 (2531)	2.3
	1.65	21 (3052)	5.4

Table B.2 Compressive strength -trial 2 (control mixture)

Temp °C (°F)	Age (Days)	Strength MPa (psi)	COV(%)
7.5 (45)	0.94	1.6 (228)	1.1
	1.87	7 (1015)	3
	3.74	12.9 (1877)	0.8
	7.48	19.1 (2776)	1.6
	14.97	23 (3328)	5
	32.14	26.5 (3845)	6.8
	69	31.6 (4582)	1.8
21.0 (70)	0.43	2.2 (318)	3.8
	0.85	8.7 (1259)	0.6
	1.7	13.1 (1902)	3
	3.41	19.1 (2767)	1.4
	6.82	22.2 (3220)	3.8
	14.47	25.2 (3652)	0.6
	30.71	29.6 (4289)	4.5
49.0 (120)	0.19	1.7 (241)	1.3
	0.36	9.7 (1401)	0.2
	0.71	15 (2179)	4
	1.41	18.6 (2692)	6.3
	2.82	21.8 (3156)	1.7
	4.59	22.7 (3293)	0.9
	7.48	25 (3620)	5.2

Table B.3 Compressive strength -trial 1 (20% FA-A)

Temp °C (°F)	Age (Days)	Strength MPa (psi)	COV(%)
7.5 (45)	1.28	1.8 (268)	0.5
	2.56	7.4 (1067)	1.3
	5.12	13.1 (1896)	1.7
	10.23	17.3 (2513)	4
	25.99	28.3 (4100)	0.8
	66	35 (5077)	0.5
21.0 (70)	0.86	7.5 (1088)	1.9
	1.73	13.5 (1956)	3.3
	3.45	19.6 (2842)	1.1
	6.9	25.2 (3654)	2.2
	14.52	30.5 (4428)	3.1
	30.56	35.6 (5166)	2.2
38.0 (100)	0.42	7.0 (1017)	0.7
	0.84	14.4 (2088)	1.5
	1.69	19.8 (2869)	4.5
	3.37	26.3 (3807)	2.8
	6.69	29.7 (4309)	2.4
	13.28	34.9 (5066)	1.9
49.0 (120)	0.25	6.4 (925)	5.8
	0.51	13.6 (1978)	4.1
	1.01	20.6 (2990)	0.3
	2.02	25.2 (3648)	1.5
	4.02	33 (4788)	0.9

Table B.4 Compressive strength –trial 1 (35% FA-A)

Temp °C (°F)	Age (Days)	Strength MPa (psi)	COV(%)
7.5 (45)	1.42	1.8 (262)	5.9
	2.85	4.9 (708)	2
	5.69	8.4 (1213)	1
	11.38	10.9 (1579)	4.8
	25.69	14.5 (2096)	0.3
	58	16.8 (2438)	3.3
21.0 (70)	1.1	6.5 (942)	2
	2.2	10.7 (1558)	2.8
	4.41	13.5 (1954)	1.6
	8.81	16.4 (2371)	0.8
	16.3	18.9 (2745)	1.3
	30.14	25 (3628)	0.4
38.0 (100)	0.59	7.5 (1083)	0.6
	1.18	11.3 (1641)	2
	2.36	14.8 (2150)	0.5
	4.71	18.3 (2656)	1.8
	8.39	23.7 (3430)	1.1
	14.94	31 (4498)	1.2
49.0 (120)	0.35	5.2 (750)	1.6
	0.71	9.4 (1369)	0.4
	1.41	12.6 (1833)	1.8
	2.83	18.2 (2646)	2.9
	5.25	28.8 (4172)	1.9

Table B.5 Compressive strength –trial 2 (35% FA-A)

Temp °C (°F)	Age (Days)	Strength MPa (psi)	COV(%)
7.5 (45)	1.42	2.0 (296)	11.2
	2.84	4.9 (715)	5.5
	5.69	8.2 (1185)	1.2
	11.37	10.5 (1521)	1.3
	22.76	13.8 (2000)	9.2
	36.27	15.2 (2208)	2.6
	58.02	16.3 (2368)	0.5
21.0 (70)	0.95	2.1 (305)	0.6
	1.65	6.7 (975)	2
	3.3	11.4 (1650)	0.5
	6.55	14.9 (2160)	1.8
	13.22	18.1 (2630)	1.1
	19.96	19.8 (2875)	1.1
49.0 (120)	30.2	22.5 (3261)	1.1
	0.26	1.4 (209)	5.3
	0.53	6.2 (896)	2.3
	1.06	13 (1886)	5.6
	2.12	17.9 (2600)	1.6
	4.24	23.5 (3403)	1.4
	6.43	27.9 (4045)	0.3
9.74	31.4 (4558)	4.1	

Table B.6 Compressive strength –trial 3 (35% FA-A)

Temp °C (°F)	Age (Days)	Strength MPa (psi)	COV(%)
21.0 (70)	0.83	1.6 (225)	7.8
	1.65	7.3 (1063)	8.3
	3.3	11.3 (1638)	0.1
	6.6	16.1 (2338)	0.7
	30.14	23.6 (3420)	4.3
	94.11	34.1 (4938)	0.7
38.0 (120)	0.26	2.2 (325)	10.8
	0.53	5.6 (819)	9.7
	1.07	9.6 (1394)	1.9
	2.12	15.1 (2196)	2.1
	4.55	22.5 (3269)	4.5
	9.75	28.4 (4125)	0.3
	26.03	37.2 (5400)	0.1

Table B.7 Compressive strength –trial 1 (50% FA-A)

Temp °C (°F)	Age (Days)	Strength MPa (psi)	COV(%)
7.5 (45)	1.66	2.3 (335)	4.6
	3.32	6.1 (879)	1.6
	6.64	13.1 (1900)	2.4
	13.29	18.2 (2646)	2.2
	26.54	25.6 (3709)	3.7
21.0 (70)	1.18	7.5 (1083)	0.6
	2.35	12.7 (1846)	0.3
	4.71	20.3 (2948)	0.3
	9.41	27.9 (4050)	1.8
	16.77	35.0 (5069)	1.4
	29.87	42.8 (6210)	3.7
38.0 (100)	0.7	11.2 (1621)	1.9
	1.4	19 (2750)	1.9
	2.79	27.4 (3975)	0.6
	5.58	36.7 (5328)	4.4
	9.5	45.1 (6546)	4.4
	16.16	50.6 (7344)	2.1
49.0 (120)	0.42	8.8 (1274)	2.4
	0.84	17.5 (2543)	3.5
	1.67	25.6 (3708)	3.7
	3.35	36.9 (5344)	1.1
	6.1	45 (6523)	0.8

Table B.8 Compressive strength –trial 2 (50% FA-A)

Temp °C (°F)	Age (Days)	Strength MPa (psi)	COV(%)
7.5 (45)	1.5	2.1 (305)	11.4
	2.98	7.4 (1068)	2.6
	5.95	14.1 (2051)	1.5
	11.95	20.3 (2946)	5.1
	23.91	28 (4061)	2.5
	35.57	31.6 (4588)	1.4
	53.5	34.2 (4965)	0.7
21.0 (70)	0.94	5.3 (762)	1.9
	1.88	12.1 (1760)	1.3
	3.8	19.0 (2760)	0.7
	7.58	25.1 (3642)	3.2
	14.96	30.6 (4430)	4.4
	29.86	37.4 (5430)	0.1
49.0 (120)	0.26	3.5 (502)	9
	0.5	11.2 (1627)	1.3
	1.0	19.9 (2883)	2.4
	2.0	27.4 (3966)	3.1
	4.02	38.8 (5631)	0.5
	6.69	44.1 (6388)	2.7
	11.12	45.7 (6620)	0.1

Table B.9 Compressive strength –trial 3 (50% FA-A)

Temp °C (°F)	Age (Days)	Strength MPa (psi)	COV(%)
21.0 (70)	0.47	1.6 (235)	12.2
	0.94	5.5 (792)	3.9
	1.88	11.2 (1625)	0.7
	4.05	17.1 (2473)	1.4
	10.54	24.7 (3575)	3.2
	29.92	35.5 (5143)	4.6
	90.95	48 (6958)	0.2
49.0 (120)	0.26	2.9 (425)	15.5
	0.52	9.8 (1423)	3.6
	1.04	18.4 (2668)	5.7
	2.08	26.8 (3880)	2.9
	4.82	40.7 (5896)	3.3
	11.12	44.7 (6479)	4.7

Table B.10 Compressive strength –trial 4 (50% FA-A)

Temp °C (°F)	Age (Days)	Strength MPa (psi)	COV(%)
21.0 (70)	0.47	1.1 (160)	2.2
	0.95	5.8 (838)	2.1
	1.89	11.1 (1613)	1
	3.76	16.6 (2400)	2.2
	30.09	38.7 (5613)	2.2
	93	50.4 (7313)	8.4
	0.26	3.5 (505)	1.4
49.0 (120)	0.51	9.2 (1331)	0.6
	1.04	15.9 (2306)	0.3
	2.08	19.0 (2751)	3.9
	4.8	35.3 (5118)	3.9
	11.08	48.1 (6975)	0.7
	30.1	53 (7688)	2.9

Table B.11 Compressive strength –trial 1 (35% FA-B)

Temp °C (°F)	Age (Days)	Strength MPa (psi)	COV(%)
7.5 (45)	1.37	2.0 (286)	2.4
	2.74	6.3 (917)	2
	5.48	12.3 (1788)	1.2
	10.96	19.7 (2854)	0.9
	25.64	25.4 (3683)	1.2
21.0 (70)	1	8.0 (1155)	3.9
	2	14.1 (2042)	1.2
	4.01	19.6 (2838)	0.7
	8.01	24.8 (3600)	4.9
	15.58	29.4 (4269)	0.3
	30.28	33 (4778)	2.1
38.0 (100)	0.52	4.6 (673)	1.4
	1.03	9 (1308)	1.1
	2.07	14.1 (2050)	1.2
	4.13	18.5 (2688)	1.2
	7.71	23.3 (3374)	3.6
	14.37	28.2 (4090)	1.6
49.0 (120)	0.31	5.5 (802)	1.1
	0.62	12.6 (1823)	3.2
	1.24	20.1 (2908)	3.2
	2.48	25.6 (3718)	0.4

Table B.12 Compressive strength –trial 2 (35% FA-B)

Temp °C (°F)	Age (Days)	Strength MPa (psi)	COV(%)
21.0 (70)	0.65	2.7 (396)	7.7
	1.3	8.4 (1221)	1.6
	2.6	14.6 (2118)	2.3
	5.21	20 (2893)	2.1
	10.37	24.4 (3538)	0.8
	17.65	28.2 (4088)	2.8
	30.28	33.2 (4818)	1.2
49.0 (120)	0.26	1.7 (250)	4.3
	0.53	10.7 (1558)	2.4
	1.05	17.6 (2550)	1.7
	2.11	23.8 (3444)	3.4
	4.2	31.4 (4551)	0.4
	6.2	35.8 (5188)	2.5
	9.1	39.0 (5654)	2.2

Table B.13 Compressive strength –trial 1 (35% FA-C)

Temp °C (°F)	Age (Days)	Strength MPa (psi)	COV(%)
7.5 (45)	1.33	0.9 (132)	0.5
	2.66	2.6 (384)	2.0
	5.33	6.9 (1004)	0.7
	10.65	12.9 (1871)	1.0
	25.91	20.6 (2983)	0.4
	63	26.7 (3877)	1.3
21.0 (70)	0.86	2.5 (363)	5.9
	1.73	8.0 (1167)	1.6
	3.45	14 (2033)	0.3
	6.9	19.8 (2872)	2.4
	14.52	25.3 (3666)	1.5
	30.56	32.1 (4657)	0.7
38.0 (100)	0.49	0.9 (133)	2.8
	0.98	4.6 (671)	1.0
	1.95	10.3 (1493)	1.0
	3.9	15.1 (2196)	1.1
	7.34	23.0 (3332)	1.2
	13.81	31.1 (4516)	1.1
49.0 (120)	0.29	1.4 (207)	3.6
	0.59	7.2 (1050)	2.7
	1.17	17.2 (2494)	0.4
	2.34	25.7 (3729)	1.6
	4.47	36.8 (5341)	3.0

Table B.14 Compressive strength –trial 2 (35% FA-C)

Temp °C (°F)	Age (Days)	Strength MPa (psi)	COV(%)
21.0 (70)	0.8	1.8 (268)	6.1
	1.62	6.2 (904)	0.7
	3.22	11.8 (1713)	3.8
	6.43	16.4 (2385)	1.6
	12.9	21.3 (3084)	2.9
	19.82	24.8 (3597)	0.5
	30.388	27.8 (4035)	2.2
49.0 (120)	0.29	1.5 (223)	3.3
	0.59	7.6 (1096)	1.7
	1.16	10.9 (1580)	3.9
	2.33	21.6 (3127)	3.1
	4.68	29.0 (4204)	1.7
	6.32	35 (5075)	5.9
	8.53	35.3 (5113)	0.2

Table B.15 Compressive strength –trial 3 (35% FA-C)

Temp °C (°F)	Age (Days)	Strength MPa (psi)	COV(%)
21.0 (70)	0.8	1.1 (156)	6.1
	1.6	5.2 (750)	0.7
	3.22	10.6 (1536)	3.8
	6.48	15.6 (2256)	1.6
	30.44	26.9 (3906)	2.9
	92.04	37.5 (5444)	0.5
49.0 (120)	0.29	1.3 (184)	2.8
	0.58	5.2 (750)	0
	1.17	11.6 (1675)	5.2
	2.34	19.6 (2838)	9.3
	4.46	31.0 (4494)	0.1
	8.54	36.3 (5263)	0.3
	23.96	42.0 (6090)	0.2

Appendix C

Appendix C summarizes compressive strength test results for field and laboratory testing.

Table C.1 Compressive strength –standard cure concrete cylinders-block (control mixture)

Age (Days)	Standard Cure MPa (psi)	COV (%)	Field Cure MPa (psi)	COV(%)	Match Cure MPa (psi)	COV(%)
1	7.1 (1023)	5.0				
2	11.8 (1714)	2.0	8.6 (1249)	2.1	19.4 (2810)	0.2
4	16.9 (2449)	3.1	13.9 (2021)	3.6	23.8 (3452)	0.2
7	18.6 (2692)	2.2	18 (2615)	4.2	26.6 (3861)	2.1
14	23.9 (3470)	5.5				
28	30.2 (4378)	2.1				

Table C.2 Compressive strength concrete cylinders-slab (control mixture)

Age (Days)	Standard Cure MPa (psi)	COV (%)	Field Cure MPa (psi)	COV(%)	Match Cure MPa (psi)	COV(%)
1						
2			11.8 (1717)	3.1	19.5 (2825)	1.3
4			15.8 (2288)	13.3	25 (3625)	3.4
7			21.7 (3148)	2.3	29.6 (4289)	0.6
14						
28	35.7 (5182)	4.4				

Table C.3 Compressive strength -concrete cylinders-block (35% FA-A)

Age (Days)	Standard Cure MPa (psi)	COV (%)	Field Cure MPa (psi)	COV(%)	Match Cure MPa (psi)	COV(%)
1	4.8 (699)	2.3				
2	7.1 (1034)	3.0	5.6 (813)	1.0	12.4 (1802)	4.2
4	9.7 (1402)	3.2	9.5 (1374)	2.2	16.9 (2450)	3.1
7	12.6 (1820)	5.5	11.9 (1722)	11.1	19.2 (2786)	5.3
14	18 (2609)	3.1				
28	24.2 (3505)	2.1				

Table C.4 Compressive strength -concrete cylinders-block (50% FA-A)

Age (days)	Standard Cure MPa (psi)	COV (%)	Field Cure MPa (psi)	COV (%)	Match Cure MPa (psi)	COV(%)
1	7.2 (1039)	5.1				
2	11.5 (1662)	2.7	8.0 (1155)	2.3	14.9 (2156)	0.8
4	16.4 (2372)	3.7	15.3 (2216)	1.5	19.5 (2823)	1.0
7	19.5 (2832)	1.1	17.9 (2599)	0.1	22.4 (3251)	3.2
14	25.3 (3668)	1.2				
28	33.2 (4811)	0.4				

Table C.5 Compressive strength -concrete cylinders-slab (50% FA-A)

Age (Days)	Field Cure MPa (psi)	COV (%)	In-Place MPa (psi)	COV (%)
2	8.7 (1263)	2.1	10.3 (1491)	3.6
4	14.9 (2159)	1.1	15.6 (2262)	1.4
7	17.1 (2485)	0.6	17.6 (2545)	3.3

Table C.6 Compressive strength -concrete cylinders-block (35% FA-C)

Age (Days)	Standard Cure MPa (psi)	COV (%)	Field Cure MPa (psi)	COV (%)	Match Cure MPa (psi)	COV (%)
1	5.6 (807)	1.8				
2	12.3 (1781)	6.1	12.0 (1732)	4.4	23.6 (3422)	3.2
4	19.5 (2822)	3.9	20.7 (2998)	1.3	30.4 (4405)	0.1
7	24.2 (3503)	0.2	25.5 (3695)	1.4	34.2 (4953)	1.71
14	38.3 (4104)	2.5				
28	36.0 (5212)	1.2				

Appendix D

This Appendix D summarizes the results for pullout force on 8 in. concrete cube and field cure blocks and slabs. The plot for compressive strength vs. pullout force for standard cure 8 in. concrete cube are also shown with best fit exponential equation used for strength vs. pullout force correlations. Finally, the calculated pullout forces for the blocks and slabs are converted to compressive strength estimates using the developed pullout load-compressive strength correlations (Figures D.1 to D.4)

Table D.1 Pullout force on 8 in. cube concrete specimen (control mixture)

Age (Days)	Pullout Force (kN)	COV(%)
1	8.45	15.4
2	12.50	8.4
4	15.63	5.4
7	17.90	3.3
14	21.61	4.7
28	26.89	8.0

Table D.2 Pullout Force on 8in. cube concrete specimen (35% FA-A)

Age (Days)	Pullout Force (kN)	COV (%)
1	7.19	6.9
2	9.40	17.8
4	10.59	5.9
7	13.41	6.9
14	18.03	9.1
28	22.86	4.3

Table D.3 Pullout force on 8in. cube concrete specimen (50% FA-A)

Age (Days)	Pullout Force (kN)	COV (%)
1	10.44	21.9
2	13.97	17.8
4	17.36	15.1
7	19.58	12.3
14	25.45	11.2
28	29.69	7.9

Table D.4 Pullout force on 8in. cube concrete specimen (35% FA-C)

Age (Days)	Pullout Force (kN)	COV (%)
1	7.16	14.0
2	12.86	11.0
4	18.30	8.7
7	20.84	4.2
14	22.49	6.1
28	30.28	7.1

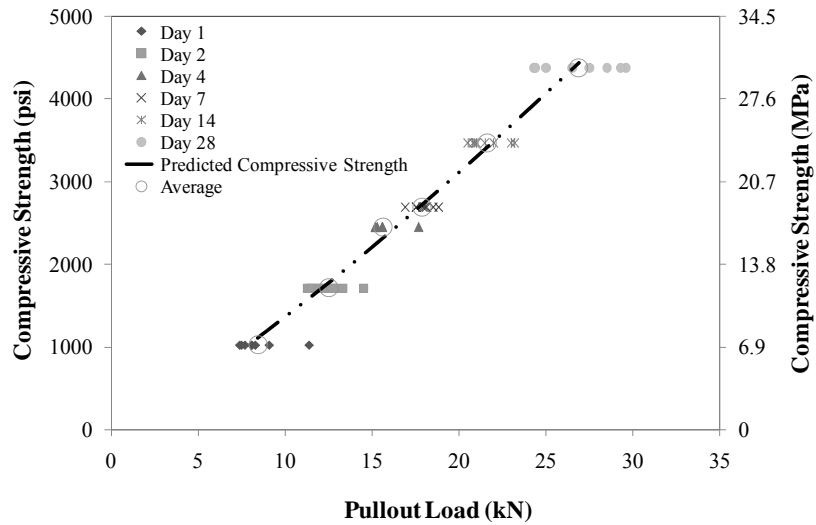


Figure D.1 Strength vs. pullout force (control mix)

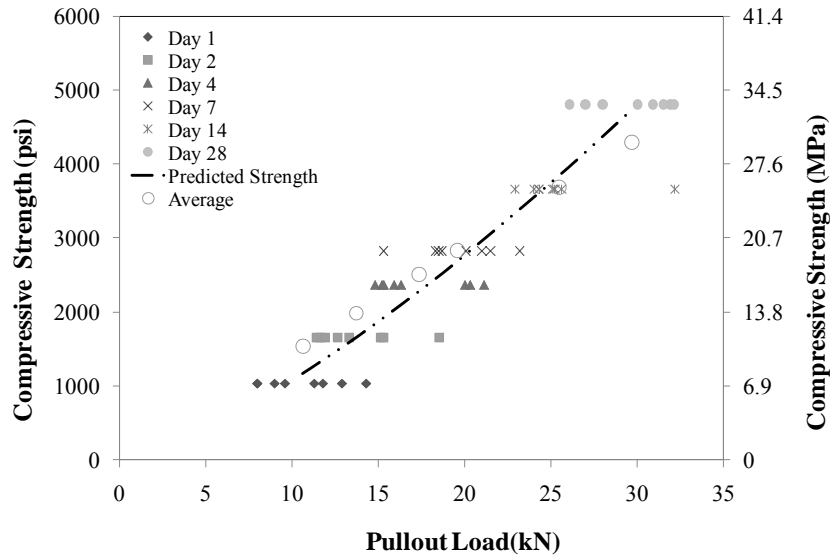


Figure D.2 Strength vs. pullout force (35% FA-A)

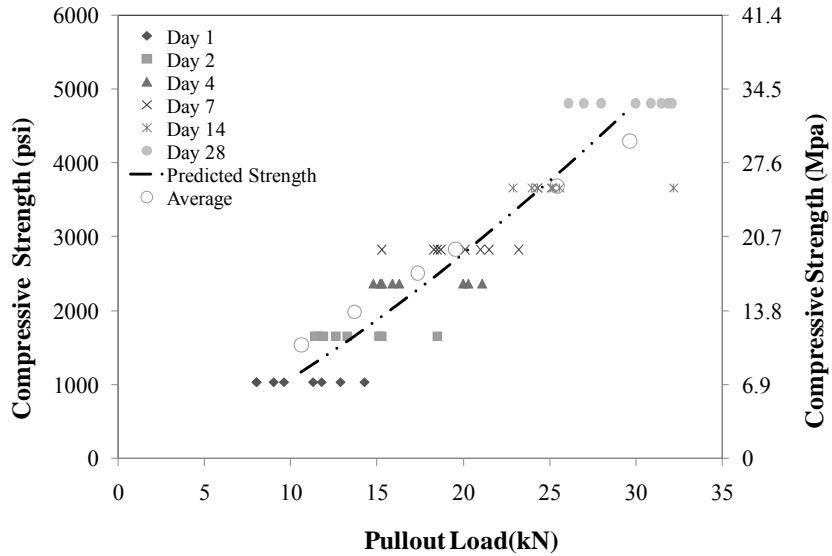


Figure D.3 Strength vs. pullout Force (50% FA-A)

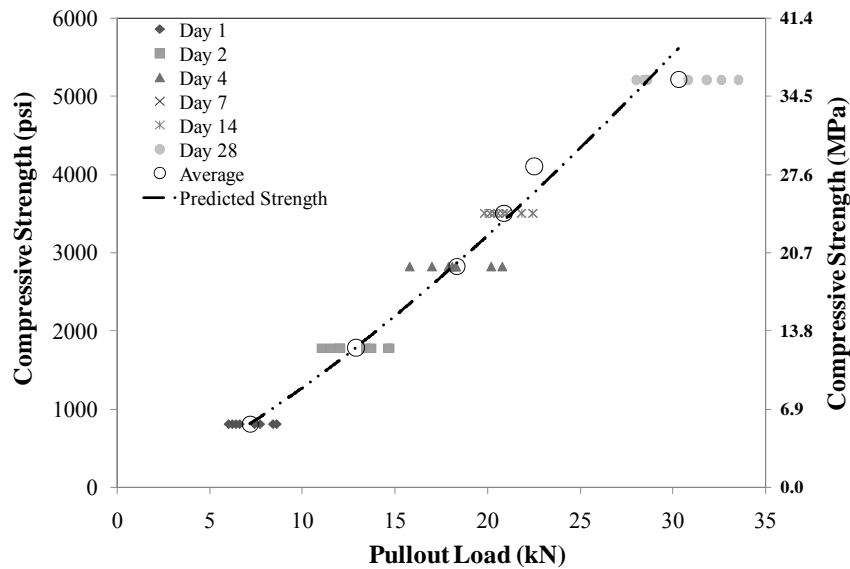


Figure D.4 Strength vs. pullout Force (35% FA-C)

Table D.5 Pullout force on concrete block field-cured (control mixture)

Age (Days)	Pullout Force (kN)	COV (%)	Estimated Strength MPa (psi)
2	17.175	6.7	17.9 (2590)
4	18.525	3.7	19.6 (2836)
7	21.525	4.2	23.4 (3395)

Table D.6 Pullout force on concrete slab field-cured (control mixture)

Age (Days)	Pullout Force (kN)	COV(%)	Estimated Strength MPa (psi)
2	16.33	7.5	16.8 (2437)
4	19.03	4.7	20.2 (2928)
7	20.69	9.1	22.3 (3237)

Table D.7 Pullout force on concrete block field-cured (35% FA-A)

Age (days)	Pullout Force (kN)	COV(%)	Estimated Strength MPa (psi)
2	10.75	4.2	9.1 (1325)
4	11.09	5.7	9.5 (1379)
7	13.64	9.1	12.4 (1804)

Table D.8 Pullout Force on concrete block field-cured (50% FA-A)

Age (Days)	Pullout Force (kN)	COV (%)	Estimated Strength MPa (psi)
2	16.60	16.4	14.8 (2151)
4	17.50	16.7	15.9 (2311)
7	18.21	10.4	16.8 (2441)

Table D.9 Pullout force on concrete slab field-cured (50% FA-A)

Age (Days)	Pullout Force (kN)	COV (%)	Estimated Strength MPa (psi)
2	11.79	6.7	9.3 (1349)
4	14.83	7.4	12.7 (1844)
7	17.10	5.7	15.4 (2240)

Table D.10 Pullout force on concrete block field-cured (35% FA-C)

Age (Days)	Pullout Force (kN)	COV (%)	Estimated Strength MPa (psi)
2	20.35	5.3	22.9 (3325)
4	22.99	2.8	26.6 (3858)
7	24.28	12.0	28.4 (4123)

Appendix E

Appendix E presents the maturity prediction plots for the setting time approach. Figure E.1 illustrates the Arrhenius plot for the hydration rate calculated based on the setting time approach using a linear trend interpolation. It is clearly observed that the reaction rate at early ages slows down as the percentage replacement of fly ash increases in the concrete mixtures

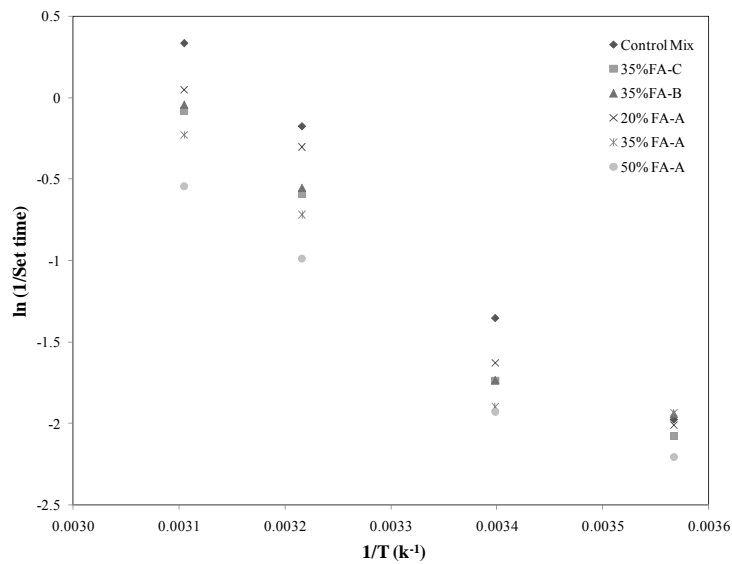


Figure E.1 Arrhenius Plot for setting time vs. temperature

Figure E.2 shows the plot of the strength maturity model for the control mixture, based on the setting time approach. Subsequent Figure E.3 shows the strength comparison between match cure, field cure and strength prediction based on the maturity method and the pullout test. Figure E.3 evidently shows that match cure cylinder provided the higher strength at any age. Maturity based strength predictions were reasonably close to the match cure strength. Even the strength

estimated based on the pullout correlations developed in this research estimates the in-place compressive strength close to the maturity model.

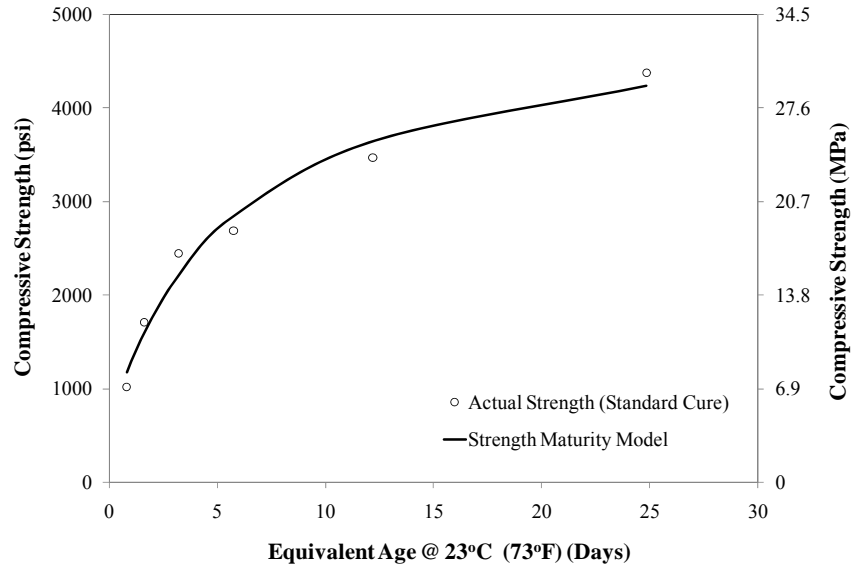


Figure E.2 Maturity model-setting time approach (Control mix)

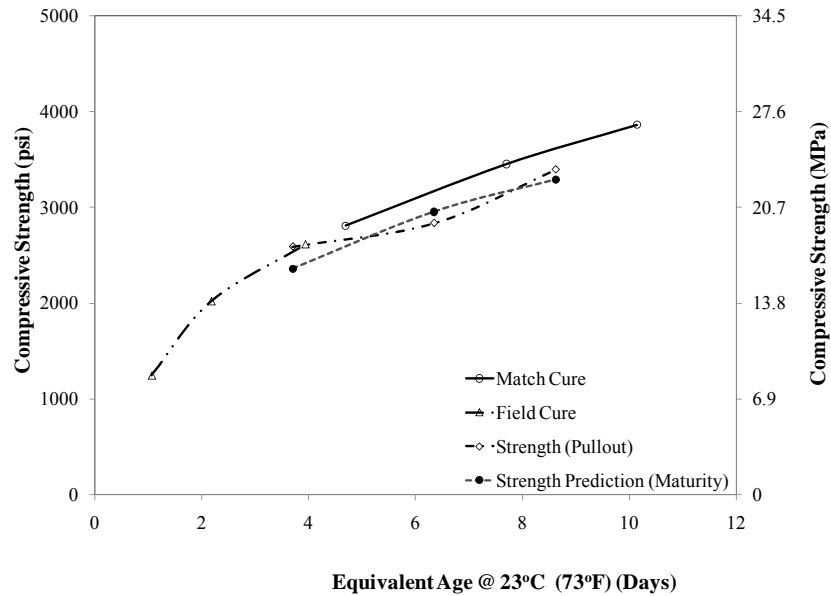


Figure E.3 Comparison of strength obtained from various methods vs. equivalent age setting time (Control mixture-block)

Figure E.4 shows the plot of the strength maturity model for 35% FA-A mixture, based on the setting time approach. Figure E.4 shows the strength comparison between the match cure, field cure and strength prediction based on the maturity method and the pullout test. Figure E.5 also evidently shows that match cure cylinders provide higher strength at any age. Field cure and maturity strength prediction are close to each other. Even though match cure cylinders and pullout test locations followed the same temperature history the strength prediction of the pullout strength are fairly low compared to the remaining strength values. This can be explained by the loose aggregate interlock, which might be possible at the testing location in the block used for the maturity model.

Figure E.6 shows the plot of the strength maturity model for the 50% FA-A mixture based on the setting time approach. Figure E.7 shows the compressive strength plot for the 50% FA-A mixture-block. It is clearly observed that the field cure and match cure cylinders have close strength at same ages. On the other hand, the maturity method slightly underestimates concrete strength.

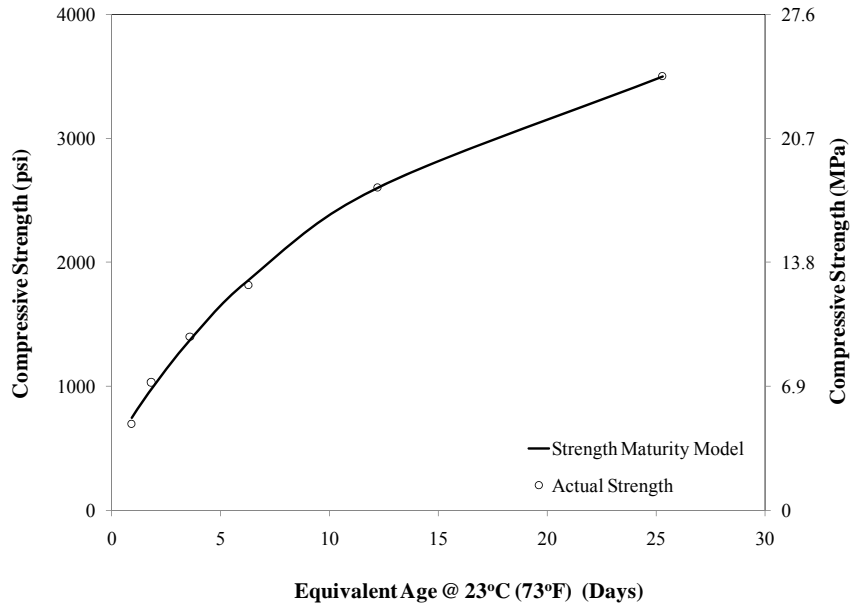


Figure E.4 Maturity model-setting time approach (35% FA-A).

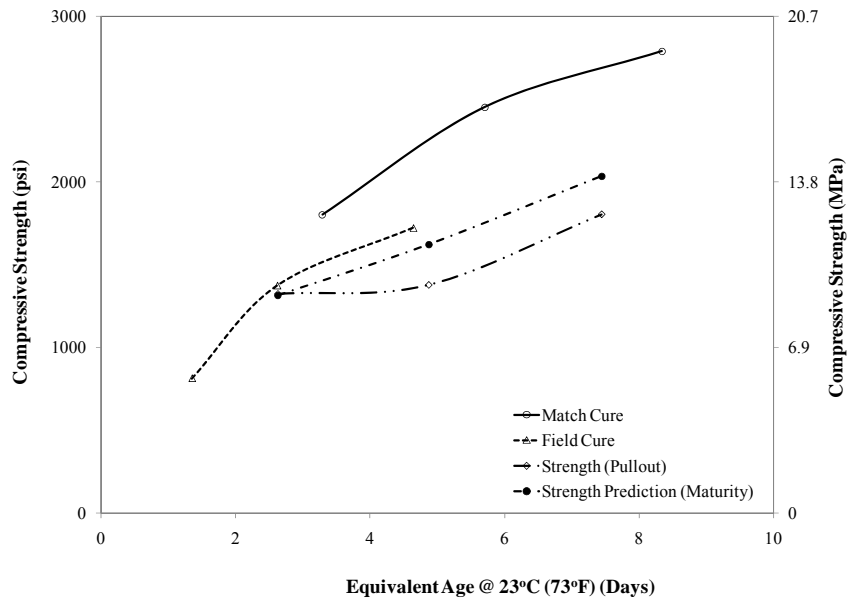


Figure E.5 Comparison of strength obtained from various methods vs. equivalent age setting time (35%FA-A mixture-block)

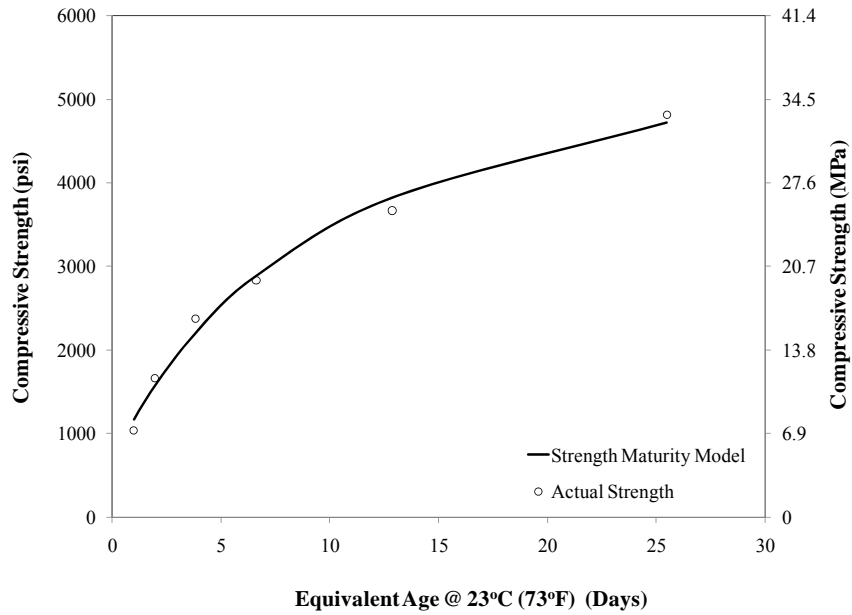


Figure E.6 Maturity model-setting time approach (50% FA-A)

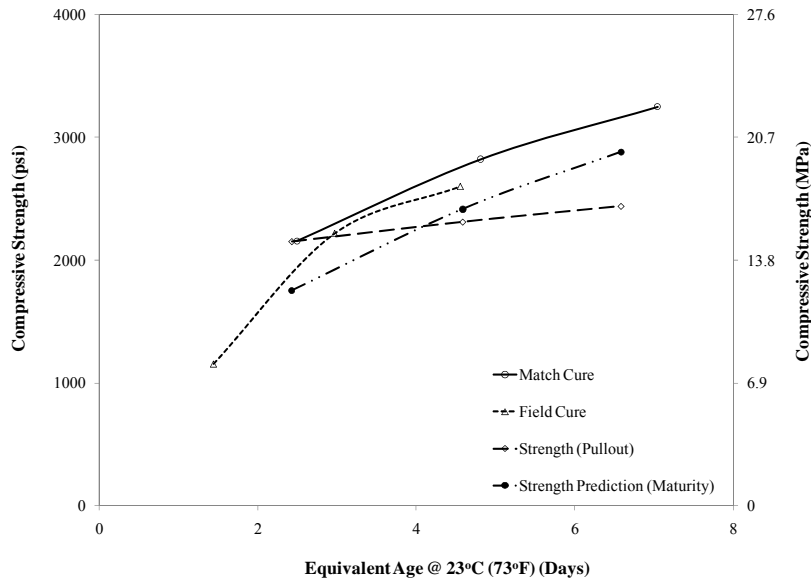


Figure E.7 Comparison of strength obtained from various methods vs. equivalent age setting time (50%FA-A mixture-block)

Figure E.8 shows the plot of the strength maturity model for the 35% FA-C mixture, based on the setting time approach. Figure E.9 shows the compressive strength plot for the 35% FA-C mixture. Same strength phenomenon was observed in Figure E.9, match cure strength is higher compared to the strength estimated based on the remaining prediction models. However, in this plot it is clearly observed that the pullout strength prediction, maturity strength prediction and the field cure strength are close to each other. On the other hand, the maturity method slightly underestimates the strength.

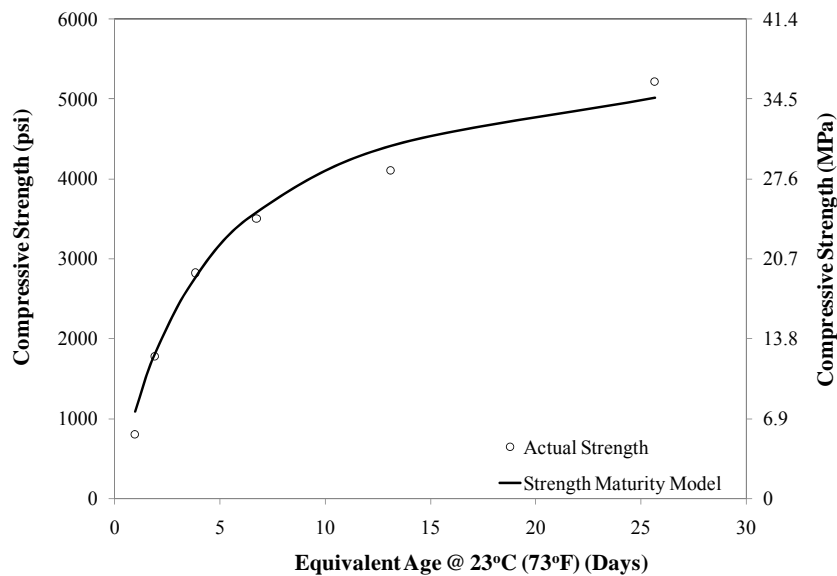


Figure E.8 Maturity model-setting time approach (35% FA-C)

Figure E.10 and Figure E.11 shows the compressive strength with curing ages for the control mix and 50% FA-A mixture slab respectively. Figure E.10 shows that maturity underestimates the strength, around 73% from the match cure strength. The reason of such variation is that the maturity model used for the strength prediction was based on block data. The slab was casted on a different date compared to the block and a maturity model was not developed for the mixture used in the slab. Furthermore, the assumption was made is that the cement used in both mixtures

was the same even though produced at a different time. Based on the plot it can be concluded that the model developed for the block mixture clearly do not applies to the mixture for the slab, which provided really low strength predictions.

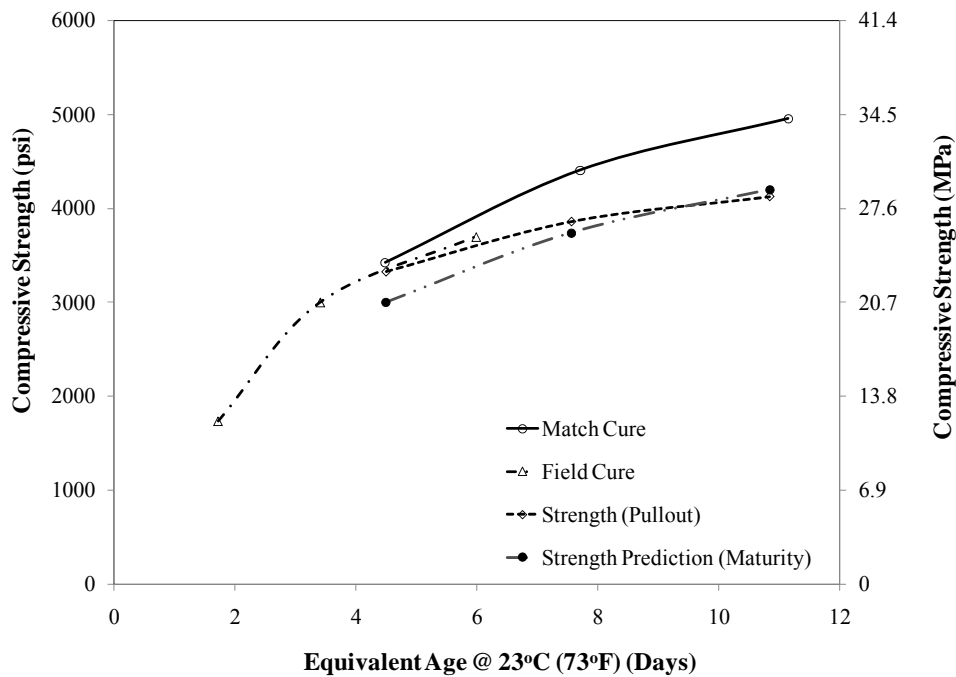


Figure E.9 Comparison of strength obtained from various methods vs. equivalent age setting time (35%FA-C mixture-block)

Figure E.11 shows the compressive strength plot for the 50% FA-A mixture-block. It is clearly observed, that the field cure and match cure cylinders have close strength at same ages. On the other hand, the maturity method slightly underestimates the strength prediction.

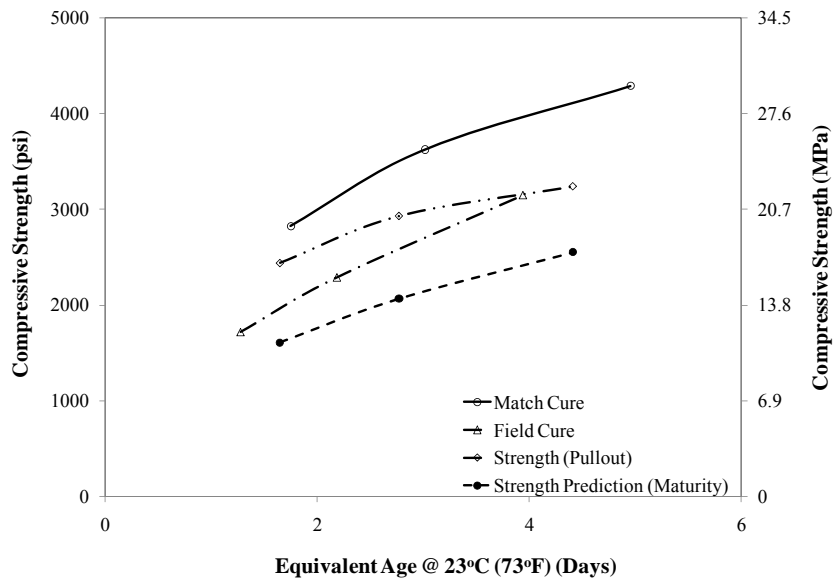


Figure E.10 Comparison of strength obtained from various methods vs. equivalent age setting time (control mixture-slab)

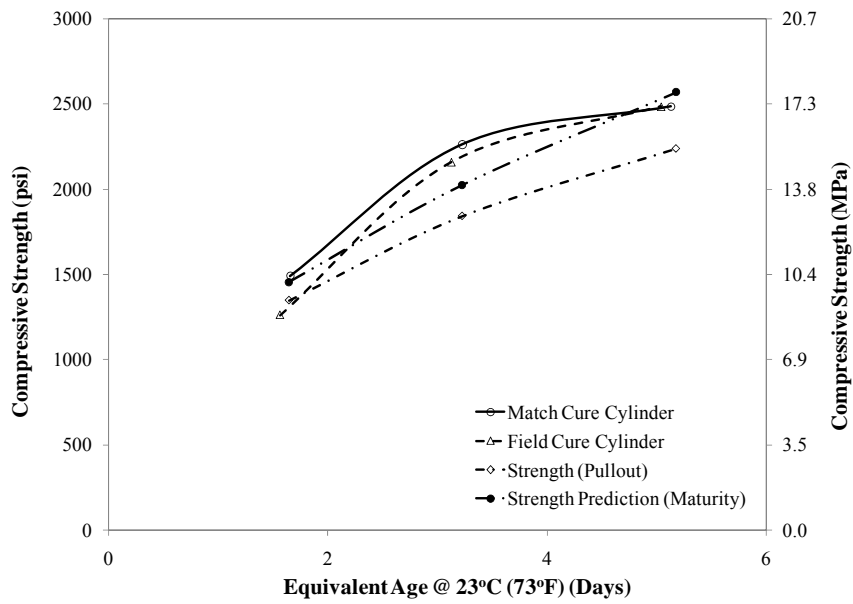


Figure E.11 Comparison of strength obtained from various methods vs. equivalent age setting time (50% FA-A-slab)

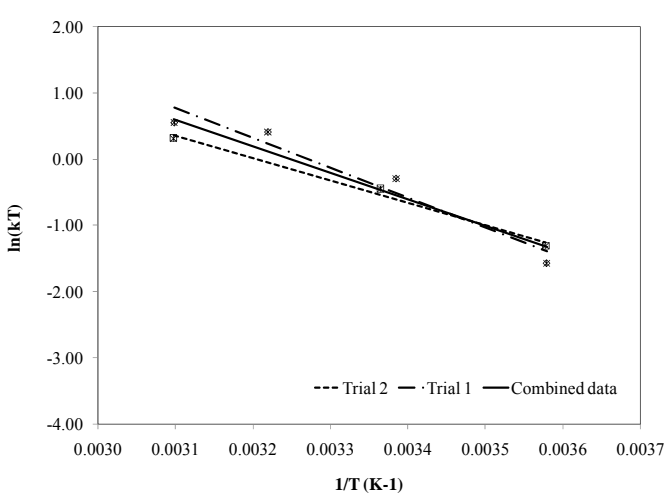
Table E.1 shows the difference in percentage between maturity predicted strength and match cure strength. It is observed that the maturity prediction strengths are lower.

Table E.1 Strength comparison between match cure and predicted strength

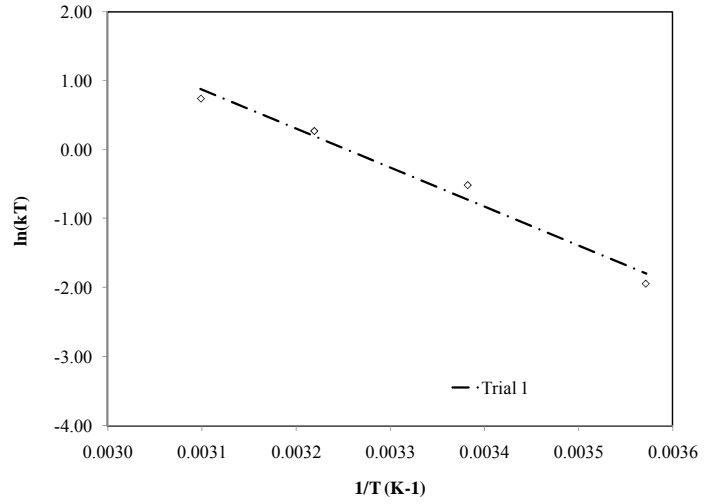
Mixture	Concrete Element	Actual Age (Days)	Match Cure Strength MPa (psi)	Strength Prediction Maturity Method MPa (psi)	Difference (%)
Control Mix	Block	2	19.4 (2810)	16.3 (2360)	-17.7
		4	23.8 (3452)	20.4 (2955)	
		7	26.6 (3861)	22.7 (3292)	
	Slab	2	19.5 (2825)	11.1 (1605)	-73.3
		4	25 (3625)	14.2 (2063)	
		7	29.6 (4289)	17.6 (2550)	
35% FA-A	Block	2	12.4 (1802)	9.1 (1314)	-41.7
		4	16.9 (2450)	11.2 (1621)	
		7	19.2 (2786)	14 (2033)	
50% FA-A	Block	2	14.9 (2156)	12.1 (1755)	-17.4
		4	19.5 (2823)	16.7 (2418)	
		7	22.4 (3251)	19.9 (2883)	
35% FA-C	Slab	2	10.3 (1491)	10 (1455)	-5.0
		4	15.6 (2262)	14 (2024)	
		7	17.6 (2545)	17.7 (2569)	
	Block	2	23.6 (3422)	20.7 (3001)	-16.6
		4	30.4 (4405)	25.8 (3740)	
		7	34.2 (4953)	29 (4198)	

Appendix F

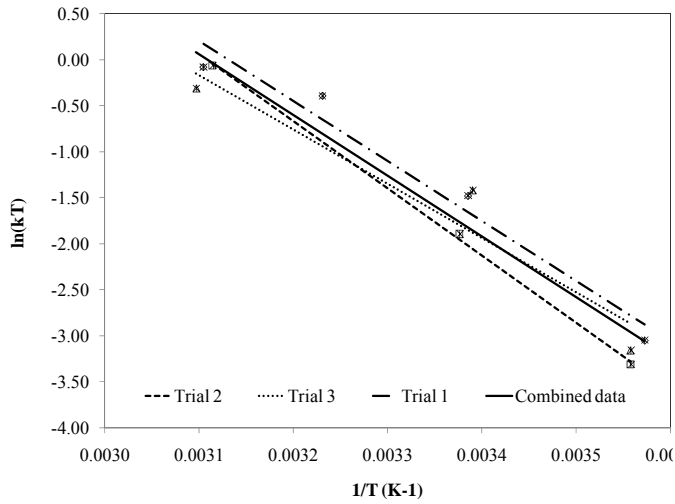
Appendix F summarizes the Arrhenius plots and maturity models for the Constant S_{uc} approach.



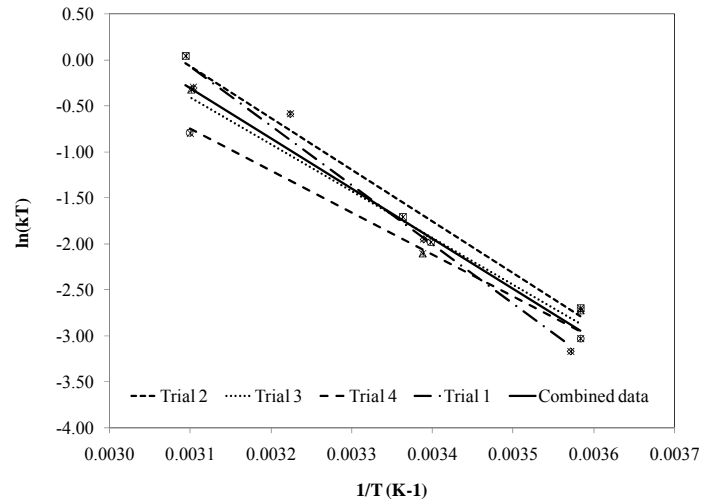
(a-Control mix)



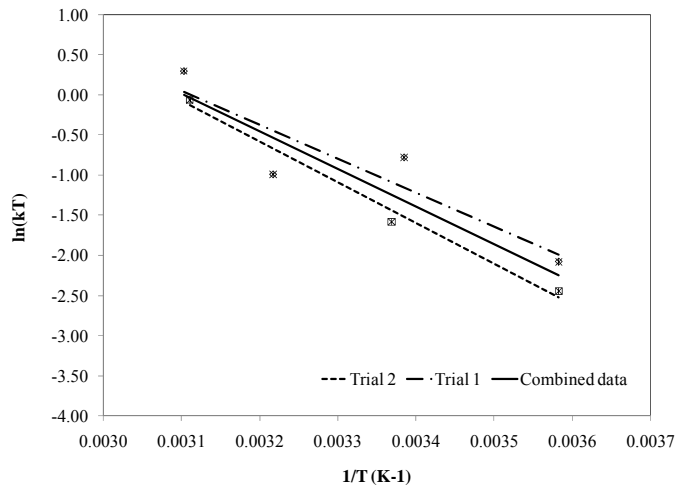
(b-20% FA-A)



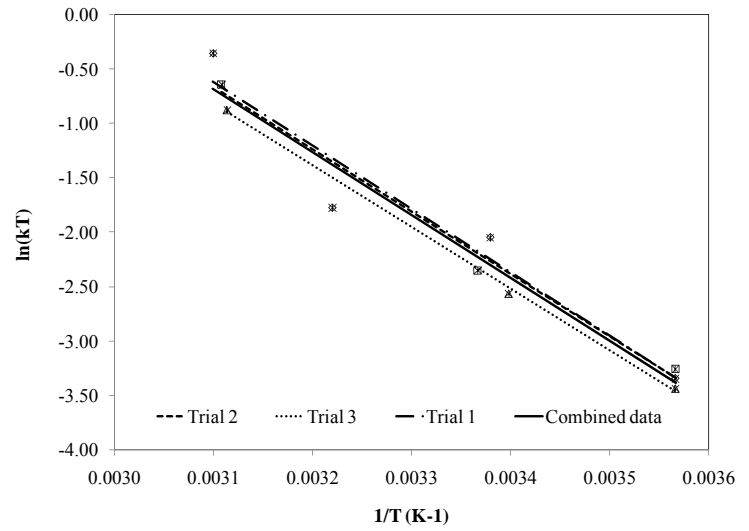
(c -35% FA-A)



(d-50% FA-A)

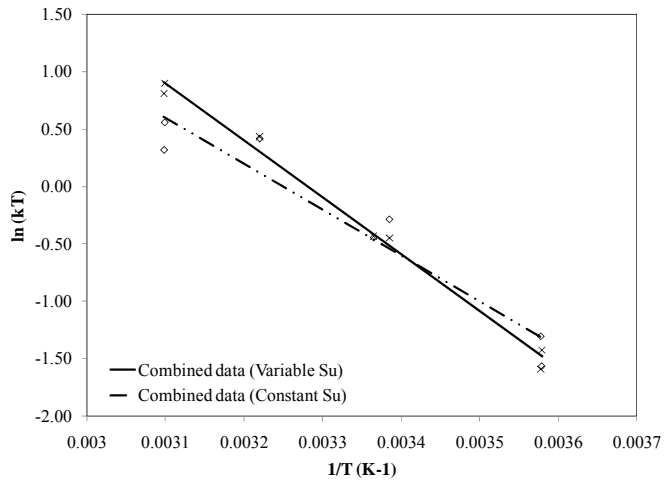


(e- 35% FA-B)

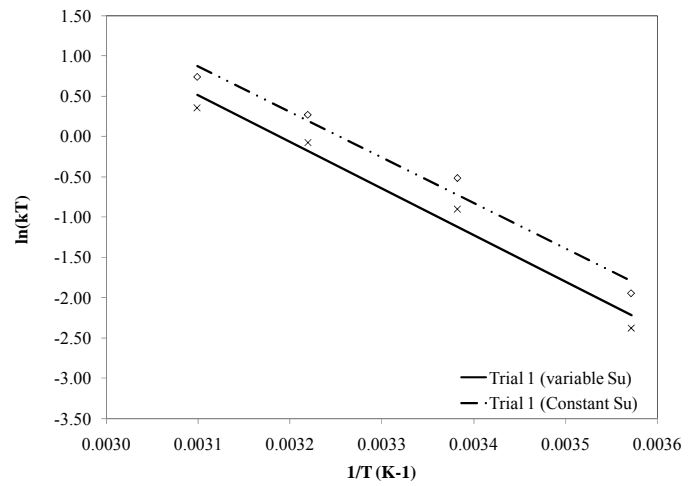


(f-35% FA-C)

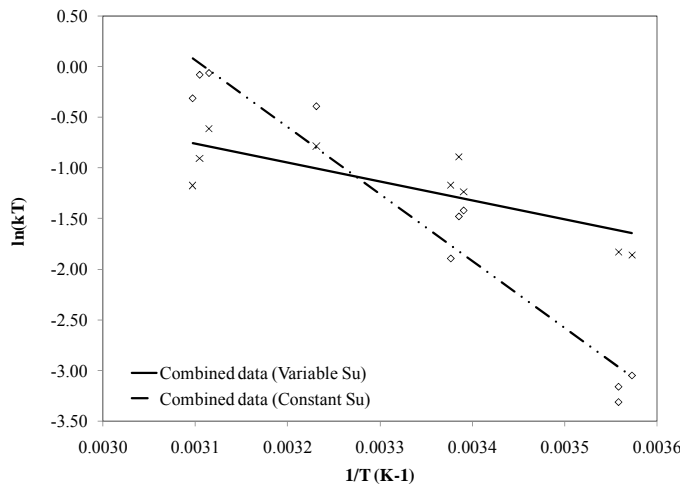
Figure F.1 Arrhenius plots (Constant S_{uc} approach)



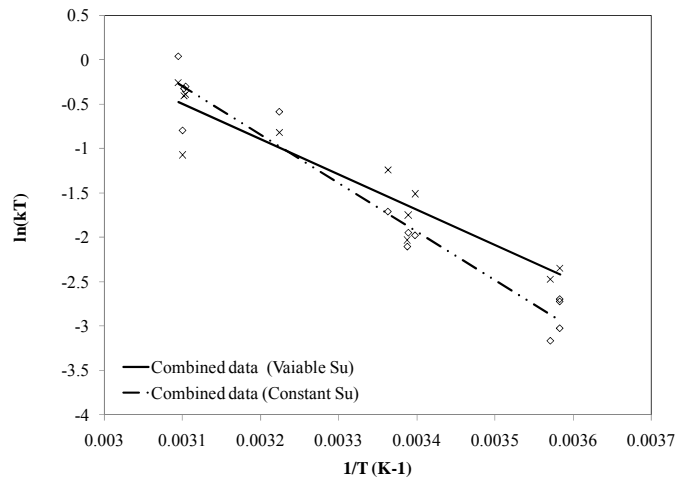
(a-Control mix)



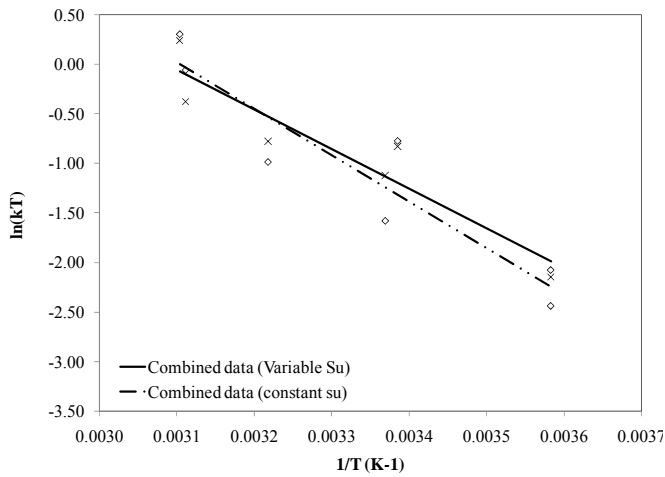
(b-20%FA-A)



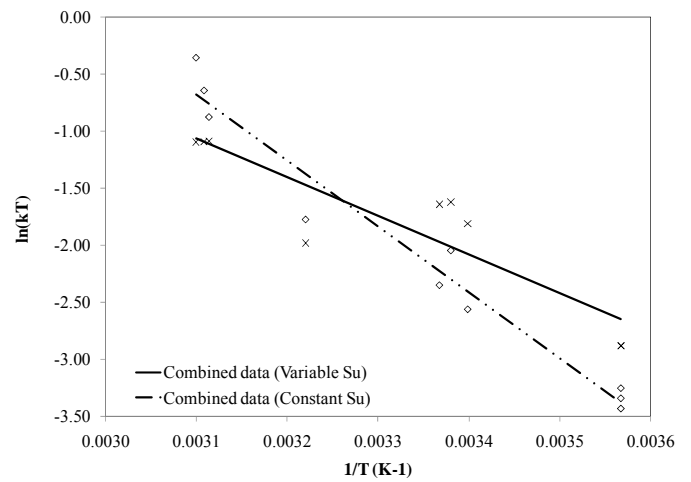
(c-35% FA-A)



(d-50% FA-A)



(e-35% FA-B)



(f-35% FA-C)

Figure F.2 Comparison of Arrhenius plot (Variable S_u and Constant S_{uc}) for combined data set

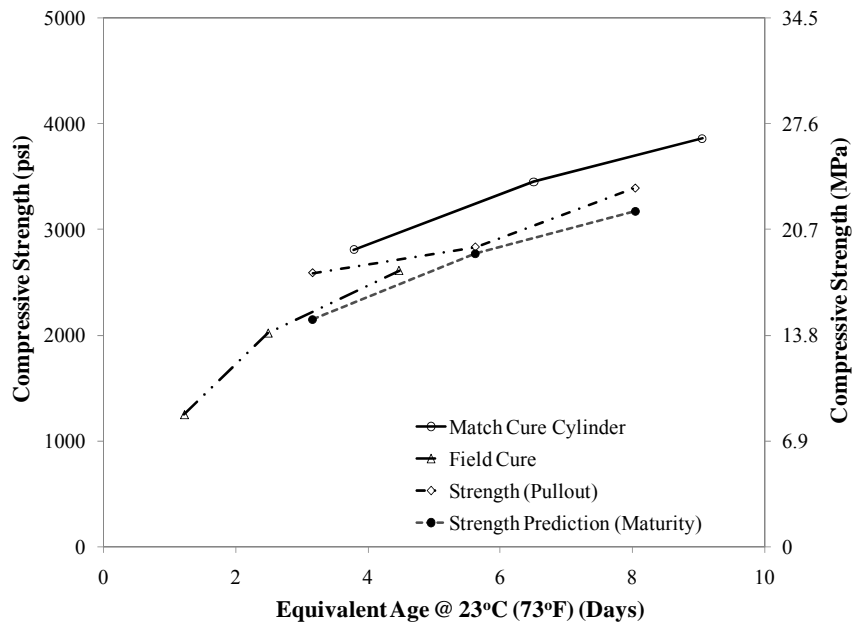


Figure F.3 Comparison of strength obtained from various methods versus equivalent age (control mixture-block)

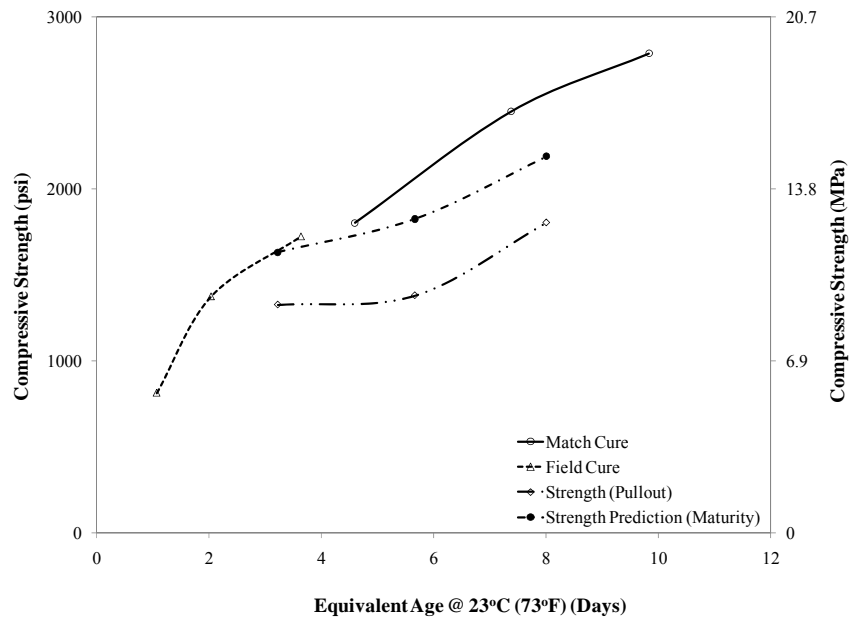


Figure F.4 Comparison of strength obtained from various methods versus equivalent age (35% FA-A-block)

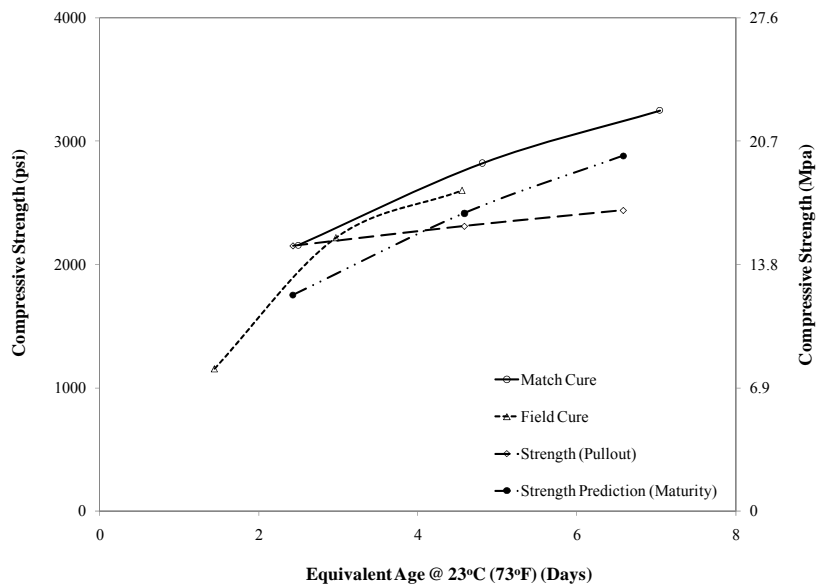


Figure F.5 Comparison of strength obtained from various methods versus equivalent age (50% FA-A-block)

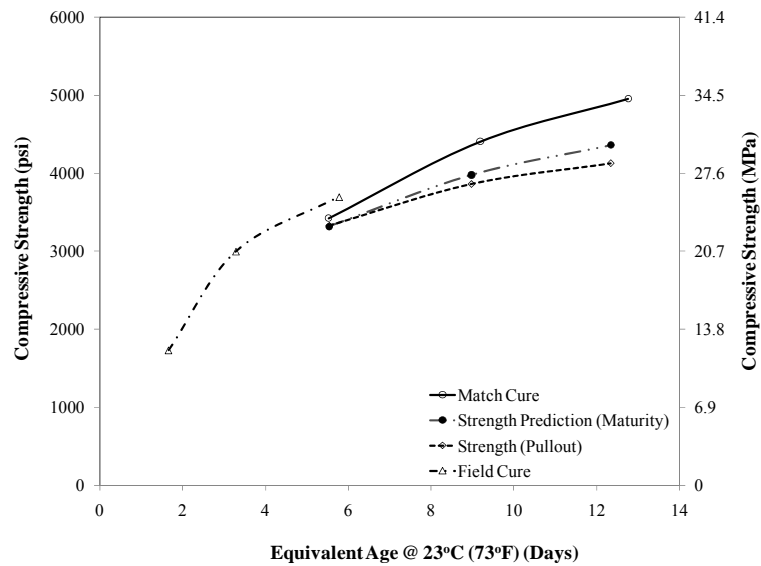


Figure F.6 Comparison of strength obtained from various methods versus equivalent age (35% FA-C-block)

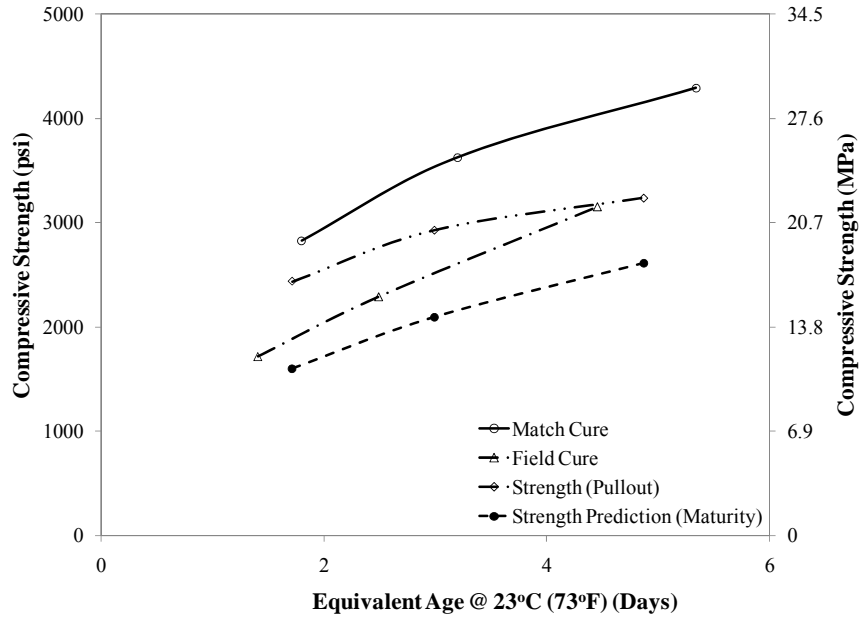


Figure F.7 Comparison of strength obtained from various methods versus equivalent age (control mixture-slab)

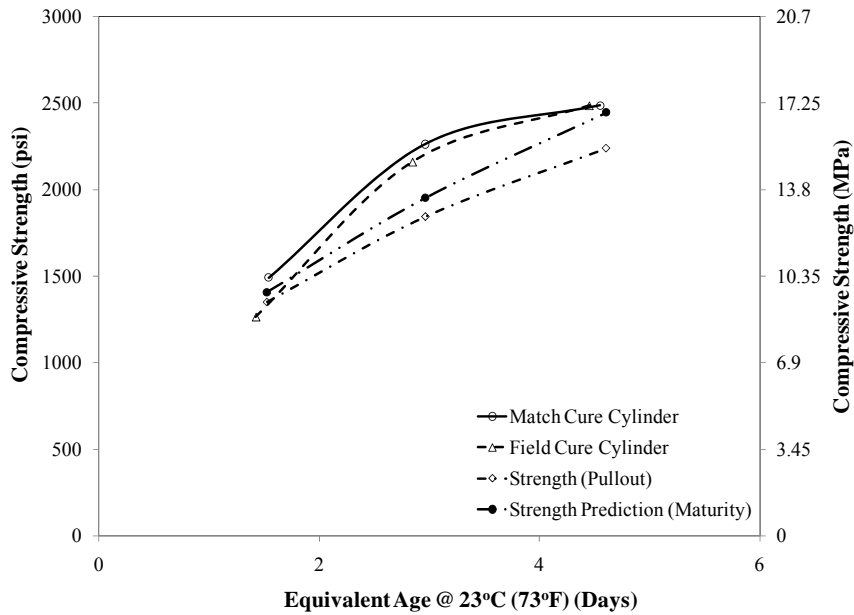


Figure F.8 Comparison of strength obtained from various methods versus equivalent age (50% FA-A -slab)

Table F.1 shows the difference in percentage between maturity predicted strength and match cure strength, with the maturity prediction strength being lower.

Table F.1 Strength comparison between various curing condition and predicted strength

Mixture	Concrete Element	Actual Age (Days)	Match Cure Strength MPa (psi)	Strength Prediction Maturity Method MPa (psi)	Difference (%)
Control Mix	Block	2	19.4 (2810)	14.8 (2152)	-25.5
		4	23.8 (3452)	19.1 (2774)	
		7	26.6 (3861)	21.9 (3174)	
	Slab	2	19.5 (2825)	11.0 (1602)	-71.1
		4	25.0 (3625)	14.4 (2095)	
		7	29.6 (4289)	18.0 (2612)	
35% FA-A	Block	2	12.4 (1802)	11.2 (1630)	-24
		4	16.9 (2450)	12.6 (1825)	
		7	19.2 (2786)	15.1 (2190)	
50% FA-A	Block	2	14.9 (2156)	12.8 (1851)	-13.2
		4	19.5 (2823)	17.4 (2525)	
		7	22.4 (3251)	20.1 (2918)	
	Slab	2	10.3 (1491)	9.7 (1409)	-8.5
		4	15.6 (2262)	13.5 (1954)	
		7	17.6 (2545)	16.9 (2446)	
35% FA-C	Block	2	23.6 (3422)	22.9 (3315)	-9.19
		4	30.4 (4405)	27.4 (3976)	
		7	34.2 (4953)	30.1 (4359)	

Appendix G

This appendix presents the temperature time profiles for the concrete mixtures. For each of the 6 field tested cases (4 blocks and 2 slabs) the temperature vs. age profiles are presented, as two plots. Figure G.1 shows the average temperature during the field-testing from October to November 2006. The temperature during this period ranged from around 30°F to 70°F.

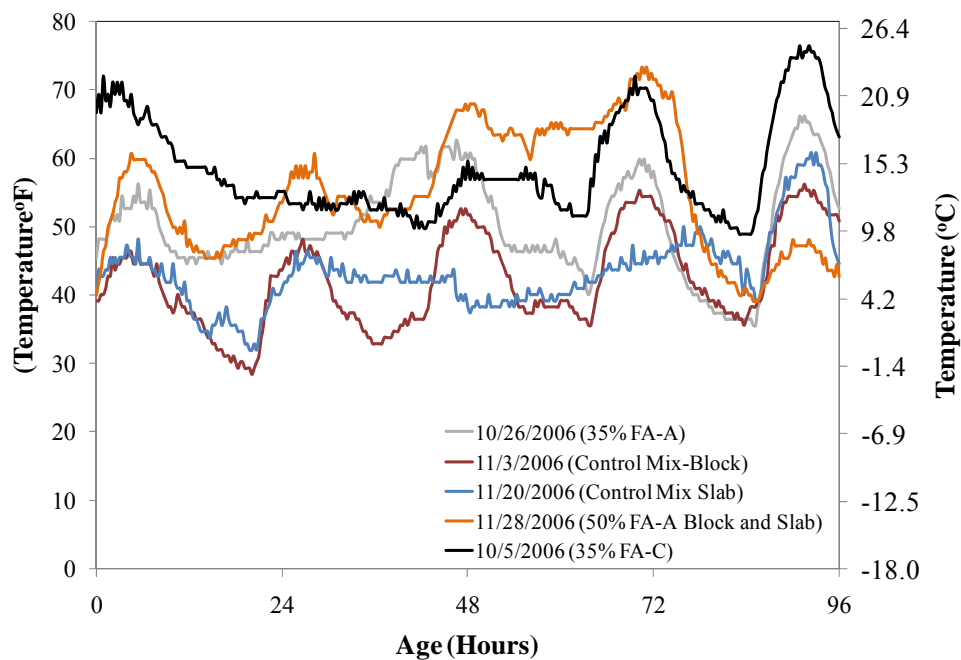


Figure G.1 Ambient temperature profile during field testing from October to November

Figure G.2 shows the thermal gradient within the block (control mix). The plot clearly shows that the iButton at the center of the block recorded the higher temperature, and the iButton closest to the edge recorded the lowest temperature during the hydration period. Figure G.3 shows the temperature profile of the concrete cured under different conditions. The temperature rise was highest in the field cured conditions despite of the lower ambient temperature. Figure

G.4 also shows that the iButton at the center of the slab recorded higher temperature. These plots clearly indicate that the mass of the structure plays a vital role in the hydration of concrete. The bigger the mass the higher the hydration rate will be. This phenomenon is observed for all the mixtures, Figure G.4 to G.11.

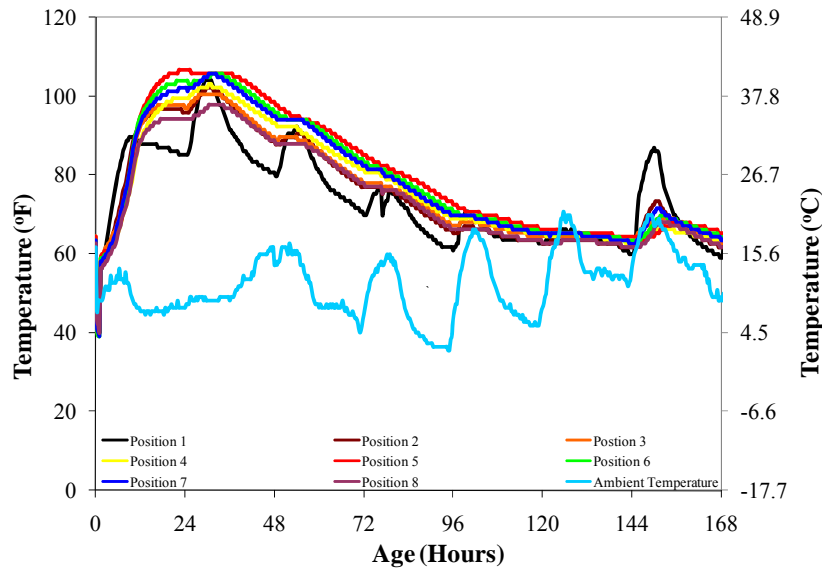


Figure G.2 Temperature Profile of block (Control mixture)

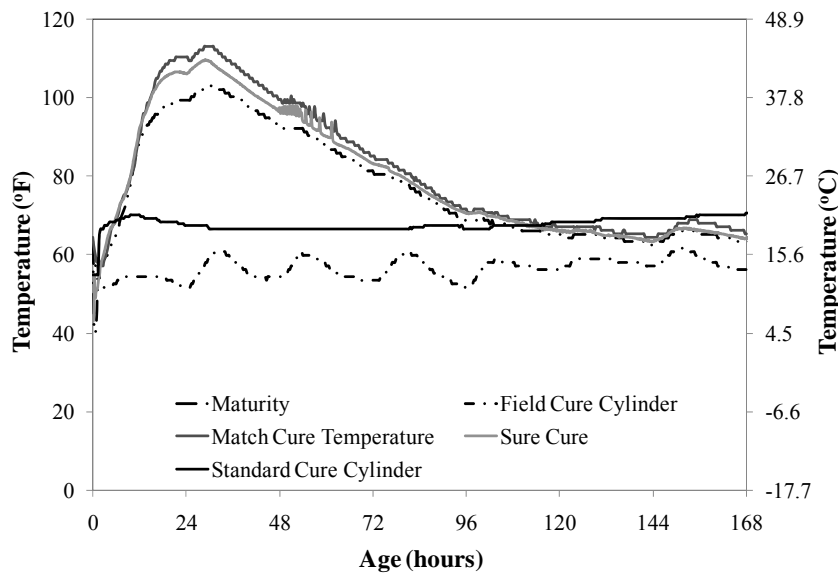


Figure G.3 Temperature Profile Control mixture

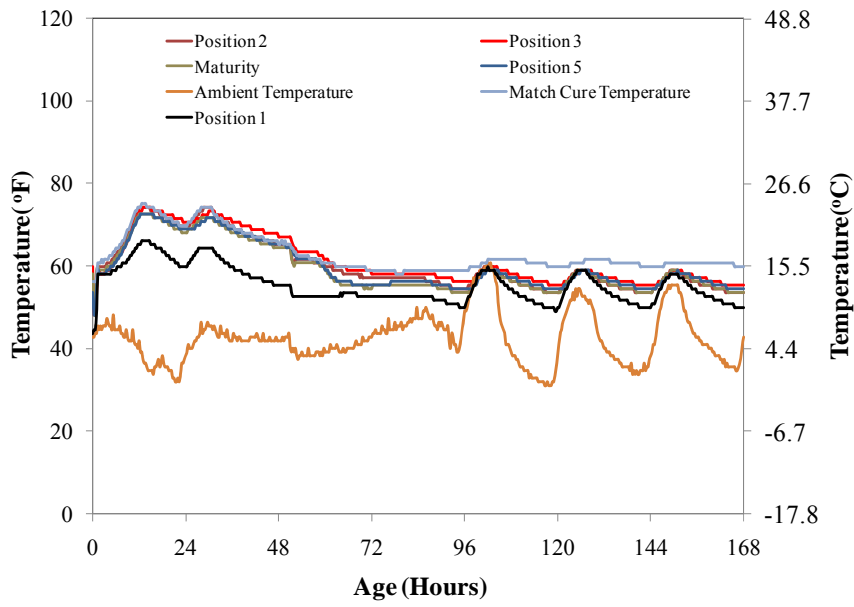


Figure G.4 Temperature Profile of Slab (Control Mixture)

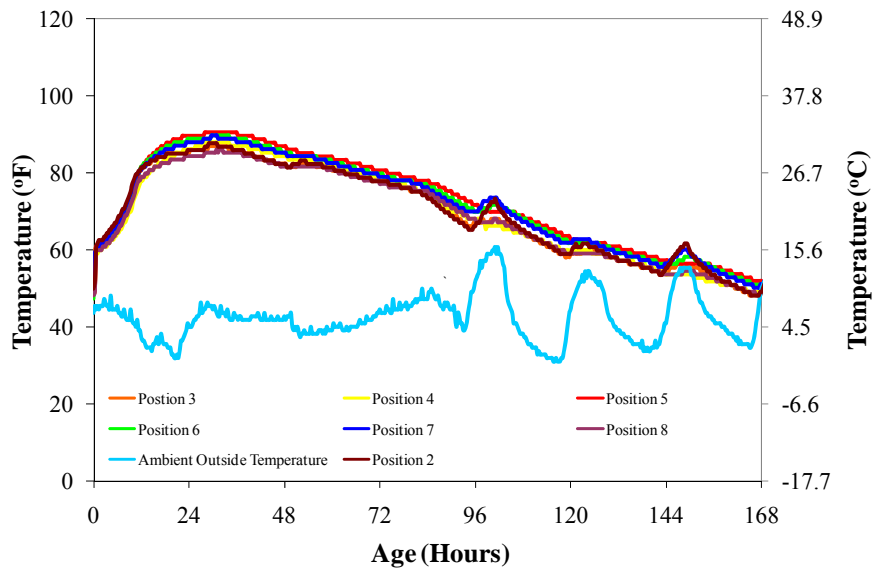


Figure G.5 Temperature Profile of block (50% FA-A)

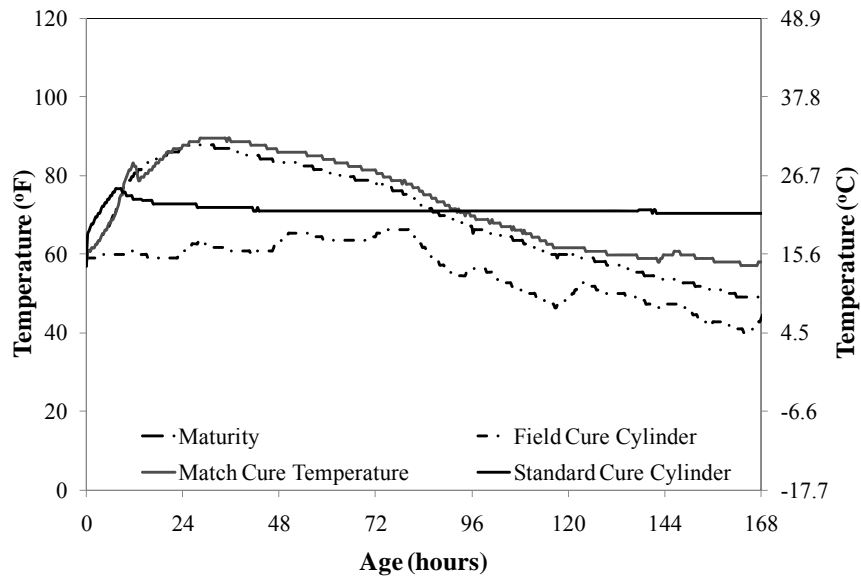


Figure G.6 Temperature Profile 50% FA-A

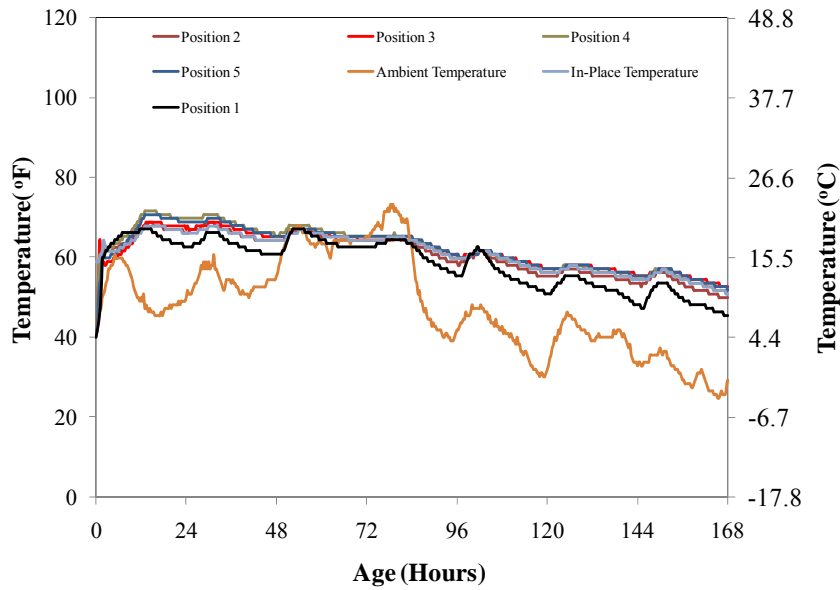


Figure G.7 Temperature Profile of Slab (50% FA-A)

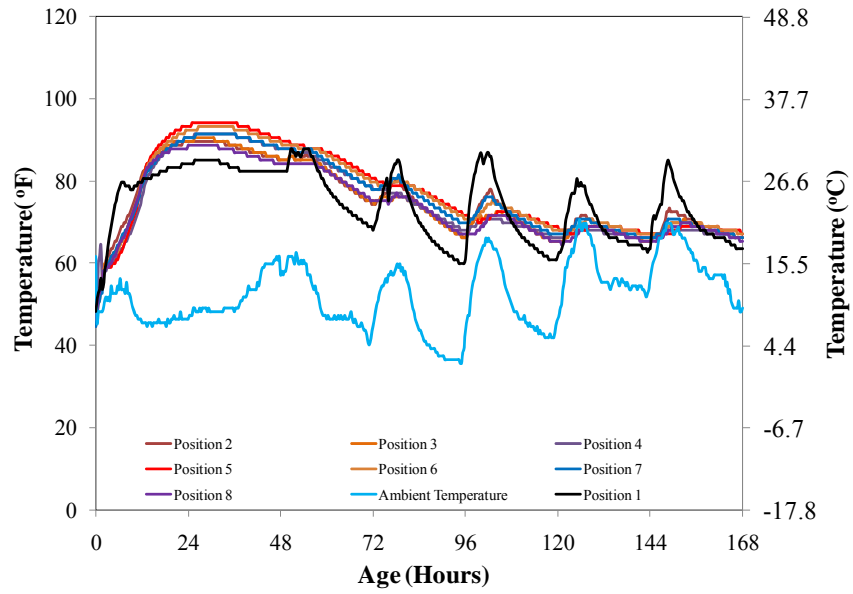


Figure G.8 Temperature Profile of block (35% FA-A)

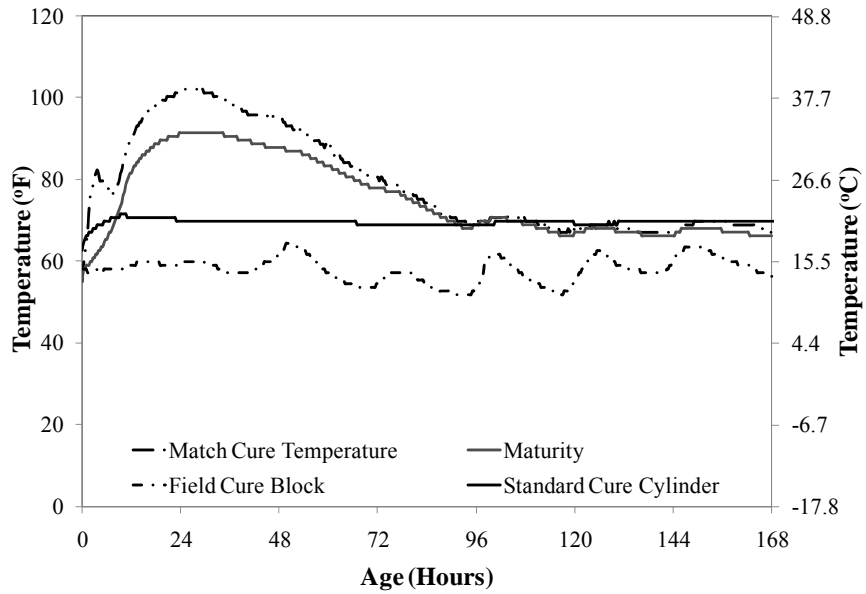


Figure G.9 Temperature Profile 35% FA-A



Figure G.10 Temperature Profile of block (35% FA-C)

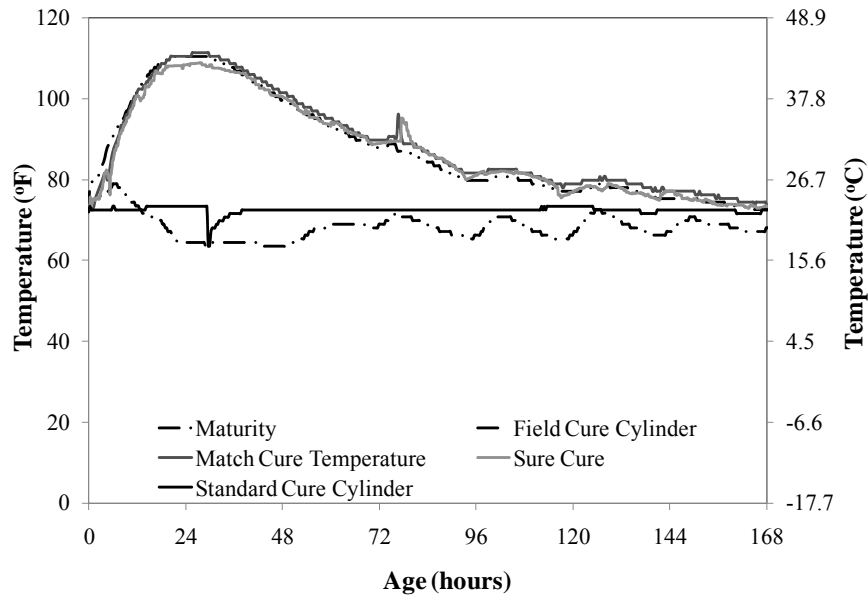


Figure G.11 Temperature Profile 35% FA-C

References

ACI Committee 228, 2003, "In-Place Methods to Estimate Concrete Strength (ACI 228.1R-03)," American Concrete Institute, *ACI Manual of Concrete Practice*.

ASTM C29/C29M, 2003 "Standard Test Method for Bulk Density ("Unit Weight") and Voids in Aggregate," Volume 04.02.

ASTM C33, 2003 "Standard Specification for Concrete Aggregates," Volume 04.02.

ASTM C39/C39M, 2005. Standard Test Method for Compressive Strength of Cylindrical Concrete Specimens," ASTM International, Volume 04.02.

ASTM C109/C109M, 2007. "Standard Test Method for Compressive Strength of Hydraulic Cement Mortars (Using 2-in. or [50-mm] Cube Specimens)," ASTM International, Volume 04.01.

ASTM C127, 2004 Standard Test Method for Density, Relative Density (Specific Gravity), and Absorption of Coarse Aggregate," Volume 04.02.

ASTM C128, 2004,” Standard Test Method for Density, Relative Density (Specific Gravity), and Absorption of Fine Aggregate,” Volume 04.02.

ASTM C136, 2006 Standard Test Method for Sieve Analysis of Fine and Coarse Aggregates, Volume 04.02.

ASTM C138/C138M 2001a,” Standard Test Method for Density (Unit Weight), Yield, and Air Content (Gravimetric) of Concrete” ASTM International, Volume 04.02.

ASTM C143/C143M, 2005a,” Standard Test Method for Slump of Hydraulic-Cement Concrete” ASTM International, Volume 04.02.

ASTM C150, 2004 “Standard Specification for Portland Cement,” ASTM International, Volume 04.01

ASTM C185, 2002,” Standard Test Method for Air Content of Hydraulic Cement Mortar,” ASTM International, Volume 04.01.

ASTM C188, 2003,” Standard Test Method for Density of Hydraulic Cement,” ASTM International, Volume 04.01.

ASTM C192/C192M, 2006 Standard Practice for Making and Curing Concrete Test Specimens in the Laboratory,” ASTM International, Volume 04.02.

ASTM C231 2004,” Standard Test Method for Air Content of Freshly Mixed Concrete by the Pressure Method” ASTM International, Volume 04.02.

ASTM C305, 2006, “Standard Practice for Mechanical Mixing of Hydraulic Cement Pastes and Mortars of Plastic Consistency,” ASTM International, Volume 04.01

ASTM C403, 2006, “Standard Test Method for Time of Setting of Concrete Mixtures by Penetration Resistance,” ASTM International, Volume 04.02

ASTM C494/C494M, 2005a, “Standard Specification for Chemical Admixtures for Concrete,” ASTM International, Volume 4.02

ASTM C618, 2005,” Standard Specification for Coal Fly Ash and Raw or Calcined Natural Pozzolan for Use in Concrete,” ASTM International, Volume 04.02.

ASTM C873, 2004, “Standard Test Method for Compressive Strength of Concrete Cylinders Cast in Place in Cylindrical Molds,” ASTM International, Volume 04.02

ASTM C900, 2006, "Standard Test Method for Pullout Strength of Hardened Concrete,"
ASTM International, Volume 04.02.

ASTM C1074, 2004, "Standard Practice for Estimating Concrete Strength by the Maturity
Method," ASTM International, Volume 04.02.

ASTM C1064/C1064M, 2005," Standard Test Method for Temperature of Freshly Mixed
Hydraulic-Cement Concrete" ASTM International, Volume 04.02.

ASTM C1231/C1231M, 2006," Standard Practice for Use of Unbonded Caps in
Determination of Compressive Strength of Hardened Concrete Cylinders" ASTM
International, Volume 04.02.

ASTM C1437, 2005,"Standard Test Method for Flow of Hydraulic Cement Mortar," ASTM
International, Volume 04.01.

Bergstrom, S.G., "Curing Temperature, Age and Strength of Concrete," *Magazine of
Concrete Research*, 5(14), 61 1953

Bernhardt, C.J., “Hardening of Concrete at Different temperatures”, *Proc. RILEM Symp. On Winter Concreting, Session BII*, Copenhagen, Danish Institute for Building Research, Copenhagen 1956

Brooks, J. J., “Prediction of Setting Time of Fly Ash Concrete,” *ACI Materials Journal*, V. 99, No. 6, November-December 2002, pp.591-597

Carette, G., Bilodeau, A., Chevrier, R. L., and Malhotra, V. M. “ Mechanical Properties of Concrete Incorporating High Volumes of fly ash from the sources in the US,” *ACI Materials Journal*, V.90, No.6 , November-December 1994 pp: 535-544

Cengiz Duran Atiş, “Heat evolution of high-volume fly ash concrete, “*Cement and Concrete Research* 32 (2002) 751–756

Carino, N.J., The Maturity Method: Theory and Application,” *ASTM J. Cement, Concrete, and Aggregates*, 6 (2), 61, 1984.

Carino, N.J and Tank, R.C., “ Maturity Functions for Concrete Made with Various Cements and Admixtures, “ *ACI Materials Journal*, Vol. 89, No.2, March-April, PP. 188-196, 1992

Carino, N.J., “The Maturity Method,” Chapter 5 in *Handbook on Nondestructive Testing of Concrete*, 2nd Edition, Malhotra, V.M., and Carino, N.J., Eds., CRC Press Inc, Boca Raton, FL, and ASTM International, 2004.

Coal Combustion Product (CCP) Production and Use Survey, 2006 from *ACAA International* . <[http://www.aaa-usa.org/associations/8003/files/2006_CCP_Survey_\(Final-8-24-07\).pdf](http://www.aaa-usa.org/associations/8003/files/2006_CCP_Survey_(Final-8-24-07).pdf)>.

Freiesleben Hansen, P., and Pedersen, J., “Maturity Computer for Controlled Curing and Hardening of Concrete,” *Nordisk Betong*, 1, 1977, pp. 19-34.

Halit Yazıcı*, Serdar Aydın, Hüseyin Yiğiter, Bülent Baradan, “Effect of steam curing on class C high-volume fly ash concrete mixtures”, *Cement and Concrete Research* 35 (2005) pp.1122–1127

Industry Fact Sheet, 2008 from *National Ready Mixed Concrete Association*<
<http://www.nrmca.org/concrete/2008.htm>>

Jonasson, J. E., Groth, P., and Hedlund, H., “ Modeling of Temperature and Moisture Field in Concrete to Study Early Age Movement as a Basis for Stress Analysis, “ *Proceedings of the International RILEM Symposium on the Thermal Cracking in the Concrete at Early Ages*, R. Springenschmid, ed., E&FN Spon, London, 1995, pp.45-52.

Maltais, Y., and Marchand, J. “ Influence of Curing Temperature on Cement hydration and Mechanical Strength Development of Fly Ash Mortars”, *Cement and Concrete Research*, Vol. 27, No. 7 pp 1009-1020, (1997)

Mills, R. H., “Factors Influencing Cessation of Hydration in Water Cured Cement Pastes, “*Special Report* No. 90, Proceedings of the Symposium on the Structure of Portland Cement Paste and Concrete, Highway Research Board, Washington, D.C., pp.406-424, 1996.

Nurse, R. W., “Steam Curing of Concrete,” *Magazine of Concrete Research*, Vol. 1, No. 2, pp. 79-88, 1949.

Obla, Karthik, Hill, Russell, and Martin Ross, “HVFA Concrete – An Industry Perspective”, *Concrete International*, Vol. 25, No. 8, 2003, pp. 49-54.

Obla, Karthik, Anton K. Schindler, and Nicholas J. Carino, “New Technology-Based Approach to Advance Higher Volume Fly Ash Concrete With Acceptable Performance-Guide for the Construction Team – An Industry Perspective”, NRMCA, pp 19. October 2008.

Papyianni, I., and Valliasis Th. “ Heat Deformation of Fly Ash Concrete”. *Cement and Concrete Composites*, Vol. 27, pp 249-254, (2005)

PCA, and NRMCA, October 2000-October 2003, Survey of Mineral Admixtures and Blended Cements in Ready Mixed Concrete, PCA/NRMCA Survey.

Sang-Hun Han, Jin-Keun Kim, Yon-Dong Park,” Prediction of compressive strength of fly ash concrete by new apparent activation energy function,” *Cement and Concrete Research* 33 (2003) pp.965–971

Saul, A.G.A., “Principles Underlying the Steam Curing of Concrete at Atmospheric Pressure,” *Magazine of Concrete Research*, Vol. 2, No. 6, March 1951, pp. 127-140.

Schindler, A.K., and Folliard, K.J., "Heat of hydration models for cementitious materials", *ACI Materials Journal*, Vol. 102, No. 1, pp 24-33, Jan. 2005.

Schindler, A.K., "Effect of temperature on the hydration of cementitious materials", *ACI Materials Journal*, Vol. 101, No. 1, pp 72-81, 2004.

Sivasundaram, V., Carette, G. G., and Malhotra, V. M., “Properties of Concrete incorporating Low Quantity of Cement and High Volumes of Low-Calcium Fly Ash,” Fly Ash, Silica Fume, Slag, and Natural Pozzolans in Concrete—*Proceedings, Third International Conference, SP-114*,

Somayaji, S., “Concrete and other Cementitious Materials,” Chapter 3 in *Civil Engineering Materials*, Prentice-Hall, Inc., Englewood Cliffs, NJ, 1995.

Subramaniam, K. V.; Gromotka, R.; Shah, S. P.; Obla, K. H.; and Hill, R.,” Influence of Ultrafine Fly Ash on the Early Age Response and the Shrinkage Cracking Potential of Concrete”, *Journal of Materials in Civil Engineering*, 2005, pp:45-53

Tank, R.C. and Carino, N.J., “ Rate Constant Functions for Strength Development of Concrete, “ *ACI Materials Journal*, Vol. 88, No.1, pp.74-83, 1991.

Upadhyaya, S., D. G. Goulias, and K. Obla, “Evaluation of In Place Strength of High-Volume Fly Ash Concrete,” The First International Conference on Recent Advances in Concrete Technology, Arlington, VA. September 18-21, 2007.

Van Breugel, K., “Simulation of Hydration and Formation of Structure in Hardening Cement Based Materials,” PhD thesis, 2nd edition, *Delft university Press*, The Netherlands, 305 pp.

Waller, V., d’Aloia, L., Cussigh, F., and Lecrux, S., “ Using the Maturity Method in Concrete Cracking Control at Early Ages”, *Cement and Concrete Composite*, Vol 26 No. 5 , pp-589-599, 2004